Imperial College London

Laboratory Investigation of the Ignition and Spread of Smouldering in Peat Samples of Different Origins and the Associated Emissions

A thesis submitted in partial fulfilment of the

requirements for the degree of

Doctor of Philosophy

in

Mechanical Engineering

by

Wuquan Cui

2022

Supervised by Prof. Guillermo Rein

Declaration of Originality

I declare that this thesis and the work described within have been completed solely by myself under the supervision of Prof. Guillermo Rein. Where others have contributed or other sources are quoted, full references are given.

Wuquan Cui

2022

Copyright Declaration

ABSTRACT

Laboratory Investigation of the Ignition and Spread of Smouldering in Peat Samples of Different Origins and the Associated Emissions

by

Wuquan Cui

Doctor of Philosophy in Mechanical Engineering

Imperial College London, 2022

Supervised by Prof. Guillermo Rein

Tackling peatland wildfires, the largest fires on Earth in terms of fuel consumption, is an emerging combustion topic in the context of climate change. The understanding of fundamental smouldering dynamics and their application to peatlands are essential to mitigation methodologies' development, but not yet fully understood in the literature. Most of the previous laboratory smouldering studies used horticultural peat which has a great advantage in controlling the influential factors, but has lower bulk density, and is not representative of some higher bulk density peat found in the field. In this thesis, a series of laboratory experiments were conducted to investigate the critical ignition conditions and governing fire spread parameters of smouldering in peat of various origins, and to quantify the associated emissions. To better understand natural variations, field samplings were conducted in Sumatra, Indonesia and Flow Country, Scotland. In addition, five types of horticultural peat were studied. The results show high bulk density peat from long-term drained peatlands experiences more extensive burning in terms of the amount of carbon and particle emitted, while newly drained peat with low bulk density is more vulnerable to fire in terms of easier ignition and faster fire spread. Evidence was found in this thesis that the heat sink density and the organic density, not only control horizontal spread and in-depth spread, but also determine ignition probability. Furthermore, as smouldering is multidimensional, a critical angle of spread direction (65˚ relative to horizontal plane) above which smouldering cannot self-sustain was found. By

studying the emissions of different types of peat, the modified combustion efficiency (MCE) range for smouldering was broadened to 0.74 – 0.88, and found to be significantly dependent on the fuel composition. This thesis provides a better understanding of how smouldering wildfires start and spread in different types of peat and the associated emissions, thus contributing to prevention and mitigation.

ACKNOWLEDGEMENTS

First I would like to thank my PhD supervisor, Prof. Guillermo Rein for giving me this opportunity to conduct research on smouldering peat fires, an emerging combustion topic in the context of climate change. I love my research and have also developed a lifetime hobby to visit as many peatlands as possible and tell as many people as possible about peatland wildfires. Thank you for all your guidance and inspirations through this journey! Thank you for your time editing my works. As saying goes, to write is human, to edit is divine. I have learned so many things from you, and would like to learn more from you in future.

I would also like to thank all members of Imperial Hazelab for the amazing journey we went through. Thank you Xinyan, Egle, Iza, Francesco, Nils, Nieves, Franz, Yuqi, Heidari, Edmund, Agung, Matt, Eirik, Han, Zhenwen, Xuanze, Ben, Guoxiang, Fahid, Dwi, Francesca, Harry, Simona, Rik, and Nik. Special thanks to team China, team GAMBUT, team WINTERFELL, team Valencia, and team Bella Ciao. Special thanks to Yuqi who helped me to start my experiments. Special thanks to Simona, Francesca and Agung for proofreading my works. Everyone here I know is so bright and I wish you all a bright future.

I appreciate in my PhD I had opportunities collaborating with and learning from some great scientists in the world. Thank you Amy, Georgia, and Dr Marc Stettler from the Department of Civil and Environmental Engineering at Imperial College for the collaboration in studying particle emissions from peat fires. Thank you Prof. Roxane Andersen from the University of the Highlands and Islands for the collaboration of WINTERFELL field study. Thank you Prof. Yulianto Nugroho and his team from the University of Indonesia for the collaboration of GAMBUT field experiment. Thank you Dr Cathelijne Stoof from Wageningen University & Research for teaching me soil geography and landscape. Thank you Dr Thomas Smith from LSE for the collaboration on emission study and teaching me Arduino. I would also like to thank Prof. Aimee Morgans and Dr Nuria Prat-Guitart for serving as my examiners of my viva. Thank you Prof. Michael Gollner who brought me to fire research, recommended me to do my PhD, and gives me the postdoc opportunity to continue my fire research at UC Berkeley.

I would like to thank all lovely people I met these years. It is difficult to list all your names. Thank you Cecily and your parents. Thank you Li Yan, FeiFan brothers, Yang Qiang and

Shangguan, and Thomas. Thank you Teresa, Antonio, Bernardo, Kathleen, Sherry, and Yifan. Thank you Xiaoying, Xiyu, Xiaotian, Shengda, Jiajie, Shinan and Wu Fan, Yurong, Gong Yu, Tianyi, Chaoxv, Dapeng, Ying Lu, Anna, Maria… Thank you my housemates at 24 Stanhope Mews W. Thank you all amazing people I met onboard MS Midnatsol, MS Fram, MS Roald Amundsen, Silver Cloud, and MV Sea Spirit.

Thank you ERC (European Research Council) for providing funding to us. Thank you all who is reading this thesis for your interest in smouldering peat fires.

I would also like to thank myself for all the days and nights in the office and in the lab, especially all the time alone in the office and in the lab during pandemic.

Thank you my parents for all your love and support! I already have more than four years not being at home. I miss you so much. This thesis is dedicated to you.

Table of Contents

Chapter 1 Introduction to Smouldering Peat Fires 1
1.1 Peatland Wildfires 2
1.2 Ignition and Spread of Smouldering Peat Fires 5
1.3 Emissions of Smouldering Peat Fires 7
1.4 Thesis Outline 12
Chapter 2 Field Peat Sampling 14
Summary 15
2.1 GAMBUT Field Sampling 15
2.2 WINTERFELL Field Sampling 30
Chapter 3 Experimental Methodology 39
Summary 40
3.1 Sample Preparation and Characterization 40
3.2 Experimental Setup 46
3.3 Spread Analysis 49
3.4 Emission Analysis 51
Chapter 4 Ignition Conditions of Self-sustained Smouldering in Peat 53
Summary 54
4.1 Introduction 54
4.2 Method 55
4.3 Results and Discussion 59
4.3.1 Ignition signature of mass loss and temperature 59
4.3.2 The influence of ignition protocol on ignition 62
4.3.3 Effects of moisture content and bulk density on ignition 66
4.3.4 Ignition signature of gas emissions 72
4.4 Conclusion 73
Chapter 5 Influence of Density on Smouldering Dynamics and Emissions 75
Summary 76
5.1 Introduction 76
5.2 Stages of Fire Evolution 77
5.3 Effect of Soil Compression on Smouldering Spread 79
5.4 Effect of Soil Compression on Emissions 81

Chapter 6 Laboratory Study of Samples from Flow Country and the Effect of Field Conditions 84
Summary 85
6.1 Introduction 85
6.2 Method 87
6.3 Results and Discussion 88
6.3.1 Overview of the burning process 88
6.3.2 Thermal residence time 92
6.3.3 Smouldering spread rate 93
6.3.4 Gas emissions 96
6.3.4 Particle emissions 97
6.3.5 Implications to the field 99
6.4 Conclusion 102
Chapter 7 Laboratory Study of Smouldering Multi-dimensional Spread in Samples of Different Origins 103
Summary 104
7.1 Introduction 104
7.2 Method 105
7.3 Results and Discussion 107
7.3.1 Overview of the smouldering dynamics 107
7.3.2 Spread rate and spread direction 110
7.3.3 Gas and particle emissions 114
7.4 Conclusion 117
Chapter 8 Laboratory Benchmark of Low-Cost Portable Gas and Particle Analysers for the Field Measurements 118
Summary 119
8.1 Introduction 119
8.2 Method 120
8.3 Results and Discussion 126
8.3.1 Performance of FLOW and SDS011 for PM measurements 126
8.3.2 Performance of KANE101 and FLOW for gas measurements 130
8.3.3 Calculating emission factors 132
8.4 Conclusions 134
Chapter 9 Conclusions of this Thesis 135
References 142

Nomenclature

Symbols	
c_i	Specific heat capacity of inorganic content (J/kgK)
c_o	Specific heat capacity of organic density (J/kgK)
c_p	Specific heat capacity (J/kgK)
c_w	Specific heat capacity of water (J/kgK)
d	Diameter of the ignition coil (cm)
L	Length of the ignition coil (cm)
k	Conductivity (W/mK)
L_w	Latent heat of evaporation (J/kg)
$\dot{m}''$	Burning rate (kg/m^{2}h)
m	Mass of sample (kg)
m_p	Mass of dry peat (kg)
m_w	Mass of water (kg)
S_d	In-depth spread rate (cm/h)
S_h	Horizontal spread rate (cm/h)
t_b	Burning time (h)
V	Reactor volume (m^3)
Δ	Compression (%)
ΔH_P	Change in enthalpy of pyrolysis (J/kg)
ΔT_d	Temperature increase of drying (°C)
ΔT_H	Temperature increase of dry matter (°C)
ρ	Density (kg/m^3)
ρ_b	Bulk density (kg/m^3)
ρ_i	Inorganic density (kg/m^3)
ρ_o	Organic density (kg/m^3)
ρ_w	Water density (kg/m^3)
ϕ	Direction of the spread direction (°)
F_c	Carbon fraction in mass of the fuel
M_i	Molar mass of species i
n_i	Number of moles of species i
n_t	Total number of moles of carbon emitted

$\dot{V}$	Volumetric flow rate inside the duct
$\dot{m}$(t)	Real-time mass loss rate of the wet peat sample

Abbreviations

MC	Moisture content (%)
IC	Inorganic content (%)
MLR	Mass loss rate (g/s)
EF	Emission factor (g/kg)
ER	Emission ratio
MCE	Modified combustion efficiency
VOCs	Volatile organic compounds
PAHs	Polycyclic aromatic hydrocarbons
PM	Particulate matter
PM1	Particle with an aerodynamic diameter ≤ 1.0 μm
PM2.5	Particle with an aerodynamic diameter ≤ 2.5 μm
PM10	Particle with an aerodynamic diameter ≤ 10 μm
TPM	Total particulate matter
IR	Infrared
NDIR	Non-dispersive infrared
FTIR	Fourier-transform infrared spectroscopy
OP-FTIR	Open-path Fourier-transform infrared spectroscopy
LAFTIR	Land-based Fourier-transform infrared spectroscopy
LAS	Laser absorption spectroscopy
PTR-MS	Proton-transfer-reaction mass spectroscopy
CLA	Chemiluminescence analyser
GC-FID	Gas chromatograph with flame ionization detector
ECS	Electrochemical sensor
WAS	Whole air sampling
LSS	Light scattering sensor
SMPS	Scanning Mobility Particle Sizer
WHO	World Health Organization
MAE	Mean absolute error
RMSE	Root mean squared error

Chapter 1

Introduction to Smouldering Peat Fires

1.1 Peatland Wildfires

Wildfire is an intrinsic and fundamental process in the Earth system, influencing the ecological evolution in the natural history for many million years, and becoming an emerging topic with the increase in the occurrence of large and uncontrolled fires over the past decade [1, 2]. Among wildfires happening in various ecosystems worldwide, peatland wildfires are known as the largest fires on Earth in terms of fuel consumption [3, 4]. It can destroy important natural habitats and soil ecosystems, releasing ancient carbon to the atmosphere, and creating regional haze episodes of severe and extensive impacts on human health [5-7].

Peatland wildfires can burn surface vegetation and also propagate underground burning peat, a type of carbon-rich organic soil containing partially decomposed vegetation, which is a typical biomass with a porous structure [5]. Peatlands cover nearly 3% of the earth's land surface and store more than 25% of the terrestrial carbon [8]. Peatlands are commonly found in tropical regions (e.g. Indonesia, Amazon and Congo), boreal regions (e.g. Siberia, Canada, Alaska, and Scandinavia), and temperate regions (e.g. British isles) [9]. They have critical roles in supporting the Earth ecosystem and preserving carbon pools formed over centuries to millennia [5]. Peat is usually formed in waterlogging and preserving conditions where the accumulation of dead vegetation is faster than the decomposition, for example, in tropical regions with seasonal raining raising the water table and in arctic regions with cold climate and high water table preserving the organic material [5, 10]. These forming conditions can naturally protect peatlands from large fires, but due to human activities (e.g. drainage, change of land use and peat mining) and climate change (warmer and dryer), peatlands are now under additional threat of wildfires [11, 12]. Figure 1.1 shows some peatlands I visited during my PhD study, and these field studies helped me tremendously in understanding the importance of peatlands in our ecosystem and the importance of protecting peatlands from large wildfires.

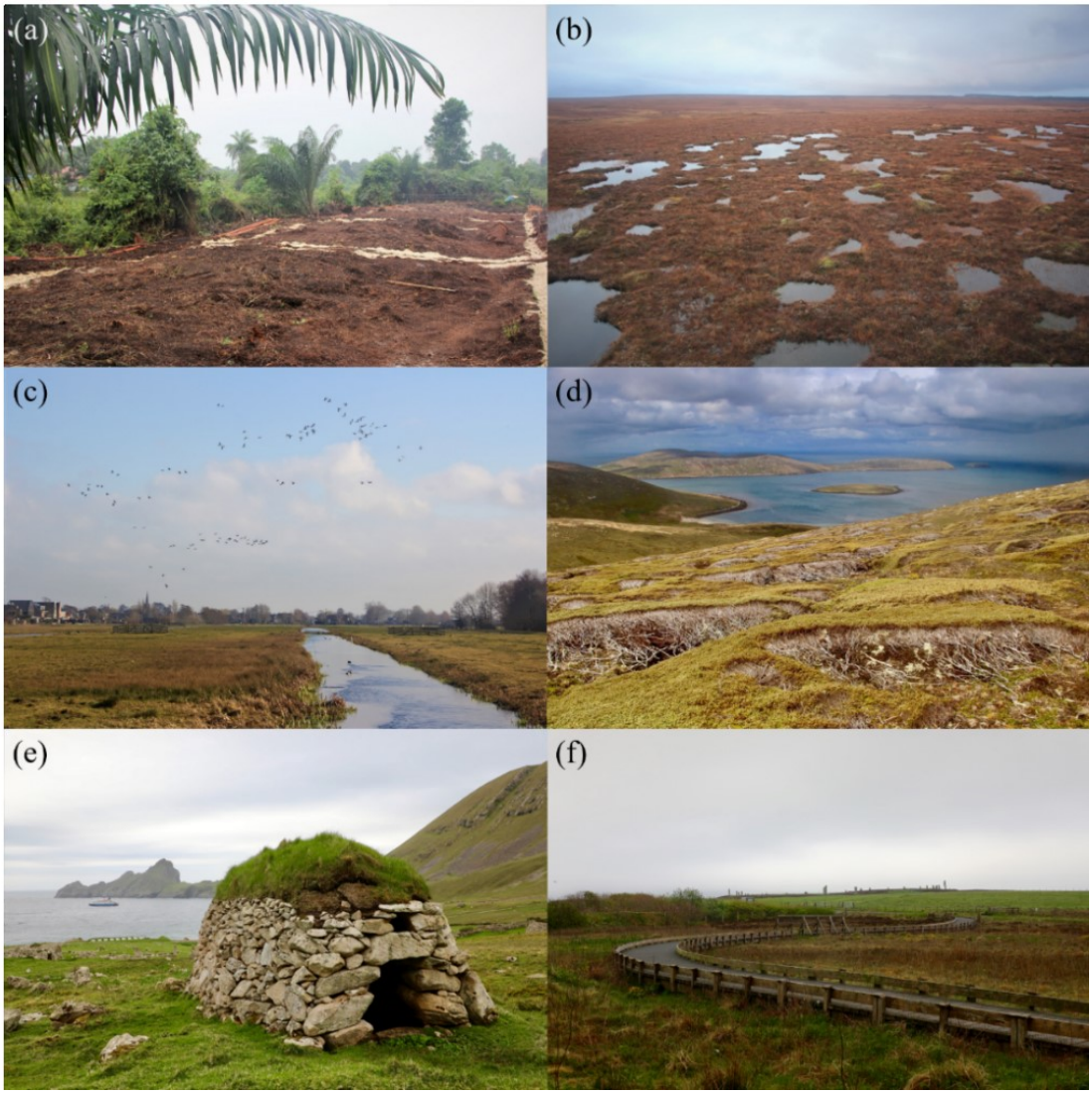

Figure 1.1 Photos of peatlands visited during my PhD study (photo copyright: Wuquan Cui). (a) A degraded peatland in Rokan Hilir, Riau Province, Sumatra, Indonesia, where we conducted GAMBUT2018 field campaign measuring peatland fires. (b) A peatland in near-pristine condition in Forsinard Flows Nature Reserve, Flow Country, Scotland, where we visited previous wildfire sites and conducted field sampling with the guidance of Prof. Roxane Andersen from the University of Highlands and Islands. (c) A restored peatland near Berkenwwoude in Netherlands, where I attended a field study led by Prof. Cathelijne Stoof from the Wageningen University. (d) A peatland in New Island, Falkland Islands. (e) A peatland in St. Kilda World Heritage Site, UK. (f) A peatland in Brodgar Nature Reserve, Orkney Islands, UK.

Smouldering combustion is the dominant mechanism of peatland fires. The process is flameless, slower (spread rate in around 1 cm h^{-1}), and occurs at a lower temperature (peak around 600 ℃) than flaming fires (around 1200 ℃), but can last for longer periods of time (months to years until fuel consumed, natural or artificial extinguishment) [3]. In terms of chemical reaction, flaming fire is homogeneous combustion with gas phase oxidation, while smouldering fire is heterogeneous combustion with oxygen directly reacting with the solid fuel particles [13]. Flaming and smouldering both present in most of the wildfires with possible transition phenomenon from one to the other [14]. Figure 1.2 shows the visual comparison of flaming and smouldering fires on peatlands with surface flaming and smouldering peat. Peat fires can be easily initiated when the organic soil is dry but challenging to be extinguished [15, 16]. The detection of smouldering in peatland wildfires is also challenging since smouldering hotspots can reach very deep underground and propagate in all directions [17]. It is important to have more research on the smouldering wildfires to help mitigate these megafires [4].

Figure 1.2 Photos of flaming and smouldering fires on peatlands (photo copyright: Wuquan Cui). These two photos were taken in GAMBUT2018 field campaign. (a) shows slash-and-burn ignition with flaming fires burning the surface vegetation. (b) shows the propagation of smouldering fires underground burning peat.

1.2 Ignition and Spread of Smouldering Peat Fires

In general, there are three main processes in smouldering, drying, pyrolysis and oxidation, which are controlled by oxygen supply and heat loss [18]. The energy of ignition has to be sufficient to initiate the process of char oxidation, with char being the product of the pyrolysis. A self-sustained smouldering needs to have enough energy produced from oxidation to overcome the heat loss and drive drying and pyrolysis [19]. The mechanism of ignition to initiate a self-sustained smouldering is complex [20-22], hence this research is essential in understanding the initiation of smouldering wildfire and developing prevention and mitigation strategies.

In the natural environment, peat fires are often initiated by flaming wildfires, lightning strikes, arson, or even self-heating [23]. The ignition criteria for self-sustained smouldering peat are influenced by many factors including soil properties, ignition source and environmental conditions. The intensity, duration and depth of the ignition source can influence the outcome of ignition [24]. Environmental conditions, such as topography, wind, precipitation and ambient temperature directly affect the oxygen supply and heat transfer on altering the process of smouldering combustion [25]. Moisture content (mass of water divided by mass of dry peat in sample), inorganic content (mass of non-combustible material divided by mass of dry peat in sample) and bulk density (mass of sample divided by volume of sample) are the three most important soil conditions to influence the ignition and propagation of smouldering [3].

Inorganic content and moisture content perform as heat sinks absorbing heat generated from the oxidation and altering heat transfer [26]. Bulk density plays an important role in limiting oxygen supply and changing heat transfer regime [27-29]. Combining the factors of

moisture content and inorganic content, a critical ignition threshold, above which ignition is not possible, was found in previous study with an approximate linear decrease of critical moisture content with increasing the inorganic content [26].

As bulk density can be changed by altering moisture content and inorganic content, and can also be influenced by many other factors such as porosity, soil structure and decomposition rate, it is very challenging to study the effect of bulk density on smouldering ignition and spread, hence very few research focused on this topic. This topic can be studied by using field peat samples with naturally different bulk densities but more uncertainties in soil properties, or by using commercial peat samples with different levels of compression to control the bulk density and other soil properties. Most of the previous studies in this topic used commercial peat samples and varied the bulk density by compression. Hu et al. [28] focused on the effect of compression on transient emissions, and Prat-Guitart et al. [27] focused more on propagation. These two studies all have one level of compression to make the bulk density higher, while Christensen [29] focusing on studying horizontal and in-depth spread by using a shallow reactor (1.6 cm depth) had three levels of compression (20%, 30%, and 40%). Huang and Rein conducted experimental and computational studies on this topic based on the experimental results using 10% moisture content peat with 0 and 40% compression [89]. No study has been conducted systematically to investigate the critical ignition conditions and the spread combining the factors of moisture content and bulk density. This topic is also very important in studying the fire dynamics of different types of peat with naturally different bulk density, and link the findings obtained in one type of peat to peat with different origins [30].

1.3 Emissions of Smouldering Peat Fires

Unlike flaming wildfires producing strongly buoyant dark smoke with abundant soot, smouldering peat fires emit weakly buoyant plumes with light smoke that stays at low altitudes and move long distances [7]. Peatland fires are responsible for regional haze episodes, of which the gas and particle emissions cause severe and extensive impacts on human health [7, 31]. For example, the 1997 haze crisis in Southeast Asia had an estimated 45,600 km^2 peatland burned for months with unprecedented haze pollution affecting a population of 100 million across five countries [32].

The emission gases from peat fires are a complex mixture of more than 90 detectable gas species [33], including carbon dioxide (CO_2), carbon monoxide (CO), methane (CH_4), ammonia (NH_3), and toxic gases such as some volatile organic compounds (VOCs), nitric oxide (NO_x), and hydrogen cyanide (HCN). Apart from their carbon emissions posing a positive feedback to climate change [6], some emitted gases have direct impact on human health, for example, some VOCs have been classified as carcinogenic to humans [34, 35]. Another important pollutant from peat fires is particulate matter, featuring in high concentrations that constitutes substantial health risks to local population [36], predominant in the respiratory and cardiovascular systems [37]. Previous research showed that smouldering peat fires emit more fine (aerodynamic diameter of 2.5 μm or less) and ultrafine (aerodynamic diameter of 0.1 μm or less) particles which can reach deeper parts of the human respiratory system [38, 39].

The adverse effects of peat fire emissions on human health, local environment and economy, and climate are raising concerns over the past decade [4, 40, 41]. However, studies with field measurement quantifying the emissions of peat fires are scarce in this emerging topic, mainly because of the challenging situation in the field and the limitations of instruments in

cost and mobility. Field experiments measure emissions directly providing the most representative data but with higher level of uncertainty, while laboratory experiments provide certainty in terms of variables controlled to study the fundamental understanding and test hypotheses formulated from field observations [24]. Both field and laboratory studies in peat fires are vital in understanding wildfires. (Figure 1.3 shows the visual scale difference in laboratory measurement and field measurement.)

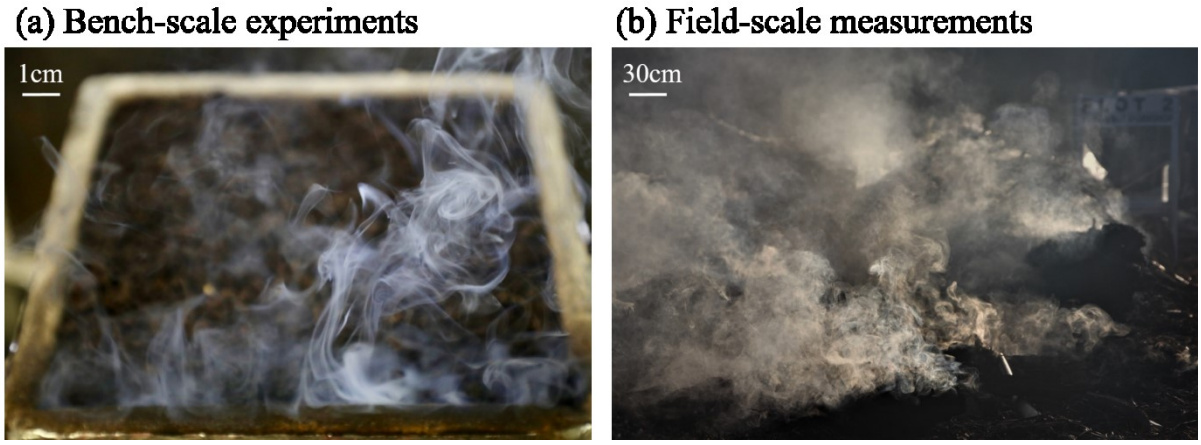

Figure 1.3 Photos showing the bench-scale and field-scale emissions of smouldering fires on peatlands (photo copyright: Wuquan Cui). Photo (a) was taken in the lab, and photo (b) was taken in GAMBUT2018 field campaign.

Figure 1.4 summarised the information of 27 literature of the past 20 years studying peat wildfire emissions in the laboratory or field. We define low-cost device to be within the range of the cost of a smartphone (below £600), and high-mobility to be handheld, medium-mobility to be portable to the field with more effort like bigger power supply and more components than handheld devices, and low-mobility to be some instruments setup in the laboratory which are not practical to be installed in the field because of fragility and extra systems needed. Figure 1.4 shows the research grade instruments used in laboratory studies of

higher accuracy and reliability are always in substantially higher cost and mostly of low or medium mobility.

The following studies of laboratory peat fire emissions are part of Figure 1.4. From the review of these studies, Fourier-transform infrared (FTIR) spectroscopy is the most commonly used instrument measuring gas emissions [28, 39, 42, 43]. The basic principle of FTIR spectroscopy is using IR radiation passing through the sampling gas to result in infrared spectrums which represent unique molecular absorptions and transmissions [44]. Comparing the infrared spectrums measured in experiments with the reference spectrums of gases in the same conditions of temperature and pressure, the concentrations of gases can be obtained. Some laboratory studies used Open-path FTIR spectroscopy (OP-FTIR) which has the same principle as FTIR but designed for field measurement [45-47]. IR or NDIR (Non-dispersive IR) based gas measurement devices are often used and reported with adequate accuracy after calibration in measuring CO_2 and CO only [48-54]. There are some more specialized instruments applied in peat fire emission measurements for gas species of VOCs, HCN, NH_3, and NO_x/NO, for example, PTR-MS (Proton-transfer-reaction mass spectroscopy) [46, 55], CLA (Chemiluminescence analyser) [43, 49, 54], and GC-FID (Gas chromatograph with flame ionization detector) [49]. In laboratory PM emission studies, filter-based and signal-based instruments are dominant, for example, filter-based PM cyclone or impactor [28, 39, 42, 46, 49, 53, 56], light scattering device DustTrak [43], and SMPS (Scanning Mobility Particle Sizer) [54].

For field gas emission measurements of peat fires, the Fourier-transform-infrared-based spectroscopy in field version (for example, Open-path FTIR spectroscopy (OP-FTIR) or Land-based FTIR spectroscopy (LAFTIR)) is a commonly used research-grade instrument that can measure a great variety of emission gases simultaneously [33, 57-59]. There are IR-based and

laser-absorption-based gas analysers developed for field measurements which are portable, but measure less variety of gases by focusing on the most abundant CO_2 and CO [51, 59-61]. Whole air sampling (WAS) is also a commonly used technique in field measurement by sampling air into bags in the field then analyse them in the lab [62, 63]. For field particle emission measurements, filter-based measurements using PM impactor or cyclone are conducted most often, which can provide the mass concentration and also allow the chemical and physical analysis of the particles later on in the lab [33, 51, 64, 65]. In recent years, the light-scattering-based devices (for example, DustTrak from TSI) are used in the field measuring the real-time mass concentration of particles [59, 61], but are relatively expensive. With the development of sensor technology, we are observing an increased utilization of air quality sensors in people's daily lives for health monitoring, however no study has been conducted to demonstrate the reliability of low-cost sensors to measure the smoke of wildfires. It is also critical to develop cost-effective air quality sensors to foster higher spatial and temporal measurements, and to be used for peat fire detection, validating remote sensing models, and estimating the health risks for residents or fire fighters.

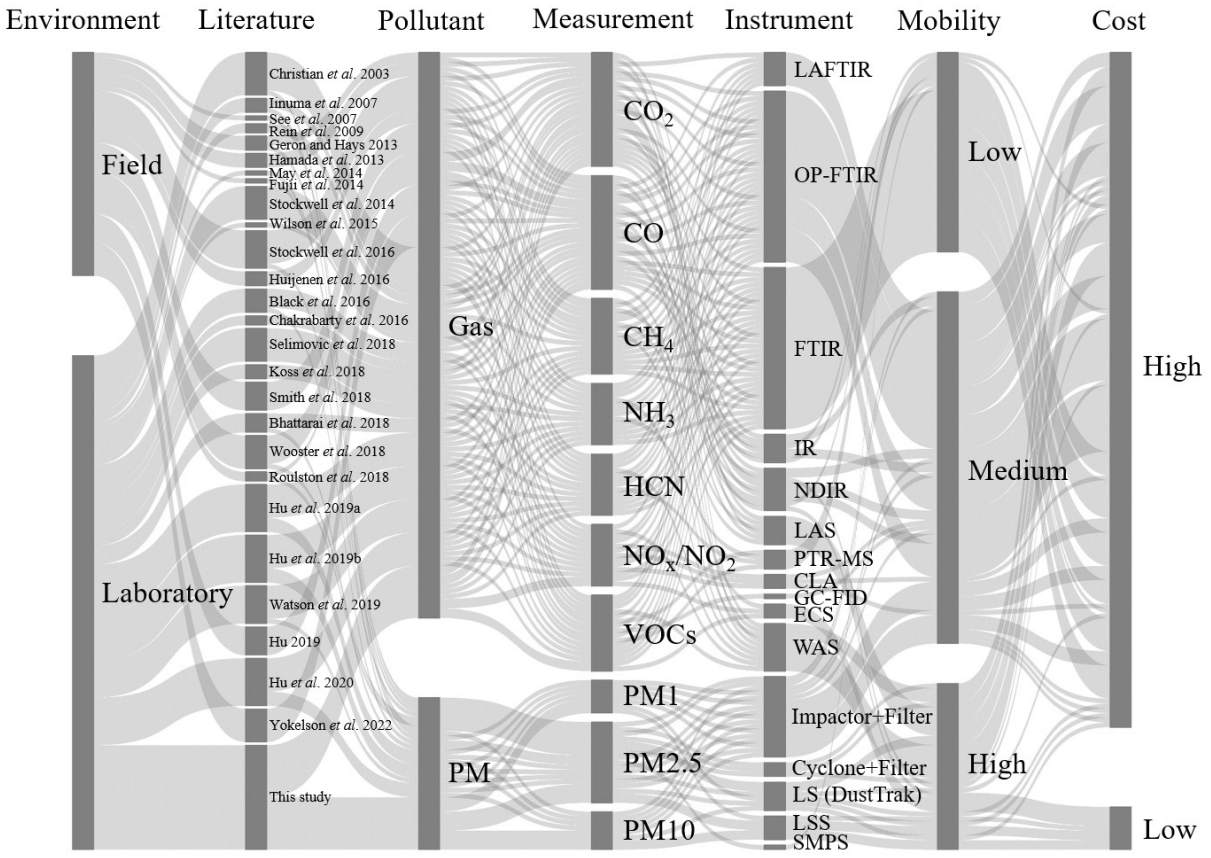

Figure 1.4 Alluvial diagram summarising the instruments used in 27 reviewed literatures studying emissions of peat fire. The measurement of gases only include the most commonly reported gases. The meanings of abbreviations of instruments are listed here: LAFTIR – Land-based FTIR spectroscopy, OP-FTIR – Open-path FTIR spectroscopy, IR – IR-based gas measurement system, NDIR – Non-dispersive IR detector, LAS – Laser absorption spectroscopy, PTR-MS – Proton-transfer-reaction mass spectroscopy, CLA – Chemiluminescence analyser, GC-FID – Gas chromatograph with flame ionization detector, ECS – Electrochemical sensor, WAS – Whole air sampling (sample air in the field and analyse in the lab), LS (DustTrak) – Light-scattering-based device DustTrak, LSS – Light scattering sensor, SMPS – Scanning Mobility Particle Sizer.

1.4 Thesis Outline

This thesis aims to investigate the ignition, spread and emissions of smouldering peat of different origins in laboratory conditions. Laboratory experiments were conducted by using a novel bench-scale experimental rig measuring the mass loss, temperature profile, visual and IR signature, and gas and particle emissions. The outline of thesis chapters is listed as follows:

Chapter 1 presents a brief introduction of the research background, aims and objectives of this thesis.

Chapter 2 presents two comprehensive field sampling in Sumatra, Indonesia, and Flow Country, Scotland. Field peat samples were obtained in these field studies, and the natural variation in the field condition were recorded.

Chapter 3 presents the experimental methodology used in this thesis. The detailed experimental setup, instrumentations, and the methods of calculating peat fire spread and emissions are presented.

Chapter 4 presents the laboratory study investigating the critical ignition conditions of self-sustained smouldering. A new ignition protocol based on mass loss is developed, and validated to be robust enough for smouldering studies of peat samples in high densities. The influence of moisture content and bulk density on ignition conditions were also investigated.

Chapter 5 presents the laboratory study investigating the influence of bulk density (changed by compression) on the horizontal spread and in-depth spread.

Chapter 6 presents a series of laboratory fire experiments using peat samples from field sampling in Flow Country, Scotland in natural peatlands, drained peatlands, and peatlands

under restoration. The effect of field condition on smouldering dynamics and emissions were investigated.

Chapter 7 presents the laboratory experiments studying smouldering ignition and spread for samples from different origins, including horticultural samples and more field samples. All spread data obtained in this thesis were summarised to develop a theory on smouldering spread in different peat.

Chapter 8 presents the laboratory assessment of low-cost and portable air quality sensors for peat fire emission measurements.

Chapter 9 summarises the main findings of this work.

Chapter 2

Field Peat Sampling

Summary

This chapter describes methods of field peat sampling conducted in GAMBUT field experiment in Rokan Hilir, Sumatra, Indonesia, and WINTERFELL field study in Flow Country, Scotland, UK. Field sampling is important in helping to understand the results of the ignition and spread of smouldering fires in the field scale and linking the findings in laboratory bench-scale studies with the fire dynamics of the field-scale. We measured soil moisture content and bulk density in our field sampling sites, and took peat samples for elemental analysis, inorganic content analysis, and laboratory bench-scale experiments quantifying fire dynamics and emissions (these field peat samples were used in experiments in Chapter 6 and 7). The sampling results indicate that peat properties are highly varied at different sampling sites with different peatland conditions both locally and globally. In general, samples from GAMBUT field sampling represent highly degraded peat with high inorganic content (23.6% - 71.2%), while samples from WINTERFELL field sampling represent peat conditions in natural peatland, drained peatland and peatland under restoration, which all have low inorganic content (2.5% - 5.4%), but have a great variation in bulk density (116 – 531 kg/m^3 in 100% moisture content). The difference in peat properties can significantly influence the fire dynamics. More research are needed to understand the effect of the complex field conditions on the ignition and spread of smouldering fires and the associated emissions, to prevent and mitigate wildfires on peatlands.

2.1 GAMBUT Field Sampling

The importance of tropical peatlands is increasingly recognised regarding to the amount of carbon storage and the role in regional and global environmental challenges. It is estimated that Indonesia has the largest tropical peat carbon pool in the world, which accounts for 65%

of the global tropical peat carbon [11]. Under the influence of climate change and anthropogenic factors, peatland fires have become a recurrent event in Indonesia during dry seasons, creating transboundary haze crisis in Southeast Asia and emitting massive greenhouse gases into the atmosphere. An example date back to 1997, the wildfires in forested peatlands in Indonesia released up to 2.57 gigatonnes of carbon into the atmosphere, which is equal to 40% of the average annual carbon emission from fossil fuels in the world [6]. Another example of peatland fires with similar severity in Indonesia shows the CO_2 release rate is 11.3 Tg per day from September to October in 2015, which is more than the average carbon emission from fossil fuels in the whole European Union [60]. Figure 2.1 shows an image from NASA taken on the 27th of September in 2015 showing the heavy smoke emitted from peatland fires in Sumatra and Borneo in Indonesia. Although these haze episodes have caused severe adverse influence to the environment and even threatened people's lives [31], the understanding of the fire dynamics and effects of the field-scale peatland fires are still very limited.

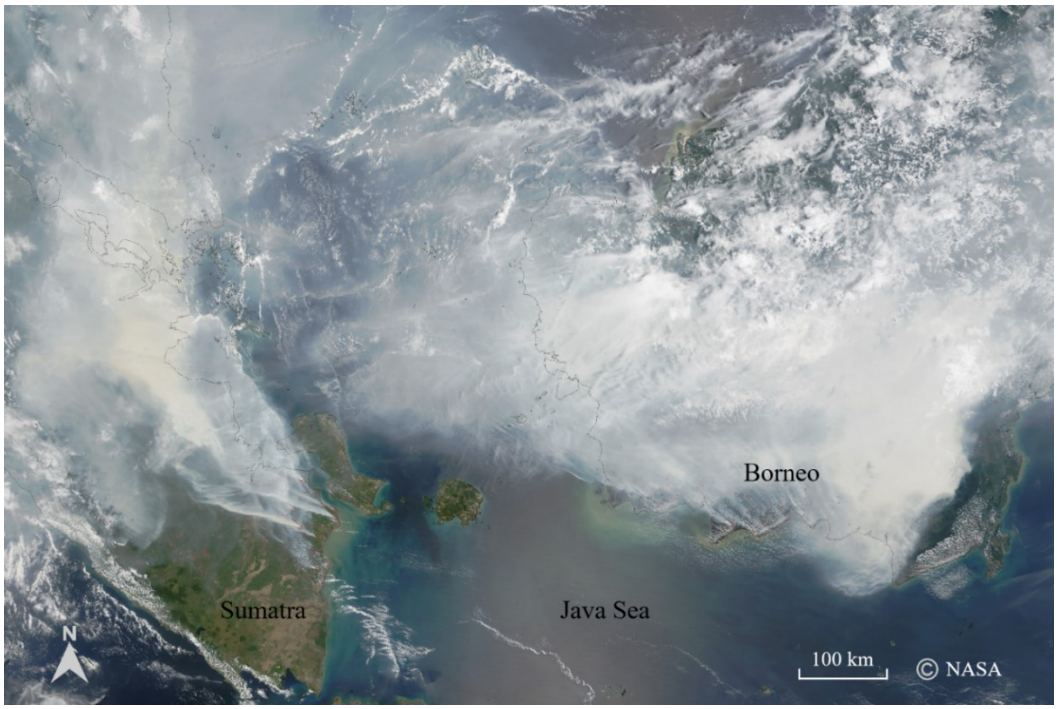

Figure 2.1 NASA satellite image shows the intensity of haze phenomenon by peatland fires in Indonesia on 27 September 2015.

GAMBUT (Gambut means peat in Indonesian) is the name of the largest to-date controlled smouldering peat fire field experiment conducted on peatlands (more details of this field campaign can be found in [66]). The site is located in Rokan Hilir, Riau Province, Sumatra, Indonesia (1°36'17.1"N 100°58'30.5"E) (Figure 2.2). From the 14th of August to the 1st of September in 2018, the experiments were conducted on a site of 400 m^2 tropical peatland (in degraded condition) to study the field-scale peatland fires. GAMBUT investigated the full life-cycle of peat fire dynamics, including ignition, spread, suppression, and emissions of the field-scale peat fires in the natural environment.

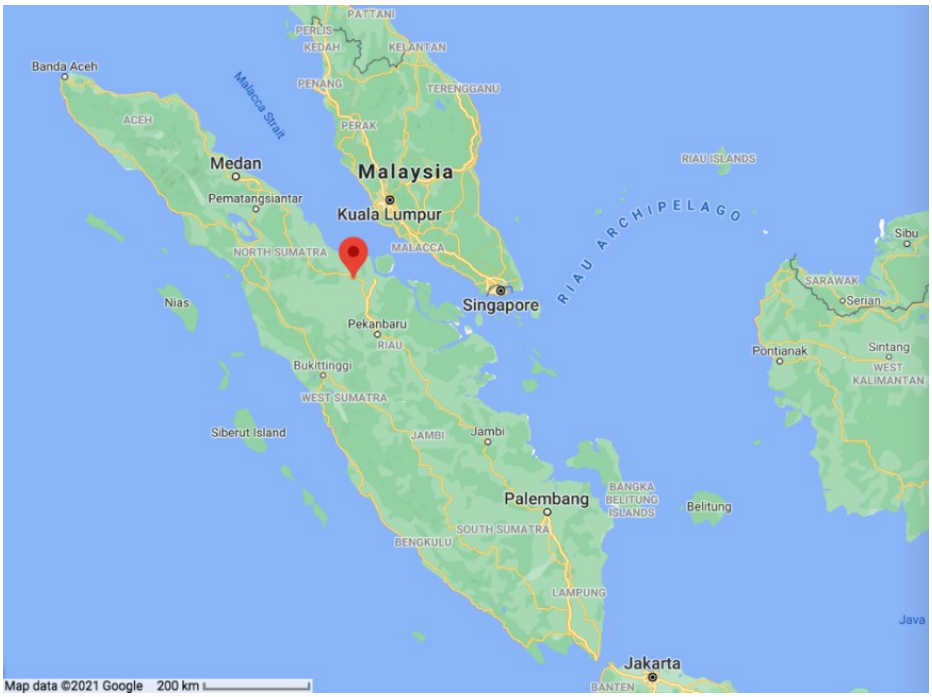

Figure 2.2 Map to show the location of the experiment site in Sumatra, Indonesia.

Site preparations were completed before ignition attempts started. The site of peatland was beside an artificial pond and originally covered by vegetation (e.g., palm trees, ferns and sedges). Four plots of peatlands with each plot in an area of 10 m by 10 m were prepared by cleaning the surface vegetation (Figure 2.3(a)). Plot 1 had the litter vegetation remaining on the surface, while Plot 2, 3 and 4 had all litter vegetation removed. Plot 4 was a backup plot,

which was not used at the end. Each plot was surrounded by sand-filled trenches (50 cm width by 50 cm depth) to control the spread of smouldering fire. The topography of the experimental plots was measured, which showed a significant elevation difference of up to 1 m between the north and south parts of the plots [66]. Site access was planned out of the plots to minimize the soil compaction made by people's steps. A tent was built at the east side of the plots and a weather station was installed at the north side of Plot 3. A suppression station was built between the pond and the plots for fire emergency and suppression study. Two ignition methods, charcoal ignition and slash-and-burn, were used to initiate the fire [66] (locations shown in Figure 2.3(b)). Smouldering fires initiated by charcoal ignition in Plot 1 and 3 sustained for 10 and 7 days, while in Plot 2 not self-sustained. Smouldering fires initiated by slash-and-burn in Plot 1 and 3 all sustained for 6 days, and in Plot 2 sustained for 4 days.

In this field experiment, I was mainly responsible for the peat soil sampling and field moisture content monitoring works. Sampling is an important procedure in field experiments to help understand the smouldering dynamics in the specific field soil conditions. Inorganic content (IC), moisture content (MC) and bulk density (BD) are the three most important soil properties which can greatly influence the fire dynamics [3]. IC and MC can perform as heat sinks absorbing energy generated and altering heat transfer. BD can play an important role in limiting oxygen supply and changing heat transfer. The main objective of sampling is to measure the IC, MC and BD of the peat soils in the experimental field and obtain field peat samples for laboratory studies.

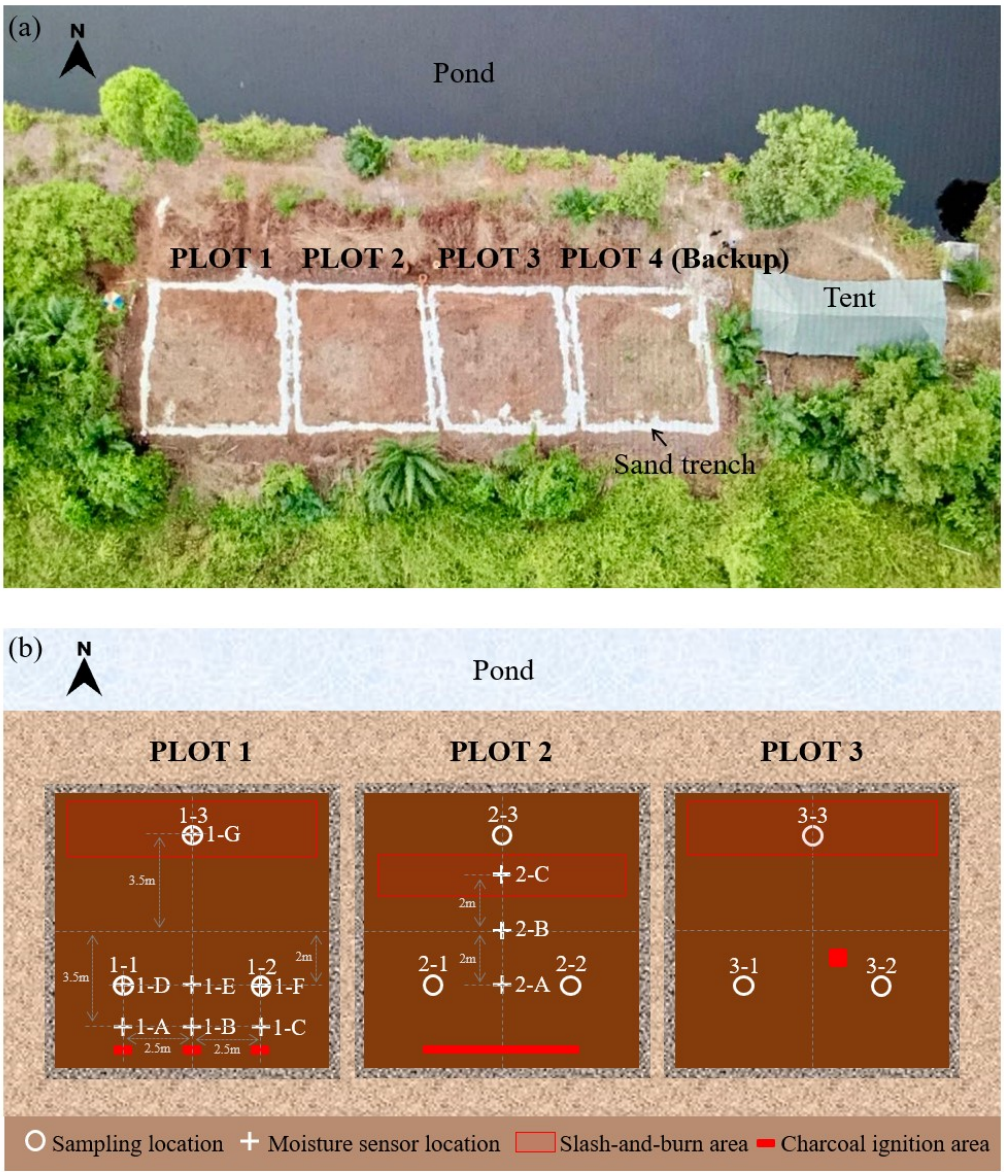

Figure 2.3 (a) Aerial view of the experimental site before ignition attempts (Photo Copyright: YS Nugroho). (b) Schematic of peat sampling, moisture sensor installation and ignition location in the experiment.

Before sampling started, a preliminary sampling was conducted at the west side out of the Plot 1 to estimate the depth of water table and the quality of the soil in this field of peatland. A Russian Corer was used to take core samples up to 1m depth (Figure 2.4(a)). From the measurement of core samples, it was estimated that the water table is around 0.7 – 1.0 m depth

from the surface. The peat soil condition above the water table close to the pond with lower elevation is much wetter than the condition at the south side of the plot with higher elevation.

Following the preliminary sampling and site topography survey, a sampling plan was made to take peat samples inside the plot. Figure 2.3(b) shows the sampling locations in all three plots. Three sampling locations were chosen in each plot with two locations at the south part and one location at the north part. The number of locations chosen at the south and the north was based on the estimation of flammability and the consideration of minimizing the disturbance of the field. The exact locations of sampling were considered not to overlap with the locations of geo-referencing plates and thermocouples (locations illustrated in [66]). Four sampling depth, 0 – 10 cm, 10 – 20 cm, 20 – 30 cm and 30 – 40 cm, were chosen at each location, which is based on the average depth of burn in peatland fires recorded in literature [10].

The measurement of BD and MC in situ were implemented simultaneously. Peat cores were taken by using four sections of PVC tubes, of which each section has a length of 10 cm and a diameter of 2.54 cm (Figure 2.4(b)). To minimize the compression from coring forces and dragging effects by soil fibers, a sharp long knife was used to cut the subterranean peat following the circle range of PVC tube on the surface of the sampling location before pushing the PVC tube down to the depth. Additional peat soils were removed behind the coring tube to leave a space to cut the bottom of the peat core and move the peat core out. The peat cores were weighed immediately for the record of wet bulk densities and sealed as samples for laboratory studies later. Since this is a destructive method taking samples directly from the experimental plots, to minimize the impact of this method, the sampling holes were filled by peat soils from the field outside of the plots and sampling locations were marked in analysis to identify if the sampling holes had a significant impact on fire dynamics. In addition, the volumetric moisture

content (VMC) of the soil at each depth was measured by using Delta-T SM150T soil moisture sensor (Figure 2.4(c)). This device was calibrated to measure the VMC with an accuracy of ±3% by detecting the variation of soil electrical conductivity. The probe of this device were inserted perpendicularly to the surface at the measuring depth before the samples were extracted. Three readings were taken at each depth.

Figure 2.4 Instruments used in peat soil sampling and moisture content monitoring in the experiment. (a) Russian corer, (b) PVC tubes, (c) Delta-T SM150T soil moisture sensor, (d) Arduino soil moisture monitoring system.

The sampling results of bulk density and moisture content are shown in Figure 2.5. The moisture content by dry mass was calculated by using the wet bulk density and the volumetric moisture content measured in the field. From the results, a significant variation is shown between the north and south part of the field plots. In general, the bulk density of peat in this field is very high, in the south part averagely ranging from 725 kg/m^3 at surface to 968 kg/m^3

at 40cm depth, and in the north part averagely ranging from 931 kg/m^3 at surface to 1450 kg/m^3 at 40cm depth. The comparison of the moisture content between the south and north part of the field plots shows in the south part the average values range from 20% at surface to 69% at 40cm depth, and in the north part the average range from 73% at surface to 334% at 40cm depth. The spatial distribution of the moisture content and bulk density can be because of the difference in elevation and the distance to the artificial pond. The north part of the plot is in lower elevation and closer to the pond, so the bulk densities at certain ranges and the moisture contents are all higher.

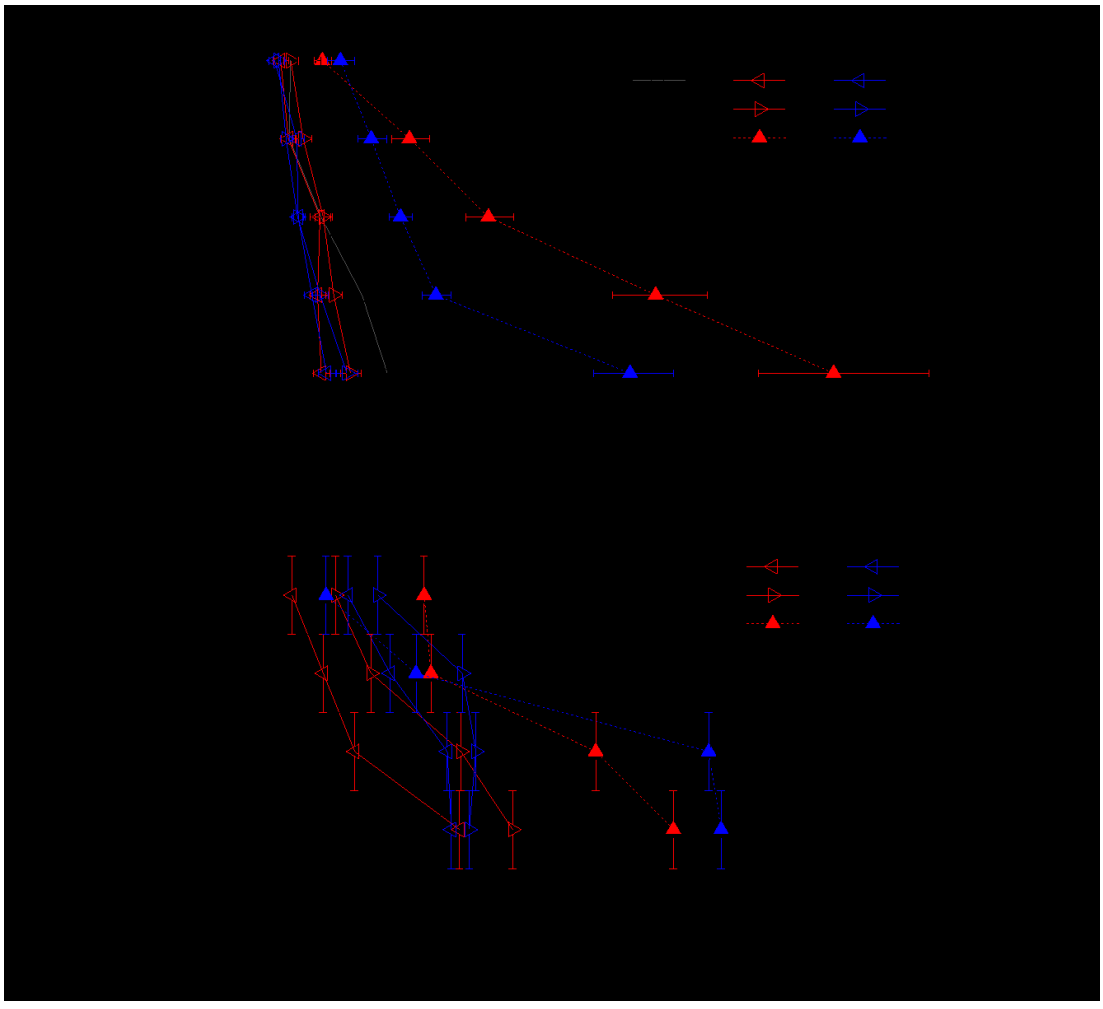

Figure 2.5 (a) Field sampling results of moisture content at different depth. (b) Field sampling results of bulk density at different depth.

As MC is considered to be the most important factor that influence the fire dynamics of smouldering in peat fires [26, 27], studying the real-time MC variation in peat under the influence of smouldering fire is of great importance not only in understanding the interaction of fire and soil, but also for developing a warning system of the smouldering fires underground. In laboratory studies, the MC of peat samples is usually controlled in sample preparation [26, 27, 42], while in the field experiments, the variation of peat MC in natural environment is complex and determined by many factors such as weather condition, water table and surface vegetation. There is no study conducting the MC live measurement in a peat fire (lab or field scale). A diagnostic apparatus monitoring soil moisture is essential to better understand the effect of smouldering fire on soil properties.

In this field experiment, a low-cost and efficient soil moisture monitoring system was built to implement in the plot and successfully captured the real-time MC variation in the soil under the influence of smouldering and suppression. The system was designed by using an open-source microcontroller and low-cost soil moisture sensors. Similar systems to monitor the soil MC are widely used in horticulture and agriculture [67]. The whole system shown in Figure 2.4(d) consisting of one microcontroller, one micro SD card module, one micro SD card and eight soil moisture sensors costs around £20.

The soil moisture sensors (YL-69) measure the soil electrical resistance between the two electrodes of the sensor, which is related to the soil VMC. The soil resistance decreases with increasing the VMC of the soil and vice versa. The comparator of the sensor activates a digital output in a predefined time interval (every one minute in this system) to the microcontroller according to the measurement of sensor. A low-cost open-source microcontroller, Arduino Uno, is programmed using the Arduino IDE through the USB interface to process data received from sensor measurements. In this system, all eight analogs

of Arduino Nano are designed to be used to control eight moisture sensors. Since the microcontroller is not able to store data, a micro SD card shield with a micro SD card is connected to the microcontroller for data collection. All these functions are programed onto the microcontroller for real-time soil moisture content monitoring.

The assembly of the system was based on the structure schematic shown in Figure 2.6. To protect the electronic components from the moist soil environment and extend the lifespan to a better ability, all the solder joints and SMD parts on the PCB of the moisture sensors to be buried in soil were coated by hot glue. The remaining part of the system consisting of the comparators of sensors, microcontroller and micro SD card module were all put into a grip seal bag and protected by a metal box covered by a rain cover in the field. The jumper wires connecting the moisture sensors and comparators were meters long according to the distance needed. Two types of power supply, power bank or field electric generator, were used to power the system according to the convenience of access in the field.

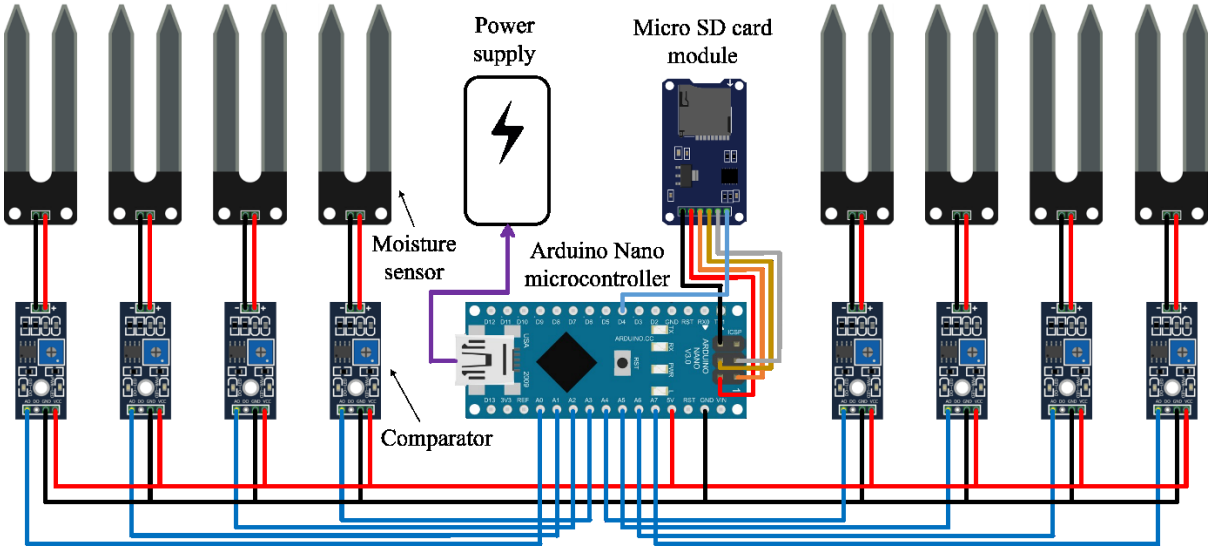

Figure 2.6 Electric diagram of the soil moisture monitoring system.

The Arduino soil moisture monitoring system was calibrated before using in the field by following the guidelines in [68]. Since the variation of soil at different location can influence the sensor signal obtained, before insert sensors at the designed position, Delta-T SM150T soil moisture sensor probe was used to measure the initial value of VMC at the position to validate the data.

The locations of live MC monitoring in the plot were designed according to the estimation of fire spread. Plot 1 and 2 were chosen to implement this system (locations shown in Figure 2.3(b)). In both plots, a location under the slash-and-burn area were chosen to study the influence of flaming fire and smouldering fire on the moisture variation of soil. In all locations, four moisture sensors were inserted into four depths (10cm, 20cm, 30cm and 40cm) to better monitor the spread of smouldering fire.

During this field experiment, the experimental plots experienced various weather conditions. From the data obtained from the weather station installed near the plots, the ambient temperature ranged from 21.6 to 35.9 ℃, and the ambient relative humidity ranged from 14.3 to 60%. There were two raining events with the averaged intensity to be 5.6 and 8.3 mm/h [66].

The moisture content monitoring system at location 2-C (under the slash-and-burn area in Plot 2, shown in Figure 2.3) captured the real-time moisture content variation from slash-and-burn ignition to all moisture sensors at all four depths failed due to the damage of high temperature. Figure 2.7 shows the results of the continuous soil moisture content measurement for nearly 72 hours. Comparing the moisture content variation when slash-and-burn ignition is applied (from time 0h) and smouldering propagates towards the location of moisture sensors (from time 30h), it is proven that flaming fire has a shallow and weak effect on the properties of the soil, which has been discussed in other literatures before [10, 18, 69]. Following the

slash-and-burn ignition, the soil moisture content from depth 10cm to 30cm decrease around 10% remarkably, but then at depth 20cm and 30cm increase promptly back to the previous level. Moisture content at depth 40cm is not severely influenced by the surface flaming (2% decrease). When the drying front of smouldering propagate through the location of sensors, the moisture content decrease dramatically to 0% (dry condition). Before smouldering reach the location of moisture sensors, the moisture content increase slowly which can be driven by the water migration from the adjacent soil in drying process of smouldering. At depth 40cm, a rally of moisture content is recorded from time 38h, which can be driven by the water migration from water table. From all these variations recorded, it is revealed that the peatlands have a natural protection regime to prevent the influence of fires [66]. Water balance is the most important component in this regime. Fire can break the balance and can only be sustained when the balance is broken.

From Figure 2.7, the downward spread rate of smouldering can be calculated following the drying process. The average spread rate from depth 10cm to 30cm is 0.89 cm/h and from depth 30cm to 40cm is 0.63 cm/h. These values agree with the spread rate values calculated from the temperature readings of thermocouples [66], and can be induced in the lower range of in-depth spread rate values recorded in the peat fire measurement in Central Kalimantan in the literature (0.5 to 6.5 cm/h) [70].

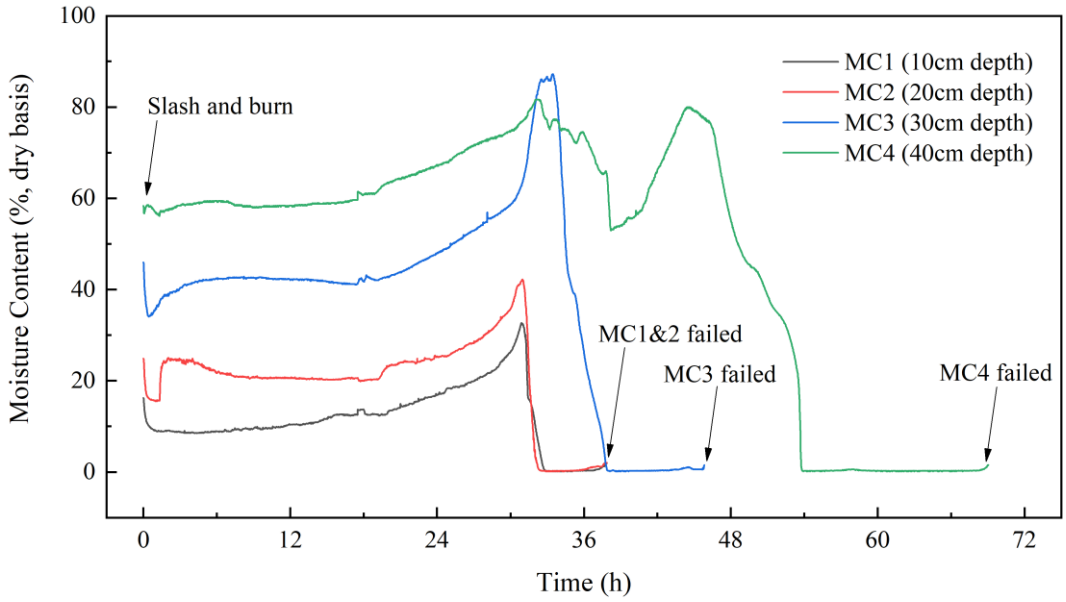

Figure 2.7 Real-time moisture content variation at location 2-C in Plot 2. MC failed means the smouldering front reached and burned the sensor to make the function failed.

The moisture content monitoring system at location 1-F (at the south part of Plot 1, shown in Figure 2.3) captured the real-time moisture content variation under the influence of smouldering spread and suppression. Figure 2.8 shows the results of the continuous soil moisture content measurement covering these influences for 72 hours and the start time (0h) in this figure is 72 hours after the slash-and-burn ignition in Plot 1. The slow increase of moisture content before smouldering front reaching the measuring locations and the rally of moisture content when smouldering propagating towards the measuring location at depth 40 cm mentioned in the analysis for location 2-C can also be found in this figure. In this location, horizontal spread of smouldering is captured when the moisture content decreasing dramatically. The values of moisture content at depth 20 cm and 30 cm drop to 0 earlier than the moisture content at depth 10 cm drop to around 10%. Evidenced by the site observation, this is due to the formation of overhang during the horizontal spread of smouldering leaving a certain depth of surface peat layer unburnt which collapses later (shown in Figure 2.9). The mechanism of overhang formation has been studied by laboratory experiments and

computational modelling in literatures [25]. According to the moisture content variation and site observation, smouldering did not reach the depth of 40 cm at this location which can be due to the shortage of oxygen penetration to the deeper layer and the close interaction with water table to maintain a certain level of moisture content. Because of the high density and inorganic content, peat soil at depth 20 cm and 30 cm are mostly charred with a small amount of ash produced at this location before suppression. From this figure, the values of soil moisture content increase dramatically above 100% when suppressions take place.

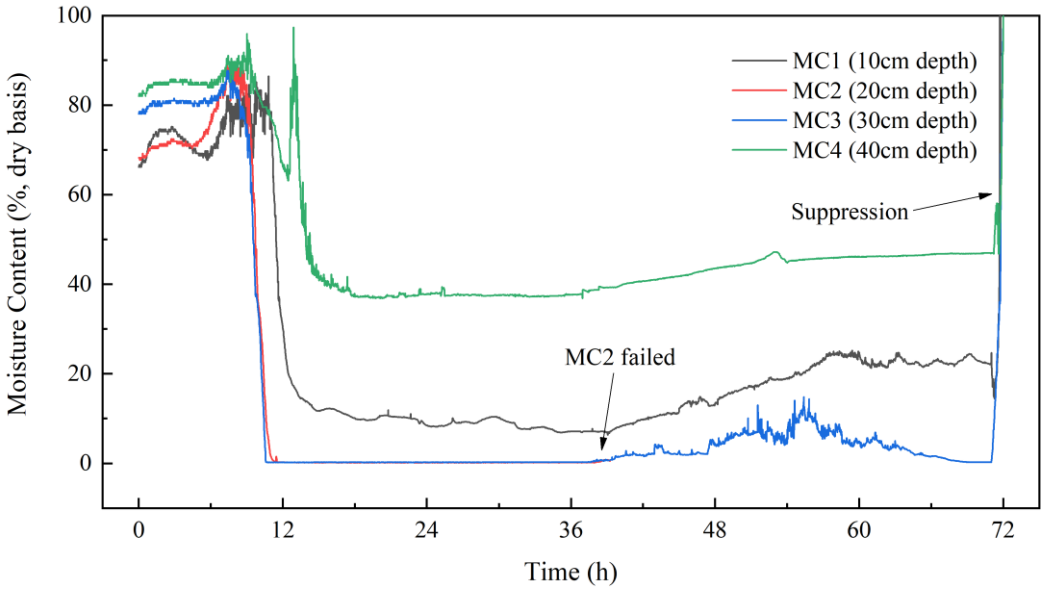

Figure 2.8 Real-time moisture content variation at location 1-F in Plot 1.

Figure 2.9 Site observation of overhang formation in smouldering propagation in Plot 1.

Following the sampling in the field in GAMBUT experiment, 36 peat samples from all three plots (three locations in each plot and four depths in each location) were shipped back to UK for laboratory studies. To measure the C/H/N content, selected samples were sent to Exeter Analytical (UK) Ltd. for elemental analysis. 27 tubes of dry samples (10g each) from three depths (0-10, 10-20, 20-30) in all sampling locations were selected according to the depth of burn measured at the end of the experiment. CE440 Elementa Analyzer were used for CHN analysis and every test had one duplicate test. The results of elemental analysis are shown in Table 2.1.

Representative samples were selected for inorganic content measurement in the lab by using Loss on Ignition (LoI) method. In this measurement, selected samples were dried first in an oven with 80 °C on set for more than 48 hours. Then the dry samples were heated in a furnace with temperature set at 1000°C until no mass loss. With the mass of remaining ash over the original dry mass, inorganic content of the peat samples can be obtained (results shown in Table 2.1).

From the results of elemental analysis, the average mass fraction of C/H/N of peat samples from the north and south part of the plots are 29.2±5.9%/6.8±4.9%/1.1±0.4% and 20.7±5.6%/2.7±1.3%/0.6±0.2%. Comparing to the analysis of commercial peat samples and other tropical peat samples which have more than 50% of carbon content in literature [7], the peat in the field experiment with much lower carbon content represents a highly degraded peat quality. The high inorganic content of the peat with an averaged value of 52.7 ± 11.6 % can also further prove it.

Table 2.1 Results of elemental content and inorganic content analysis of GAMBUT field peat samples

Plot	Location	Depth (cm)	Elemental analysis			Inorganic content (%)
			C (%)	H (%)	N (%)	
1	North (1-3)	0 - 10	33.73	3.20	0.88	44.8
		10 - 20	30.73	16.46	0.82	23.6
		20 - 30	25.97	10.21	0.62	
	South (1-1&1-2)	0 - 10	21.94	2.43	0.57	63.5
		10 - 20	23.81	2.48	0.55	57.6
		20 - 30	26.05	2.11	2.51	54.9
2	North (2-3)	0 - 10	22.56	3.86	0.69	49.5
		10 - 20	34.77	6.34	1.69	
		20 - 30	36.56	6.67	1.53	38.4
	South (2-1&2-2)	0 - 10	22.37	2.66	0.63	53.2
		10 - 20	17.89	3.46	0.50	
		20 - 30	24.76	5.39	0.74	53.5
3	North (3-3)	0 - 10	23.22	2.66	1.09	49.8
		10 - 20	32.92	3.38	1.57	
		20 - 30	22.21	8.34	0.61	55.0
	South (3-1&3-2)	0 - 10	17.19	1.81	0.49	71.2
		10 - 20	14.20	1.53	0.40	
		20 - 30	17.98	1.96	0.46	62.3

2.2 WINTERFELL Field Sampling

Northern peatlands have an important role in maintaining the global carbon cycle and store an estimated one third of the global terrestrial carbon [8]. Different with the formation process of tropical peat which mainly origin from trees in rainforests and form under a nearly constant high temperature environment, northern peatlands are mainly formed from bryophytes experiencing low temperatures in winter and high water tables with reduced decomposition

rate. As a consequence of the continuous climate change, northern peatlands are more vulnerable to fires in frequency and severity due to drier soil and increasing global atmospheric temperature [71]. Although peatlands in UK account for a relatively small portion of northern peatlands, they are nationally and internationally important and more vulnerable because of the unique variable maritime climate comparing with the continental climate of peatlands formed in areas such as Canada and Siberia [72]. Scotland holds the majority of peatlands in UK and the blanket bog peat in Flow Country is estimated to be the largest single expanse in Europe, and possibly in the world (Figure 2.10) [73]. In recent years, the peatland nature reserve in Flow Country is in application for UNESCO World Heritage Site because of the unparalleled blanket peat ecosystem, while one of the largest peat restoration project is ongoing to increase the resilience of peatlands to withstand more challenges in future.

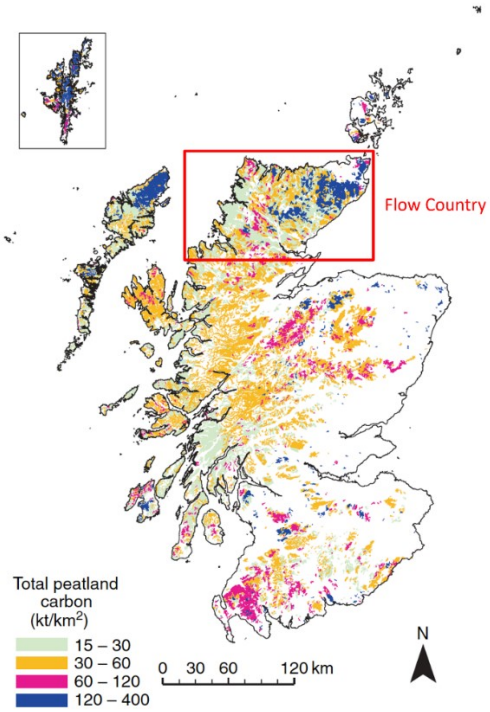

Figure 2.10 Peatland carbon stocks in Scotland (figure reproduced from [8]).

From 12 May 2019 to 17 May 2019, an active wildfire in Flow country burned around 53.8 km^2 of peatland (Figure 2.11), which is one of the largest peatland fires recorded in recent

years in UK. The effect of this peatland fire in ecology and the process of recovery is under investigation. It is also very important to understand the fire dynamics and fire emissions of this peatland fire. In collaboration with the Environmental Research Institute in the University of Highlands and Islands, we conducted a field study six months after the wildfire event in fire affected areas with peat sampling in adjacent unaffected peatlands in Flow Country, and planned to conduct experiments in lab-scale by using field samples to quantify the fire dynamics and emissions.

Figure 2.11 A satellite image of the peatland fires in Flow Country on 16 May 2019.

The field visit was in mid-November when winter is coming in the northernmost region in UK of which the scenes remind us the north region in the famous TV series Game of Thrones, so we name this field study WINTERFELL. In this field study I acted as a team leader, spending four days in Flow Country with three other colleagues, Eirik G. Christensen, Muhammed Agung Santoso and Dwi Marhaendro Jati Purnomo, to visit the post-fire sites and take peat samples under the guidance of Prof. Roxane Andersen, a senior research fellow from

the Environmental Research Institute in the University of Highlands and Islands, who also leads a research project studying the peatland resilience and has a wealth of knowledge in peatland ecology and peatland fires happened in Flow Country.

The climate in Flow Country is very important for the formation of peatlands, and climate change is influencing the fire severity in this area. According to the climate history in Forsinard, this area in general has a cool and wet climate condition. According to the weather records in 2019 from the Met office, the average daily relative humidity for the whole year is around 81% which represents a high atmospheric humidity. The precipitation is a combination of high and regular conditions of which the average monthly amount of precipitation from October to February is above 100 mm and from May to August is below 60 mm. This area has relatively cool mean temperatures. In winter from December to February the daily average maximum temperature is 6 °C with the average minimum -1 °C, while in summer from June to August the average maximum is 17 °C with a minimum of 8 °C. In recent years the highest temperature in record in summer is around 30 °C.

During the wildfire event in May, the fire spread from the peatland area close to Melvich on the north coast to the Forsinard Flows Nature Reserve in the central area of the Flow Country (Figure 2.12). The burned area extends across peatlands with different conditions: peatland in natural condition, drained peatland, and peatland under restoration. Three sampling sites were chosen based on the peatland conditions and the distances between the sampling locations and burned areas in same conditions before the wildfire event were within 200 m, so the peat samples taken from these locations can represent the peatlands burned with different conditions in the fire event. Lab experiments are designed by burning these peat samples in the emission rig [39] and measuring temperature, burning rate, infrared and visual signature, and gaseous and particle emissions. These lab-scale experiments make possible the estimation of

the ignition probability, spread rate and emissions. Then these experimental results can be used to compare the fire dynamics of peat samples from different field conditions to better understand the fire severity and emission in field scale. Three sampling locations are named by using three letters that can represent the peatland conditions: NAT (samples from peatland in natural conditions), DRA (samples from drained peatland), and RES (samples from peatland under restoration). Figure 2.12 shows the general landscape and detailed surface condition of the three sampling sites.

The samples from NAT and RES were both collected in the RSPB's Forsinard Flows National Nature Reserve, part of the Flow Country peatlands of Caithness and Sutherland. NAT samples were collected approximately 200 m south of the fire scar in an area locally referred to as the "Uair" (58°25'9.99"N, 3°59'44.58"W), representing near-natural condition. The area includes a network of well-developed pool systems with a bryophyte cover dominated by Sphagnum sp. (S. capillifolium, S. austinii, S. cuspidatum, S. medium, S. papillosum), red-stem moss (Pleurozium shreberi) and wolly fringe-moss (Racomitrium lanuginosum) and a vascular cover dominated by the cross-leave heath (Erica tetralix), common heather (Calluna vulgaris) as well as sedges including common cottongrass (Eriophorum angustifolium), common cottongrass (E. vaginatum) and deer grass (Tricophorum cespitosum). The area is managed for conservation and has low-level grazing by red deer.

RES samples were also collected approximately 200m south of the fire scar, this time in an area locally referred to as the "Dyke plantation" (58°25'40.06"N 3°59'16.98"W). This area of deep peat was planted with non-native conifers Lodgepole pine and Sitka spruce in the 1980s as part of a controversial tax incentive scheme [74]. The afforestation has caused significant damage to peatlands [75], notably significant dewatering and compaction of the peat [76], as well as loss of typical bog vegetation [77]. Large areas of afforested peatlands

have been undergoing restoration since the late 1990s, and in 2017-18, the area around RES, including the area that burned, was targeted by the first step of a large-scale "forest-to-bog" restoration intervention: the extraction of timber. The area was due to be re-wetted with a combination of drain blocking and re-profiling to eliminate the microtopographic features created by the planting (plough throw ridges and furrows), but these interventions were delayed because of the 2019 fire. As such, at the time of sampling RES was still be considered a degraded area but one that was actively managed, and therefore "under restoration". The samples were taken on the "original surface" of the bog, (avoiding the furrows and plough throw ridges) where only a sparse cover of mosses (bog haircap moss, Polytrichum strictum and red-stem moss, Pleurozium shreberi), common heather (Calluna vulgaris) and hares-tail cotton grass (E. vaginatum) can be found.

Site DRA is located close to the north coast by the road A836 around 2 km west of Melvich (58°33'31.20"N 3°58'28.33"W) within an area where peat has historically been hand cut for fuel and drained in the early 20th century in an unsuccessful initiative to turn this area into a more productive land. The area was also rotationally burned in the past and is still used for grazing cattle and sheep. The long history of degradation and drainage in this area has led to increased compaction of the peat and dominance of heather (Calluna vulgaris), with the peat generally thinner (~0.3 – 1 m). An access track to the Strathy North windfarm intersects the wider area and acted as a fire break during the fire event in May 2019, with the east side of the track severely impacted, and the west side where samples were taken unburnt but otherwise similar.

Figure 2.12 Sampling site location and condition in WINTERFELL field study. The image (from Google Map) on the left shows the location of three sampling sites (NAT, DRA, RES). The photos in the middle column show the general landscape of the three sampling sites, and on the right column show detailed surface conditions of the three sampling locations.

There are two objectives for peat sampling, understanding the physical and chemical conditions of peat in the field and obtaining enough peat samples for lab experiments. A Russian Corer was used to take peat samples from the field. Samples at three depth ranges, 0 – 10 cm, 10 – 20 cm and 20 – 30 cm, were taken at all three sites, which is based on the average depth of burn in the peatland fires in May. Samples were stored and labelled in Lock & Lock storage containers. Mini peat cores were taken at three depths, 10cm, 20 cm and 30 cm, by using a cylindrical container with a very thin metal wall, which has a length of 6.95 cm and a diameter of 5.25 cm. These mini peat cores (in total 9 samples) were sealed separately in grip seal bags to preserve the moisture content and shipped back to the lab in London with samples in containers for laboratory studies.

When receiving peat samples in the lab, peat samples of the nine mini peat cores were put in aluminium trays separately for drying in an oven with the temperature set to 80 °C. The initial mass of these samples and the mass after drying (until no mass loss) were recorded to calculate the wet bulk density ($\rho_{f,w}$, mass of wet sample divided by the volume of the sample), dry bulk density ($\rho_{f,d}$, mass of dry peat in sample divided by the volume of the sample), and moisture content (MC_f, by dry mass). All these sampling results represent the physical condition of peat soil in November when precipitation level is high. From the results shown in Figure 2.13, the moisture content of peat samples at site NAT is much higher than the ones at site DRA and RES, which indicates the peatlands at site NAT is in a healthy water condition. The peatlands at site RES were drained before for plantation, but the hydrological condition of the peat is improving when restoration started. The moisture content of the peat at site DRA is the lowest and can be much lower in summer with less precipitation, which has a higher probability to be affected by fire events. From the results of bulk density, peatlands at site DRA and RES have higher density than the peatland at site NAT, which can prove the effect of consolidation and compression of drainage in peatlands.

The C/H/N contents of the peat samples were measured by Exeter Analytical (UK) Ltd. Nine tubes of dry samples (10g each) from three depths (0-10, 10-20, 20-30) in all three sampling locations were analysed by using CE440 Elementa Analyzer and every test had one duplicate test. Regarding to the results of elemental analysis shown in Figure 2.13, these peat samples have high combustibility when moisture content is low. The inorganic contents were measured in the lab by using the LoI method introduced in 2.1. The results shows the inorganic content of all these samples are very low, which indicates these samples are very easy to ignite when moisture content is low [26].

All these nine samples were dried naturally in room temperature of laboratory environment to 100% moisture content (by dry mass) for smouldering experiments. As all samples from the field were sealed when they were taken from the peatlands, the original moisture contents of all samples can be obtained by drying 50 g sub-samples. With the original mass and moisture content, the targeted sample mass in 100% moisture content can be calculated. In the drying process, each type of sample were mixed everyday to make the moisture content homogenous. The wet bulk density ($\rho_{l,w}$) and dry bulk density ($\rho_{l,d}$) of these samples in 100% moisture content are also shown in Figure 2.13. The sample properties show the dry bulk density and decomposition rate (color of the peat profile) increase with the depth, and the dry bulk density at the same depth range increases in the order of NAT, RES and DRA.

Type	Depth (cm)	C / H / N (%)	IC (%)	MC_f (%)	$\rho_{f,w}$ / $\rho_{f,d}$ (kg/m^3)	$\rho_{l,w}$ / $\rho_{l,d}$ (kg/m^3)	Peat Profile 2 cm
NAT	0-10	44.0/5.3/0.8	3.8	1149	540 / 43	116 / 58	
	10-20	42.0/5.1/0.5	3.5	1880	527 / 27	186 / 93	
	20-30	45.5/5.5/1.2	2.5	1898	611 / 31	240 / 120	
DRA	0-10	45.5/5.2/1.2	5.4	316	769 / 185	262 / 131	
	10-20	51.7/6.3/1.2	4.8	218	961 / 303	445 / 222	
	20-30	56.3/5.9/0.9	5.3	377	882 / 185	531 / 266	
RES	0-10	46.7/5.3/1.4	4.9	724	920 / 112	213 / 106	
	10-20	50.3/6.3/2.1	3.1	606	849 / 120	220 / 110	
	20-30	54.0/6.6/1.8	3.8	558	906 / 138	400 / 200	

Figure 2.13 Results of the physical and chemical analysis of WINTERFELL peat samples. MC_f represents the moisture content measured in the field. $\rho_{f,w}$ and $\rho_{f,d}$ are the wet and dry bulk density measured in the field. As all these peat samples were conditioned to 100% moisture content for laboratory experiments, $\rho_{l,w}$ and $\rho_{l,d}$ are the wet and dry bulk density measured in the lab in 100% moisture content.

Chapter 3

Experimental Methodology

Summary

This chapter describes the main experimental methodology used in this thesis, including peat sample preparation, laboratory experimental set-up, and the method of analysing fire spread and emissions. This thesis studied peat samples of different origins of which the characterisation and preparation methods were introduced. The bench-scale experimental rig to study the fire dynamics and emissions of these peat samples were described along with the diagnostics of mass loss, temperature profile, IR and visual images, and gas and particle emissions. These experimental methods are used in Chapter 4 – 8. This chapter also introduced the methods of calculating the horizontal and in-depth spread based on our experimental set-up, and the correlation with heat sink density and organic density. The methods of quantifying gas and particle emissions, including the calculation methods of emission ratio (ER), modified combustion efficiency (MCE), and emission factor (EF), were also introduced.

3.1 Sample Preparation and Characterization

In previous laboratory peat fire studies, horticultural peat which is mainly used as a soil improver in horticulture is the most commonly used peat [15, 19, 23, 25, 27, 42, 78, 79]. This type of peat is commercially available with good consistency between bags and already processed by peat mining company to a relatively uniform condition in soil properties, which is suitable for studying the fundamental parameters under controlled conditions and can meet the need of experimental repeats [24]. Some studies used peat samples taken from the field [18, 80-82], which has more complexities in soil properties but close to the natural conditions. Field peat sample is more challenging to obtain and limited in quantity, which also has issues of transportation and time. Studying field peat samples is meaningful and necessary in linking the lab experiments with field measurements. Figure 3.1 shows the general features of horticultural

peat and field peat. In this thesis, both horticultural peat and field peat samples were studied in smouldering experiments. Table 3.1 shows the physical and chemical properties of the peat samples of different origins. In the names of these peat samples, (H) represents horticultural peat and (F) represents field peat.

Figure 3.1 Photos of horticultural peat and field peat samples.

In this thesis, five types of horticultural peat were studied in smouldering experiments. The packages of these samples all wrote sphagnum moss peat, which indicate these horticultural peat were sampled in peatlands with sphagnum moss as dominant forming vegetation. Irish 2020 (H) was the most used peat sample in this thesis (Chapter 4, 5, and 8). It is a type of Irish horticultural peat which is commercially available from Bord na Mona Horticulture Ltd. Irish 2020 (H) was purchased from the same horticultural peat company of the previous Irish horticultural peat, Irish 2018 (H), which was used in many previous studies [15, 42, 78] and this thesis (Chapter 7). Both Irish 2020 (H) and Irish 2018 (H) were mined in peatlands in Irland, but Irish 2020 (H) has naturally higher inorganic content (5.1% vs 2.5%) and bulk density (shown in Figure 3.2) than Irish 2018 (H). The third type of horticultural peat used in this thesis (Chapter 7) is Canadian (H) which was mined in peatlands in Canada by Hoffman Horticulture Ltd. Canadian (H) has the lowest bulk density (shown in Figure 3.2) in all horticultural peat used in this thesis. The last two types of horticultural peat are from

peatlands in Latvia named as Latvian Black (H) and Latvian White (H) with “black” and “white” representing the dark and light color, and also high and low decomposition rates. These two types of peat samples sent by Hortimed Horticulture Ltd. are commercially available for large orders, but in this thesis (Chapter 7) we only used the requested trial samples which were enough to do one set of smouldering experiment each.

The sample preparation for smouldering experiments followed the previous protocol [24, 25, 42] by drying the raw peat at a fixed temperature of 80 ℃ until no further mass loss, then conditioning the dry peat to targeted moisture content, and sealing it for at least 48 hours before experiments. Figure 3.2 shows the bulk density values of Irish 2020 (H), Irish 2018 (H), and Canadian (H) from dry condition to 200% moisture content. The dry bulk density values show these peat samples expand significantly when increasing moisture content from dry condition to 100% moisture content, and maintain at a relatively stable dry bulk density when increasing moisture content from 100% moisture content to 200% moisture content. The turning point of moisture content at which peat does not expand when absorbing more water can be different in different types of peat, but in these three types of horticultural peat it is around 100% moisture content. This observation is very important in explaining the effect of moisture content on smouldering dynamics, since from dry condition to around 100% moisture content in these types of peat, the effect of moisture content includes the heat sink effect of water in drying process and the volume expansion effect decreasing the density of organic content to burn, while from around 100% moisture content to higher moisture content, the heat sink effect dominates the effect of moisture content on fire dynamics.

The range of bulk density values of Canadian (H) (the lowest) and Irish 2020 (H) (the highest) covers the range of horticultural peat used in other studies [25, 27, 79]. The range of moisture content in Figure 3.2 did not include moisture content above 200% because the

experimental results in this thesis shows the critical moisture content for Irish 2020 (H), Irish 2018 (H), and Canadian (H) are 160%, 200%, and 180%, which are introduced in Chapter 4 and 7.

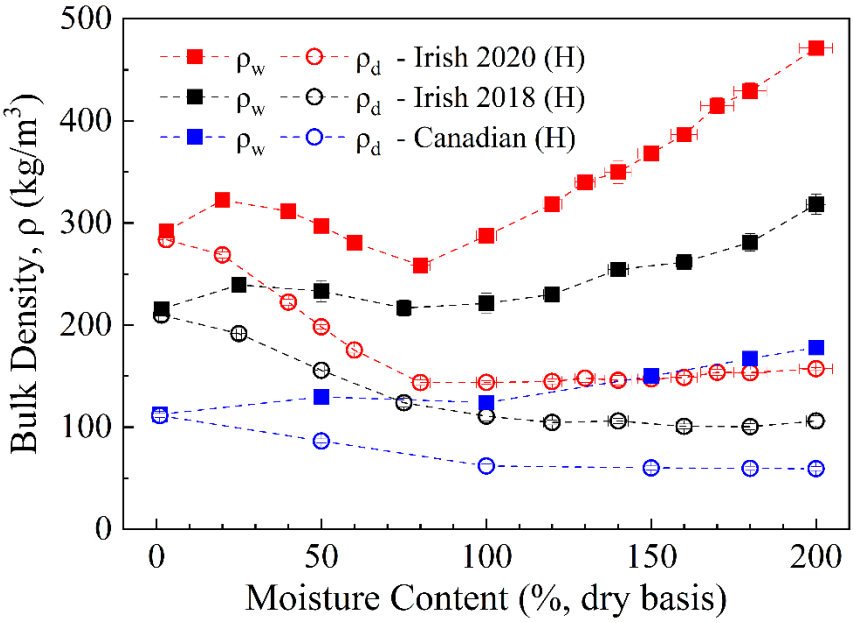

Figure 3.2 Measurements of the moisture content and bulk density of horticultural peat samples of Irish 2020 (H), Irish 2018 (H), and Canadian (H). These horticultural peat samples are commercially available and efficient for repeat experiments. The data of Irish 2020 (H) (5 repeats for each moisture content below 100% and more than 10 repeats for each moisture content above 100%) and Canadian (H) (3 repeats for each moisture content) are from this thesis. The data of Irish 2018 (H) is the average of previous works (3 repeats for each moisture content) [42] and works presented in Chapter 7 (3 repeats for 100% and 200% moisture content). Each point shows the averaged value and the standard deviation of moisture content and bulk density are all included in this figure. Wet bulk density (ρ_w) is the mass of wet peat sample divided by the volume of sample. Dry bulk density (ρ_d) is the mass of dry peat in sample divided by the volume of sample. The initial mass of sample is measured in reactor before each experiment to estimate the bulk density.

Apart from horticultural peat samples, field peat samples from Indonesia and Scotland were also studied in this thesis. Chapter 2 has introduced the field peat sampling and characterization process for samples taken from the GAMBUT field experiment in Indonesia and WINTERFELL field study in Scotland. The nine field peat samples (naturally dried to 100% moisture content) from WINTERFELL field study presented in Figure 2.10 were studied in Chapter 6. Most of the WINTERFELL samples were only enough to conduct one smouldering experiment except samples from site DRA at the depth range of 0 - 20 cm and 20 – 30 cm (named as Scottish DRA0-20 (F) and Scottish DRA20-30 (F) in Table 3.1), which were enough to do another experiment (presented in Chapter 7). There are two types of Indonesia field peat studied in Chapter 8 (properties summarised in Table 3.1). One is the sample from GAMBUT field experiment in Sumatra named as Indonesian GAMBUT (F). Another sample named as Indonesian Palangkaraya (F) was collected by the research team of Prof. Yulianto Sulistyo Nugroho from the University of Indonesia in a drained peatland from the depth range of 0 – 30 cm in Palangkaraya, Central Kalimantan, Indonesia. Indonesian Palangkaraya (F) had enough samples for four smouldering experiments. From the summary of sample properties in Table 3.1, the inorganic content of these peat samples are lower than 7% except Indonesian GAMBUT (F) which is over 50% representing a highly degraded condition.

The bulk density of these peat samples can cover a large range, which is important in studying how the natural variations in bulk density influence the smouldering dynamics and emissions. As one of the most important usage of horticultural peat is for improving the soil structure to allow roots to breathe, the sample has to be porous enough with less consolidation, thus horticultural peat samples are always in low bulk density. However, in the natural field conditions, the bulk density of peat has a larger variation. The dry bulk density can be as low as 4 kg/m^3 (in 105% moisture content) [80], but can be much higher in some peatlands, for example, peatlands experienced long-term drainage and peat at deeper region with high

decomposition rate [24]. These peatlands with peat in high bulk density has much higher carbon density and more vulnerable to wildfires when they are in low moisture content. In this study, the dry bulk density of Indonesian Palangkaraya (F) and Scottish DRA20-30 (F) in dry condition can reach as high as 475.7 and 520.0 kg/m^3, which are all at the high limit comparing to literature values [25, 27, 79]. In all research studying smouldering peat fires, the only work found using high bulk density peat is the work of smouldering characteristics of Brazilian field peat which has an averaged dry bulk density of 468.5 kg/m^3 (dry condition) [82]. As most of the previous research conducted smouldering experiments using low bulk density peat (dry bulk density lower than 250 kg/m^3 in dry condition), it is important to conduct research to investigate if high bulk density peat burn differently in smouldering experiments.

Table 3.1 Physical and chemical properties of peat samples used in Chapter 7

Peat Type	Elemental Analysis (%)			IC (%)	Dry Bulk Density (kg/m^3)		
	C	H	N		MC=1%	MC=50%	MC=100%
Irish 2020 (H)	50.21 ±1.36	5.14 ±0.18	1.65 ±0.82	5.10 ±0.60	283.7 ±5.6	198.2 ±2.2	143.7 ±1.8
Irish 2018 (H)	54.10 ±0.46	5.11 ±0.09	1.30 ±0.10	2.50 ±0.60	209.6 ±5.8	155.5 ±6.9	110.7 ±5.0
Canadian (H)	47.56 ±1.52	5.94 ±0.04	0.65 ±0.03	2.80 ±0.05	111.4 ±2.0	86.4 ±2.0	62.0 ±3.0
Latvian Black (H)	48.55 ±1.99	5.64 ±0.35	1.02 ±0.78	3.66 ±0.60	234.6 ±6.0	171.3 ±7.0	121.5 ±5.0
Latvian White (H)	48.60 ±0.27	5.89 ±0.03	0.71 ±0.25	3.06 ±0.60	127.3 ±6.0	98.0 ±7.0	70.4 ±5.0
Indonesian Palangkaraya (F)	51.19 ±7.49	4.04 ±0.56	1.15 ±0.17	6.12 ±0.17	475.7 ±8.0	306.6 ±10.9	278.4 ±10.0
Indonesian GAMBUT (F)	23.09 ±1.02	2.66 ±0.13	0.63 ±0.06	53.2 ±3.11	527.8 ±10.0	412.5 ±10.0	258.5 ±6.7
Scottish DRA0-20 (F)	52.42 ±0.71	6.17 ±0.13	1.40 ±0.01	3.14 ±0.60	370.0 ±8.0	251.6 ±11.0	192.4 ±10.0
Scottish DRA20-30 (F)	56.34 ±1.44	5.85 ±0.40	0.87 ±0.01	5.30 ±0.60	520.0 ±8.0	380.0 ±11.0	265.5 ±10.0

MC=1% represents oven-dried peat, because it is not possible to have samples dried to 0% since dry peat absorbs moisture in the air once exposed to the ambient environment.

3.2 Experimental Setup

Most of the experiments in this thesis were conducted using the emission rig developed in previous research [39]. This experimental rig was designed to investigate peat fire dynamics and emissions. Figure 3.3 shows the schematic of the emission rig. In this setup, an emission hood connected with a duct to an adjustable fan can collect smoke produced by controlled peat fire. The setup was calibrated to set the duct center-line flow rate to 2 m s^{-1} and the skirt free height (the distance between the hood and the reactor) to be 2 cm [39]. This allows the smoke produced to be completely collected in the hood and well mixed in the duct, while the impact of experimental setup to fire dynamics can be reduced to the minimum (the impact of fan on the experimental results is discussed in section 5.2).

The other experimental setup used in Chapter 8 did not use the emission hood to collect emission gases and particles. The smoke released by smouldering peat was naturally diluted inside the combustion fume hood (1.2 × 1.2 × 3 m^3) connecting to exhaust. The averaged velocity across the section of the fume hood is 0.6 m s^{-1}. A metal structure was built to lift diagnostic devices if they need to be at a certain height.

All experiments in this thesis used horizontal reactor which was designed to study the horizontal spread of smouldering peat (design details are introduced in [24]). Figure 3.3 shows a section view of this reactor. This open-top reactor has an internal dimension of 20 × 20 × 10 cm, built by mineral fibre boards, which is in consistent with previous works [25, 39]. The ignitor is a metal coil with a length of 18 cm and an outer helical diameter of 1 cm fixed at one side board of the reactor (5 cm from the open-top). At the ignition stage, the ignition coil had a constant power supply of 100 W, and was turned off when the sample had 10% mass loss.

This is a new ignition protocol developed in this thesis based on mass loss, which is introduced in Chapter 4.

To monitor the fire dynamics, a mass balance (Mettler Toledo, resolution 0.01g, frequency 0.1 Hz) was used to record the real time mass loss in the burning process. Twelve thermocouples (K-type, frequency 0.1 Hz) were inserted into the reactor in three depths (positions shown in Figure 3.3) to measure the temperature profile during smouldering propagation. Gopro and FLIR camera were installed to record the visual and infrared signature of the experiments (in this thesis Gopro and FLIR images are only used in monitoring the experimental progress and assisting as visual evidence to explain the results). These four diagnostics were used in all experiments in all chapters of this thesis.

To measure the fire emissions, Fourier-transform infrared (FTIR) spectroscopy (Thermo Scientific Nicolet iG50) was used to measure emission gases, and Dekati 4-stage PM cascade impactor was used to collect size-fractioned particles ($D \leq 1$ μm, 1 μm $\leq D \leq 2.5$ μm, 2.5 μm $\leq D \leq 10$ μm, $D \geq 10$ μm) onto the filters in each of the stages of the cascade impactor. The FTIR used in this research was calibrated by previous studies [39, 42], and can measure 20 different gas species which are commonly reported in peat fire studies: carbon dioxide (CO_2), carbon monoxide (CO), methane (CH_4), acetylene (C_2H_2), ethylene (C_2H_4), ethane (C_2H_6), propylene (C_3H_6), propane (C_3H_8), butane (C_4H_{10}), methanol (CH_3OH), formaldehyde (CH_2O), nitric oxide (NO as NO_x), nitrogen dioxide (NO_2), hydrogen cyanide (HCN), acetic acid (CH_3COOH), acetaldehyde (C_2H_4O), formic acid (CH_2O_2), hydrogen chloride (HCl), ammonia (NH_3), and sulphur dioxide (SO_2).

The operation of PM cascade impactor followed the protocol of previous research [28, 39, 42] to set the sampling flow rate to be 0.0005 $m^3\ s^{-1}$ ± 5.0% by adjusting the setup of the

pump (leading to an accuracy of ± 2.8% for the size of particles). The sampling duration was 10 min each time, and the filters were weighed immediately after sampling by using a Sartorius balance (resolution 0.01 mg). The PM1, PM2.5 and PM10 were calculated by the measured mass gain of filters at each stage of the impactor.

Apart from FTIR and PM cascade impactor, in Chapter 8 we calibrated another research-grade device DustTrak DRX aerosol monitor which can provide real-time mass fraction concentrations including PM1, PM2.5 and PM10 for measuring peat fire smoke. Chapter 8 also evaluated three low-cost and portable air quality sensors (KANE101, SDS011, and FLOW) against research-grade reference instruments (FTIR, PM Cascade Impactor, and DustTrak).

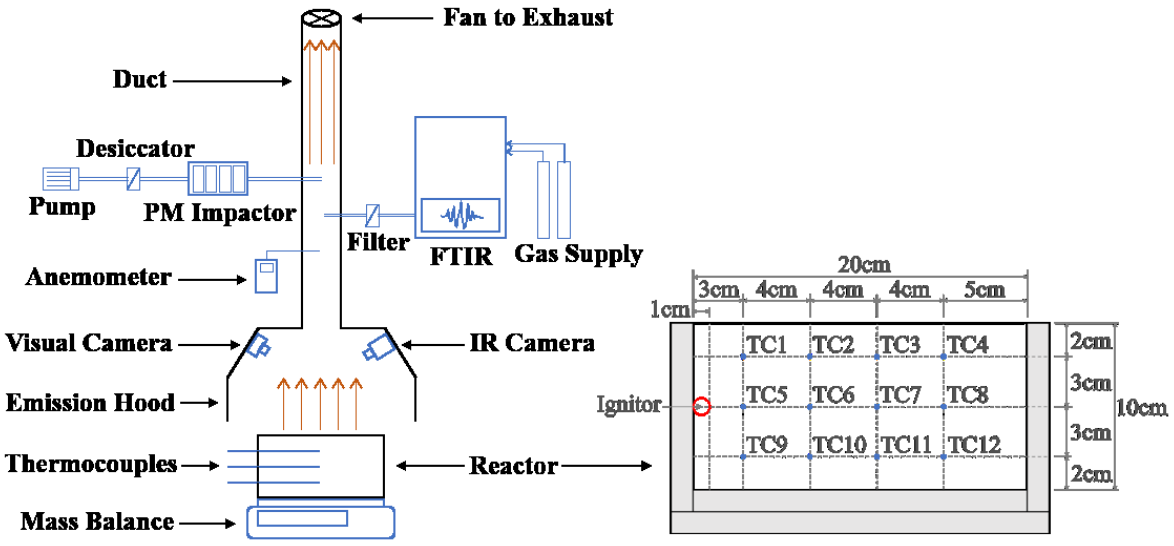

Figure 3.3 Schematic of the emission rig to measure the fire dynamics and emissions of peat fire. A section view of the reactor for smouldering peat experiments is shown on the right with detailed positions of thermocouples and ignitor.

3.3 Spread Analysis

A previous peat fire study [29] has found a smouldering spread theory, which suggests the horizontal spread rate is linearly correlated with the inverse of heat sink density (energy needed to heat a unit volume of peat to a typical smouldering peak temperature), and the in-depth spread rate is linearly correlated with the inverse of organic density. This thesis applied this spread theory in analysing the horizontal spread and in-depth spread. The calculation method of heat sink density and organic density are shown below.

The moisture density (ρ_w), organic density (ρ_o), and inorganic density (ρ_i) are calculated using Eq. (3.1), (3.1), and (3.3) for each soil condition of moisture content (MC) and bulk density (ρ_b), and substituted into Eq. (3.4) to calculate the heat sink density (ΔH_s), the energy needed to heat a unit volume of peat sample to a typical smouldering peak temperature (550 ℃). The values of heat of pyrolysis (ΔH_p), latent heat of water (L_w), and other thermal properties in Eq. (3.4) are introduced in Table 3.2.

$$\rho_w = \rho_b * MC/(MC + 1) \tag{3.1}$$

$$\rho_o = \rho_b * (1 - IC)/(MC + 1) \tag{3.2}$$

$$\rho_i = \rho_b * IC/(MC + 1) \tag{3.3}$$

$$\Delta H_s\ (units\ of\ J/m^3) = \rho_w\ (c_w \Delta T_d + L_w) + \rho_o \left(c_p \Delta T_H + \Delta H_p\right) + \rho_i\ c_i \Delta T_H \tag{3.4}$$

Table 3.2 List of values used for calculating heat sink density [29].

Variable	Value	Unit	Description
c_w	4186	J/kg·K	Specific heat of water
c_o	1840	J/kg·K	Specific heat of organic matter
c_i	880	J/kg·K	Specific heat of inorganic matter
ΔT_d	80	°C	Temperature increase to drying temperature 100°C
ΔT_H	530	°C	Temperature increase to peak smouldering temperature 550°C
L_w	2256	kJ/kg	Latent heat of water vaporisation
ΔH_P	500	kJ/kg	Heat of pyrolysis

The study developed this theory used IR signature to track the moving speed of smouldering leading edge to obtain horizontal spread rate, and used the time difference between the leading edge and the trailing edge of smouldering passing by the same location as the time of in-depth spread from the surface to the bottom of the reactor (1.6 cm depth) [29]. In this thesis, temperature data measured by thermocouples were used to calculate the horizontal spread rate and in-depth spread rate with the similar mechanism as used in previous study by using IR camera. By using the thermocouple data, 200 ℃, a typical smouldering temperature represent the start of pyrolysis used as the threshold calculating the depth of burning [25], is used as the threshold for tracking the leading edge and trailing edge of smouldering. The data from the bottom thermocouples at 8 cm depth were used to calculate the horizontal spread and in-depth spread. This method of calculating horizontal spread is used in previous studies [25, 42], while for in-depth spread is similar to the method of [29] but new. This method to estimate in-depth spread was validated by using the visual footage (shown in Figure 3.4).

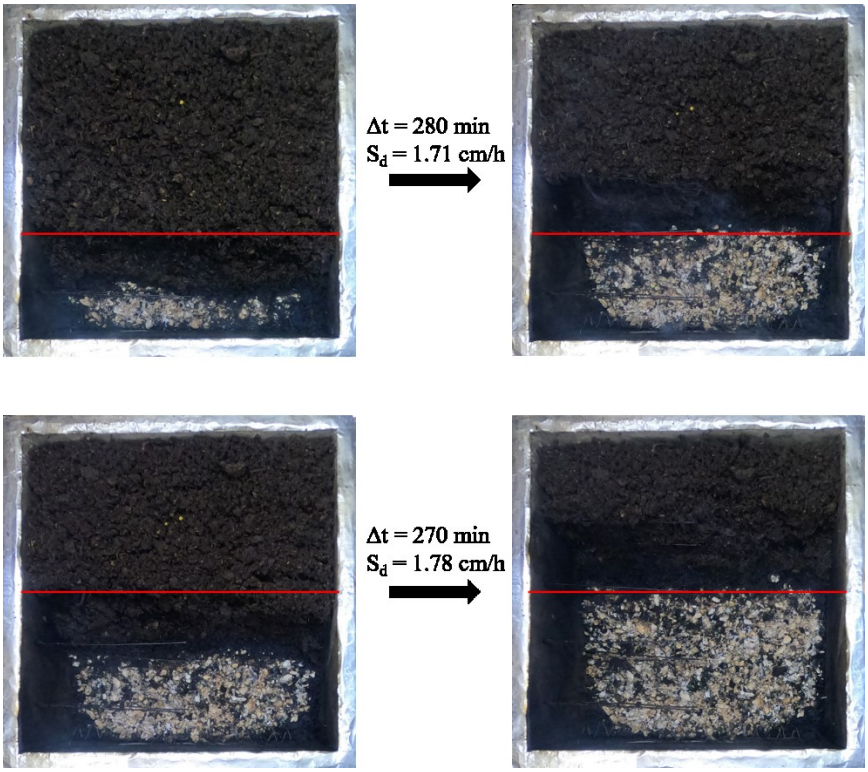

Figure 3.4 An example of top-view visual footage with time recorded to validate the method estimating the in-depth spread. Two vertical planes, one at the second column of thermocouples and one at the third column of thermocouples from the ignition source, are chosen to show the in-depth spread from the surface to the bottom (10 cm depth).

3.4 Emission Analysis

Emission ratio (ER) and modified combustion efficiency (MCE) are two important characteristics in emission studies to indicate the combustion regimes [48, 83, 84]. The methods of calculation are shown in Eq. (3.5) and (3.6), where ΔCO_2 and ΔCO are the excess concentration of CO_2 and CO. Previous research revealed that the MCE threshold of smouldering is 0.75 – 0.85, and flaming is above 0.9 in peat fires [33]. The averaged MCE at steady stage in this study was 0.85 ± 0.01.

$$ER_{CO/CO_2} = \frac{\Delta CO}{\Delta CO_2} \tag{3.5}$$

$$MCE = \frac{\Delta CO_2}{\Delta CO + \Delta CO_2} \tag{3.6}$$

A convenient way of quantifying emissions from wildfires is calculating emission factors. The emission factor is the ratio of the mass of a pollutant emitted per unit mass of fuel consumed. Previous works discussed different methods to calculate emission factors in peat fires [39]. The most commonly used method in atmospheric science and remote sensing is carbon balance method. This approach, particularly useful in the field, assumes emissions containing carbon are all measured, given by Equation 3.

$$EF_b(i) = F_c \cdot 1000\ (g\ kg^{-1}) \cdot \frac{M_i}{12} \cdot \frac{n_i}{n_t} \tag{3}$$

Where F_c is the carbon fraction in mass of the fuel, M_i is the molar mass of species i, n_i is the number of moles of species i, and n_t is the total number of moles of carbon emitted.

In the field, it is nearly impossible to measure the real-time fuel consumption, but in laboratory studies, real-time mass loss rate can be obtained along with gas concentrations. A method using mass loss data in laboratory experiments to calculate emission factors can be applied to validate the calculation of carbon balance method, given by Equation 4 [39].

$$EF_m(i) = \frac{\rho_i c_i(t) \dot{V}}{\left(\frac{\dot{m}(t)}{1+MC}\right)} \tag{4}$$

Where ρ_i is the density of species i, $c_i(t)$ is the real-time concentration of species i (background concentrations were subtracted), $\dot{V}$ is the volumetric flow rate inside the duct (0.035 $m^3\ s^{-1}$ ± 2.5% for our rig), $\dot{m}(t)$ is the real-time mass loss rate of the wet peat sample, and MC is the sample moisture content by dry mass.

Chapter 4

Ignition Conditions of Self-sustained Smouldering in Peat

Summary

The understanding of the basic mechanisms of ignition of peat to initiate self-sustained smouldering is essential in the development of mitigation technologies, but not well studied yet in the literature. In this research, laboratory experiments were conducted to improve the understanding of how peat conditions (moisture content and bulk density) and ignition protocols influence the ignition probability. A modified ignition protocol was developed by stopping the heat source when 10% mass of the sample is lost. This mass-based ignition protocol was found to be robust to initiate self-sustained smouldering in peat samples for a wide range of soil conditions. By using the new ignition protocol, experiments using peat samples of moisture content from 100% to 180% with a range of bulk density via compression were conducted to investigate how both moisture content and bulk density together influence the critical ignition conditions. Results show that although the moisture content plays a major role in the ignition probability, bulk density is also important. Increasing density decreases the critical moisture content by increasing the mass of water in a unit volume. This increase of heat sink makes the ignition more difficult. These findings contribute to studying smouldering peat fires and improve the understanding on the ignition of different types of peat.

4.1 Introduction

Moisture content (mass of water divided by mass of dry peat in sample), inorganic content (mass of non-combustible material divided by mass of dry peat in sample) and bulk density (mass of sample divided by volume of sample) are the three most important soil conditions to influence the ignition of smouldering [3]. Inorganic content and moisture content perform as heat sinks absorbing heat generated from the oxidation and altering heat transfer [26]. Bulk density plays an important role in limiting oxygen supply and changing heat transfer

regime [27-29]. Combining the factors of moisture content and inorganic content, a critical ignition threshold, above which ignition is not possible, was found in previous study with an approximate linear decrease of critical moisture content with increasing the inorganic content [26]. As bulk density can be changed by altering moisture content and inorganic content, and can also be influenced by many other factors such as porosity and decomposition rate, it is very challenging to study the effect of bulk density on smouldering ignition, hence very few research focused on this topic. This topic is also very important in studying the fire dynamics of different types of peat with naturally different bulk density, and link the findings obtained in one type of peat to peat with different origins [30].

In this chapter, experiments were conducted under controlled laboratory conditions to investigate the critical ignition conditions for self-sustained smouldering peat under different moisture content and bulk density utilizing diagnostics of mass loss, temperature, gas emissions, and visual/IR imaging.

4.2 Method

Experiments were conducted using the emission rig developed previously in [39]. This experimental rig was designed to investigate peat fire dynamics and emissions. There are five types of diagnostics set up used in this study. A mass balance was used to record the real time mass loss in the burning process. Twelve thermocouples were inserted into the reactor in three depths to measure the temperature profile during smouldering propagation. Gopro and FLIR camera were installed to record the visual and infrared signature of the experiments. Fourier-transform infrared (FTIR) spectroscopy (Thermo Scientific Nicolet iG50) was used to measure emission gases. Details of the experimental setup was introduced in Chapter 3.

The duct system is designed to collect the emissions from the combustion process and the fan at the top of the duct is calibrated to ensure the center-line flow velocity inside the duct stabilized at 2 m/s. The open-top reactor has an internal dimension of 20 × 20 × 10 cm, built by mineral fibre boards. The ignitor is a metal coil with a length of 18 cm and an outer helical diameter of 1 cm fixed at one side board of the reactor. Power of 100 W was applied to the coil to ignite the peat samples [24].

To investigate the ignition conditions of smouldering peat, two main variables are studied in this research: different ignition protocols (time-based and mass-based ignition protocols, and the depth of ignitor), and peat with different physical conditions (moisture content and bulk density).

Different ignition protocols were tested by varying the duration of ignition protocol and the depth of ignitor in the reactor. In previous studies, an ignition protocol of keeping the ignitor on for 30 min was widely used and considered to be sufficiently strong to ignite dry peat [27, 39, 42]. In this study, the duration of 20 min, 30 min, 60 min, 120 min and 180 min of ignition protocol were tested for different level of energy input to initiate a self-sustained smouldering in peat samples with variable physical conditions. The ignition duration was not extended when the smouldering front detached from the ignition coil to make sure the smouldering can be self-sustained without aiding of radiation heat transfer from the coil. Based on the experimental observation (shown in Figure 4.1) and estimation (equivalent to the amount of sample 2 cm from the side wall consumed), when the mass loss of sample reaches 10%, the smouldering front is detached from the ignition coil. A new ignition protocol, turning off ignitor when sample consumption reaches 10% mass loss, is defined and tested in the experiments. To study the influence of the depth of ignitor on ignition, three depths of 2 cm, 5 cm and 8 cm (following the depths of thermocouples in the reactor) were tested to ignite peat samples with moisture

content from 80% to 180% moisture using both the original time-based ignition protocol and the new mass-based ignition protocol.

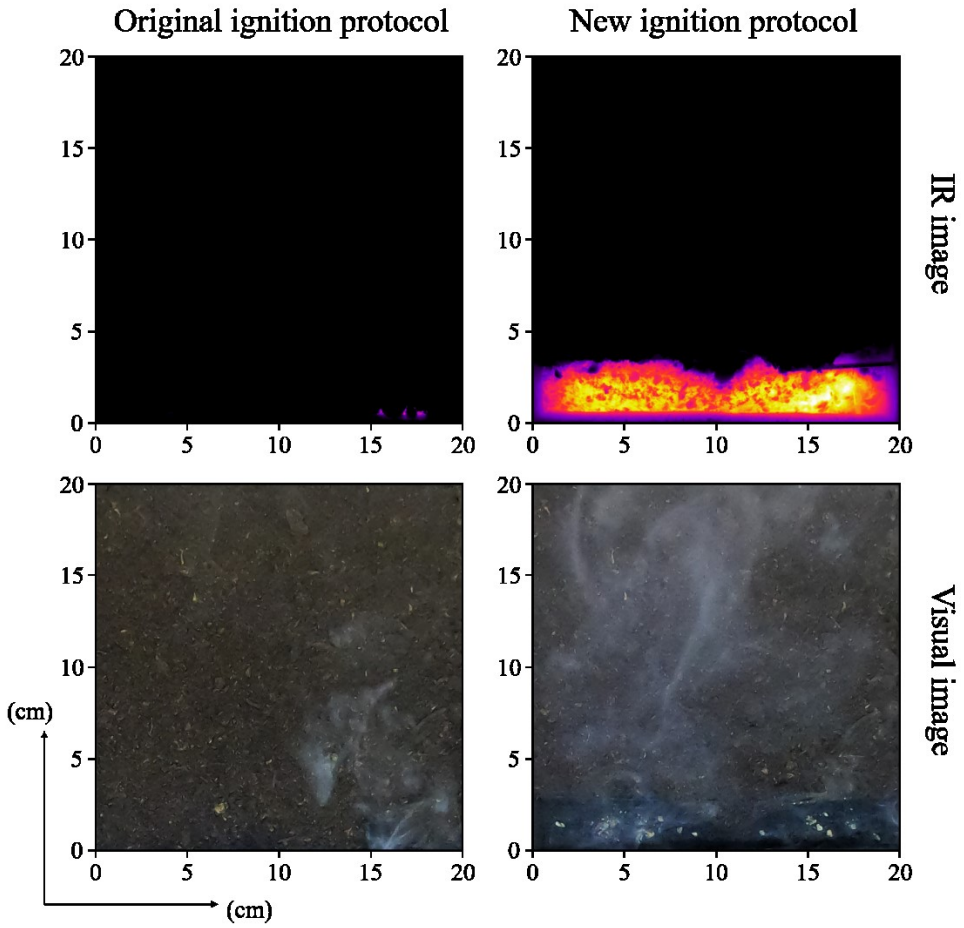

Figure 4.1 Top view of IR and visual images when the ignitor was turned off by using the original time-based ignition protocol (left) and the new mass-loss-based ignition protocol (right). The original ignition protocol kept the ignitor on for 30 min and the new ignition protocol kept ignitor on until reaching 10% sample mass loss. This set of example is from smouldering experiments of 100% moisture content peat.

Two most important physical conditions, moisture content and bulk density, were varied to find the ignition limit and the difference in fire dynamics between the self-sustained and not self-sustained smouldering. This study uses a new type of Irish horticultural peat (Irish

2020 (H)) which is similar to the peat used in previous studies (Irish 2018 (H)) [29, 39], but has naturally higher inorganic content and bulk density. To study the effect of moisture content on ignition, peat samples were treated to moisture content (mass of water per mass of dry peat) of 20%, 40%, 50%, 60%, 80%, 100%, 120%, 140%, 150%, 160%, 170%, 180% and 200% following the protocol of sample preparation in [24]. Experiments were repeated ten times for each moisture content from 100% to 200% in using the original ignition protocol, and five times for each moisture content from 100% to 200% in using the new ignition protocol. To test whether the new ignition protocol is sufficient to initiate a self-sustained smouldering and to verify the moisture content threshold, additional experiments extending the ignition protocol to 20% and 30% mass loss (ignitor keeps drying samples until reaching 20% or 30% mass loss) were conducted with three repeats in peat sample with 180% and 200% moisture content.

To study the ignition threshold combining the factors of moisture content and bulk density, peat samples with moisture content of 100%, 120%, 140%, 160%, 180% were treated by compression in reactor to 20%, 40%, 60%, 80% and 100% more of the original bulk density. Compression (Δ, %) is defined as the number of percentage increase in bulk density after compression. 100% is the maximum compression that can be achieved for each moisture content in this study. From the experimental observation, peat samples inside the reactor remain compressed during the experiments. Experiments were repeated three times for every combination of moisture content and bulk density by using the new mass-based ignition protocol. To compare the effect of ignition protocol on igniting peat with different level of compression, time-based ignition protocol was used in experiments of 100% moisture content in compression of 20%, 40%, 60%, and 80%.

In this study, a self-sustained smouldering is defined as a smouldering process persisting from the end of the ignition protocol to consistently burn all available fuel ahead.

Since the fuel in the reactor is nearly uniform and the lab environmental conditions are stable, an independent self-sustained smouldering front can propagate until the end of the reactor without extra external energy input. The result of each experiment is categorised into either self-sustained (ignition probability = 1) or not self-sustained (ignition probability = 0). Logistic regression is used to analyze the results of ignition probability and verify the efficiency of ignition protocol. The ignition outcomes, self-sustained and not self-sustained, are dichotomous dependent variables. Mass loss and temperature data during the ignition process are used as independent variables to find the signature of self-sustained smouldering. To compare the efficiency of the original and new ignition protocol, logistic regression analysis is conducted to predict the ignition probability over a range of single independent variables of moisture content and bulk density by using different ignition protocols. To combine factors of moisture content and bulk density, multiple logistic regression is used on two independent variables to predict the ignition probability.

4.3 Results and Discussion

4.3.1 Ignition signature of mass loss and temperature

By using the original time-based ignition protocol, all repeats of experiments done for each moisture content from 100% to 200% show when turning off the ignitor at 30 min, the temperature values at thermocouples are below 100 ℃, and the values of mass loss are below 6%. The original ignition protocol can provide a near-limit ignition condition and the data are valuable for finding the critical ignition threshold. It is found that the temperature value at TC9 (at the bottom layer near the ignition coil, location shown in Chapter 3) is a potential indicator of ignition after analyzing the thermal residence time (the time duration above a temperature

threshold at a certain location [18], shown in Figure 4.2) at the location of TC1, TC5 and TC9 (three thermocouples near ignition coil).

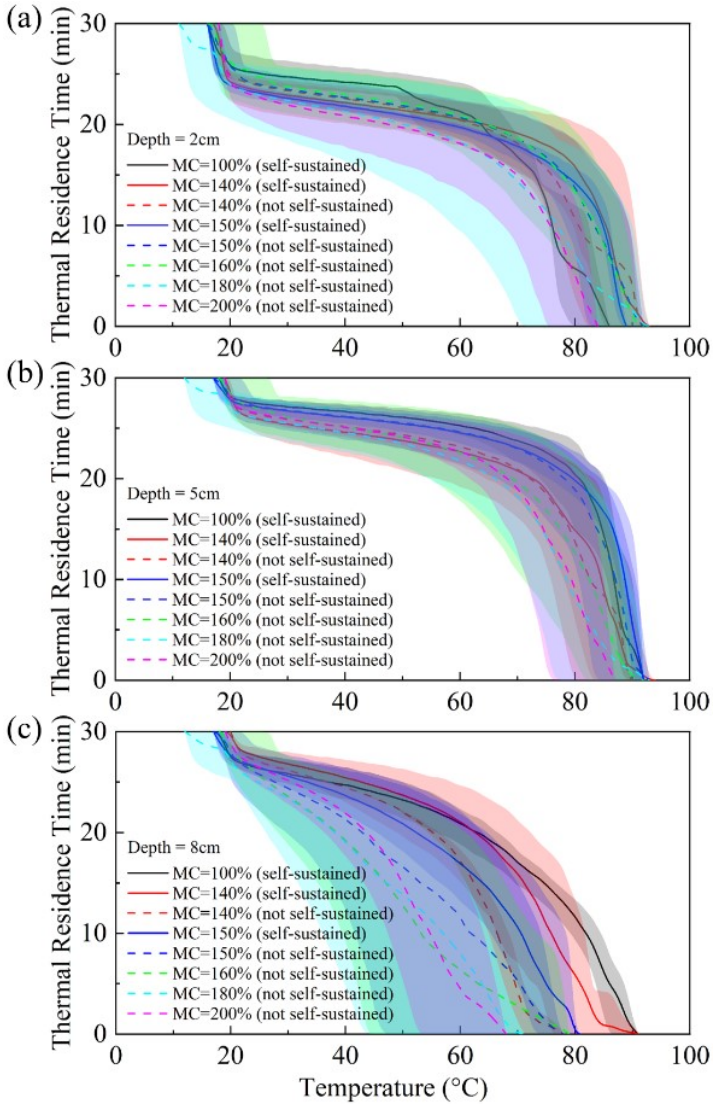

Figure 4.2 Thermal residence time at the location of (a) TC1 (depth of 2cm), (b) TC5 (depth of 5cm), and (c) TC9 (depth of 8cm) in the duration of 30min ignition protocol. Thermal residence time is the time duration above a temperature threshold at a certain location.

The raw data of temperature at TC9 and sample mass loss when turning off ignitor were analyzed by logistic regression. Figure 4.3 shows the estimated ignition probability in relation to independent variables of temperature (at TC9) and mass loss when turning off ignitor. This

method is useful since the ranges of temperature and mass loss of self-sustained cases have overlaps with those of not self-sustained cases. Results show that when temperature at TC9 can reach 80 ℃, or the sample mass loss can reach 4% before turning off ignitor, the probability of ignition is 50%. 80 ℃ is also found as a turning point in propagation process after which the temperature increasing rate start to increase dramatically.

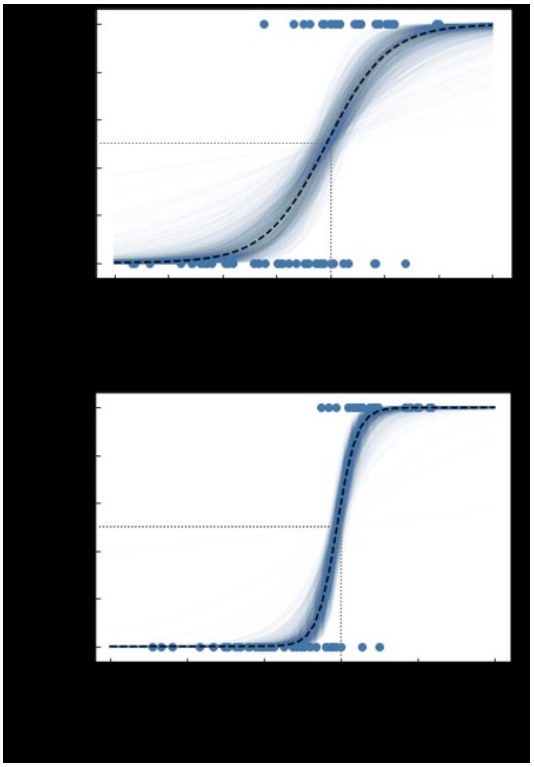

Figure 4.3 Probability of initiating self-sustained smouldering in terms of ignition temperature and mass loss. The probability distribution is analysed by using logistic regression for self-sustained (probability = 1) and not self-sustained (probability = 0) data from experiments of using moisture content from 100% to 200% by original ignition protocol. In (a), the temperature data is the temperature shown in TC9 at the end of the ignition protocol. In (b), mass loss is the percentage of sample mass loss in reactor at the end of the ignition protocol. Blue dots represent all data points. Blue curves represent all possible fits using logistic function and darker regions represent higher probability of a good fit. The dashed black line represents the best fit of logistic regression.

4.3.2 The influence of ignition protocol on ignition

Figure 4.4 summarizes the influence of ignition protocol on the critical moisture content for ignition by placing the ignition coil to depths of 2 cm, 5 cm (standard protocol) and 8 cm. By using the original time-based ignition protocol, in 30 min ignitor at depth of 2 cm, 5 cm, and 8 cm can ignite samples with up to 120%, 150%, and 80% moisture content. By using the new mass-based ignition protocol, until 10% mass loss ignitor at depth of 2 cm, 5 cm, and 8 cm can all ignite samples with up to 160% moisture content. This means the mass-based ignition protocol is sufficient to initiate self-sustained smouldering within ignition limit regardless of the depth of ignitor, and in the time-based ignition protocol, the depth of ignitor can influence the result of ignition.

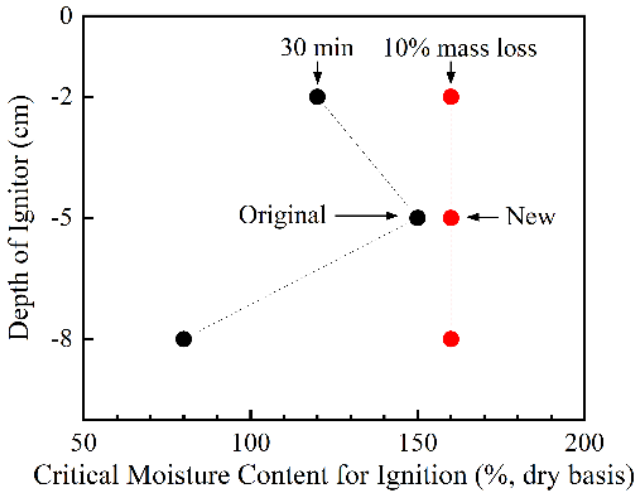

Figure 4.4 Summary of experiment results studying the influence of ignition protocol on the critical moisture content for ignition. Three depths (2 cm, 5 cm, and 8 cm) and two protocols (time-based and mass-based) were tested in experiments. The original protocol is to keep ignitor at depth 5 cm on for 30 min, and the new protocol is to keep ignitor at depth 5 cm on until reaching 10% sample mass loss.

An example is given in Figure 4.5 for experiments using the original time-based ignition protocol to ignite samples with 140% moisture content. It shows the difference of thermal residence time for temperature threshold that can reach at different depth, and normalized mass (remaining mass over original mass of samples in reactor) in the duration of ignition protocol by changing ignition depth. The results show when changing the depth of ignitor from 5 cm to 2 cm and 8cm, all repeats cannot become self-sustained. This can be explained by the mechanism of heat transfer and oxygen supply [18]. When ignitor is located at 2 cm from the surface, the mass loss is higher than the mass loss of self-sustained cases when the ignitor is at 5 cm. This is because when the ignition location is near surface, the oxygen supply is more sufficient for the combustion process to consume more peat samples, while the heat loss is increased to a higher level. The heat generated in smouldering process cannot overcome the heat loss, so smouldering is not self-sustained in this case. When the ignition coil is at 8 cm, the mass loss during the ignition process is less than the case of ignition coil at 5 cm, because insufficient oxygen supply limits the combustion process. In this case, smouldering cannot be self-sustained although the thermal residence time at 80℃ at TC9 is higher than the self-sustained cases.

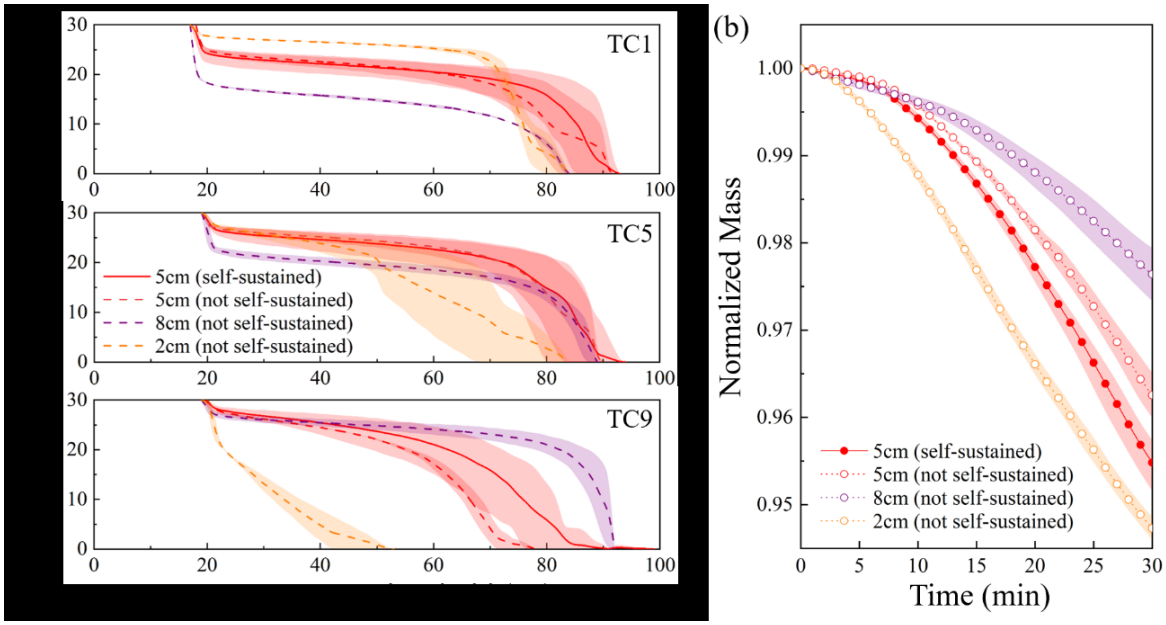

Figure 4.5 (a) Thermal residence time at the location of TC1, TC5 and TC9 in the duration of ignition protocol with ignitor at the depth of 2cm, 5cm and 8cm. (b) Normalized mass loss in the duration of ignition protocol with ignitor at the depth of 2cm, 5cm and 8cm.

By testing different durations of ignition protocol, the new ignition protocol based on mass loss is found to be robust to initiate self-sustained smouldering to ignite peat samples within the critical ignition threshold of moisture content and bulk density. Figure 4.6 shows the improvement of probability estimation for initiating self-sustained smouldering by using the new ignition protocol. In all repeats of experiments using the new ignition protocol, peat samples below critical ignition conditions (for both moisture content and bulk density) have 100% successful ignition, and peat samples above critical ignition conditions have 0% successful ignition. The original time-based ignition protocol is not strong enough to reach the same efficiency in igniting peat samples like Irish 2020 (H) with naturally higher bulk density in near limit conditions. To study the critical ignition threshold, the ignition protocol has to be strong enough to minimize the influence of ignition protocol on ignition. The new mass-based

ignition protocol is proposed as the universal method in ignition study for peat samples with different physical and chemical conditions.

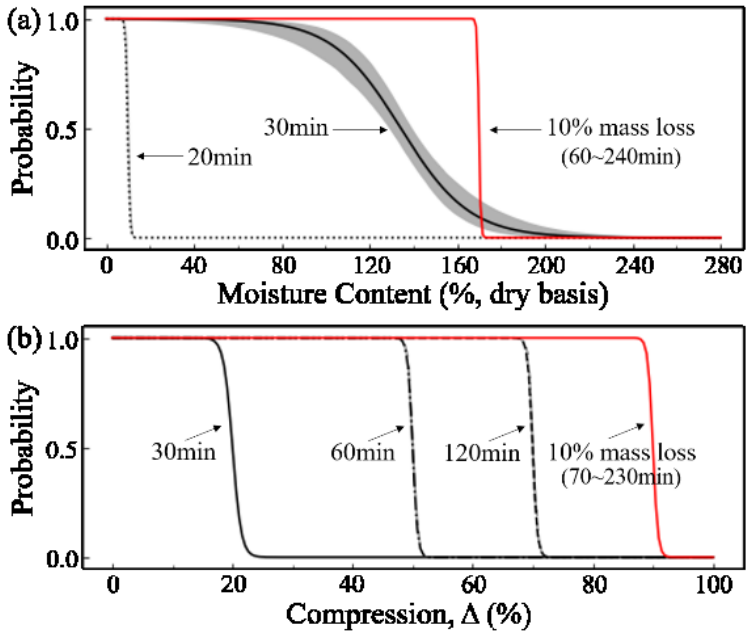

Figure 4.6 Probability of initiating self-sustained smouldering in peat with different moisture and density conditions by changing the ignition protocol from time-based to mass-based protocol. The probability distribution is analysed by using logistic regression for self-sustained (probability = 1) and not self-sustained (probability = 0) data. In (a), all experiments with different moisture content used original bulk density without compression. In (b), probability estimation is based on the results of experiments using 100% moisture content peat with different levels of compression. 100% is the maximum compression that can be achieved in laboratory study.

The scaling of this ignition protocol to other configurations of experimental reactors can be done by defining the ignition zone based on the dimensions of ignitor (L, d) and volume factor (V1/V2) considering the size of different configurations. Ignitor initiates smouldering in consuming the mass in ignition zone which is equivalent to 10% mass loss in this configuration,

and in new configurations the mass loss is calculated by using Eq. (4.1). The alternative method if mass loss cannot be recorded could be monitoring the ignition process by using IR and visual cameras and turning off the ignitor when smouldering front spreads away from the ignition coil.

$$\mathrm{m}_l = \frac{2d*V_1}{L*V_2} \tag{4.1}$$

4.3.3 Effects of moisture content and bulk density on ignition

In finding the critical moisture content for the new Irish horticultural peat (Irish 2020 (H)), the original ignition protocol (30 min) can ignite samples with up to 150% moisture content. For samples with or less than 100% moisture content, self-sustained smouldering were observed in all repeats of experiments. When increasing moisture content to 120%, 140% and 150%, 5 out of 10, 4 out of 10, and 10 out of 15 repeats were not self-sustained. When using the new ignition protocol (10% mass loss), all repeats for each moisture content up to 160% can initiate self-sustained smouldering. None of the repeats for 180% and 200% moisture content peat sustained smouldering after turning off the ignitor. The evolutions of mass loss in the duration of the original time-based ignition protocol and the new mass-based ignition protocol are shown in Figure 4.7. This figure suggests that moisture content significantly influences the ignition dynamics. Ignition of samples with higher moisture content requires more energy supply to evaporate more water contents to reach the following ignition process [20].

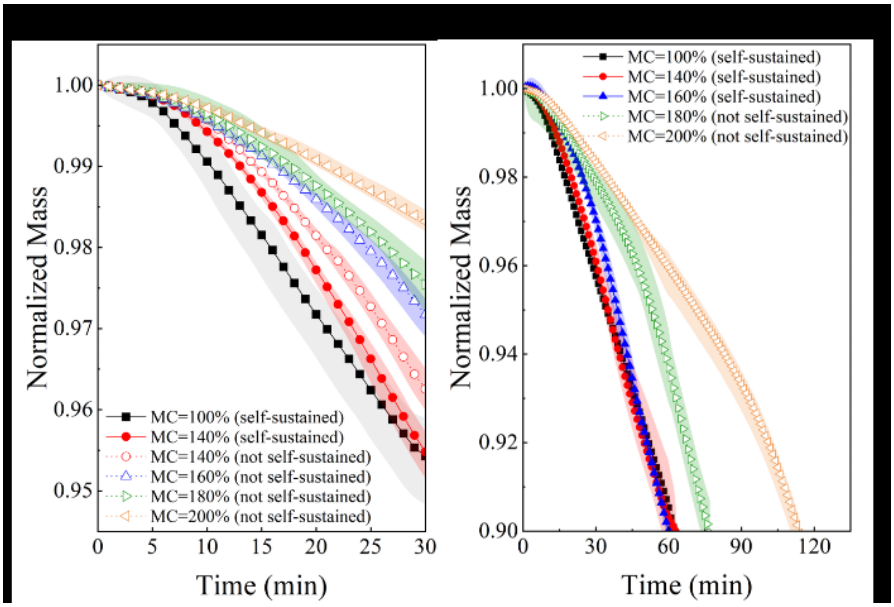

Figure 4.7 Normalized mass loss of peat with different moisture content in the duration of ignition protocol. Normalized mass is the fraction of the remaining mass in reactor compared to the original mass.

To test whether the new mass-based ignition protocol is sufficient to initiate a self-sustained smouldering and to verify the moisture content threshold, additional experiments extending the ignition duration to 20% or 30% mass loss (ignitor keeps drying samples until reaching 20% or 30% mass loss) were conducted in 180% and 200% moisture content peat. None of the experiments shows a self-sustained propagation. Figure 4.8 shows the temperature profile of the bottom layer of the fuel in the reactor (TC9, TC10 and TC11 are at the depth of 8 cm and usually used to track smouldering spread [25]) in experiments using 200% moisture content peat. After turning off the ignitor when reaching 30% mass loss, the temperature at TC9 can reach 490 ℃ and persist for one hours above 350 ℃. However, smouldering cannot sustain to the location of TC10 (4 cm from TC9) from which the temperature peaked at around 284 ℃, below the typical char oxidation temperature 350 ℃ [85].

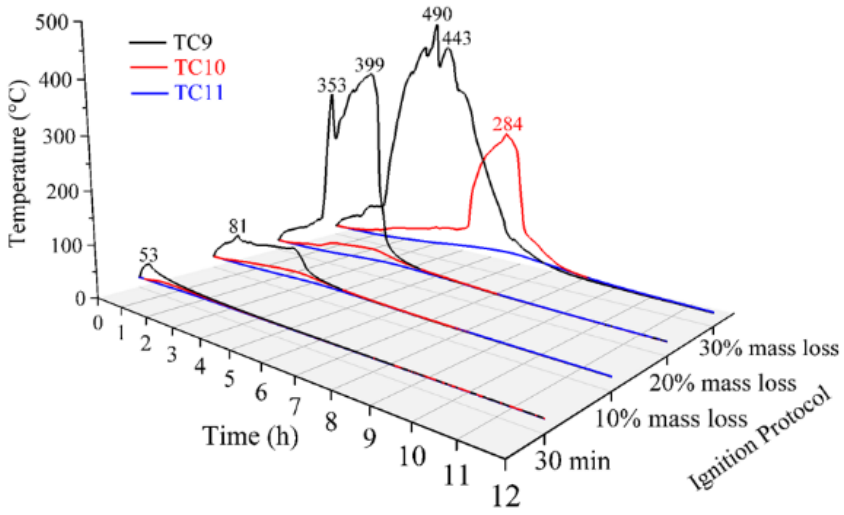

Figure 4.8 Temperature evolution at the location of TC9, TC10 and TC11 for additional experiments with 200% moisture content by extending the duration of ignition protocol from 30 min time-based protocol to 10%, 20%, and 30% mass-based protocol. The temperature profiles show smouldering were not self-sustained in all cases.

In studying the influence of bulk density on ignition, a variety of modified bulk densities were tested. Figure 4.9 shows the evolutions of mass loss in the duration of original time-based ignition protocol and new mass-based ignition protocol igniting peat samples of 100% moisture content in 0%, 20%, 40%, 60% and 80% compression. The results show bulk density can greatly affect the mass loss rate in ignition. Samples with higher bulk density require higher amount of energy supply to sustain until enough fuel oxidized to continue the smouldering process [27]. Once smouldering in high density peat can sustain to get enough oxygen supply to the depth of burning, the process can be self-sustained. In contrast, the original ignition protocol can only initiate self-sustained smouldering up to 20% compression, while the 60 min, 120 min and 180 min ignition protocols can ignite samples up to 40%, 60% and 80% compression. The new ignition protocol is sufficient to initiate self-sustained smouldering for all these levels of compression since the reaction at deeper layers can get

enough oxygen supply when smouldering front is detached from the ignitor when there is 10% mass loss in sample.

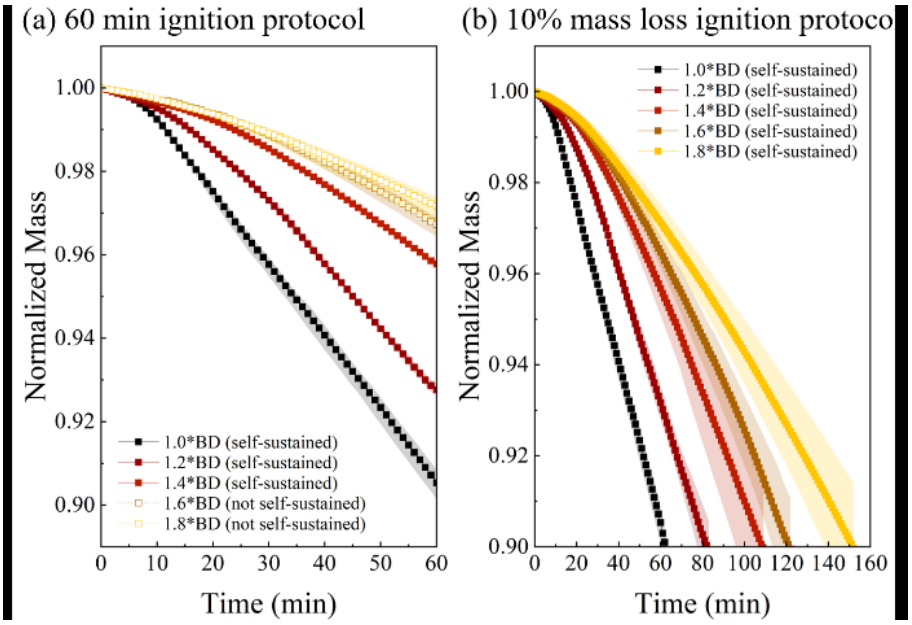

Figure 4.9 Normalized mass loss of peat with different bulk density in the duration of ignition protocol. BD (286 kg/m3) is the original bulk density of the samples without compression in 100% moisture content.

Figure 4.10(a) shows the outcomes of experiments using the new mass-based ignition protocol to ignite peat samples above 100% moisture content with modified bulk density by compression. This figure shows the effect of compression in limiting the ignition probability is increasing when moisture content is increased above 100%. This finding agrees with the literature that the effect of moisture content on smouldering propagation is enhanced by the increase of bulk density [27, 29].

The results of experiments show moisture content and bulk density are two important variables in predicting the probability of ignition. Increasing the moisture content or the level of compression are all correlated with a decreasing of ignition probability. By using multiple variable logistic regression analysis, Eq. (4.2) is found to predict the probability of ignition (P_i)

for this type of peat. To make the P_i to be 50%, Eq. (4.3) is found to be the critical line for ignition threshold of moisture content and bulk density.

$$P_i = 1/(1 + e^{-(976.78-5.97MC-4.01\Delta)}) \quad (4.2)$$

$$P_i = 50\%, \Delta = 243.62 - 1.49MC \quad (4.3)$$

When igniting peat samples in the same moisture content but higher bulk density, more water content in a certain volume around ignition coil has to be evaporated, and there are less oxygen penetration to the ignition zone for char oxidation. To further investigate the controlling factors of the critical ignition criteria for moisture content and bulk density, the methodology developed in previous research [29] analyzing the influence of bulk density in smouldering propagation is used in analyzing the ignition criteria in this research. The method of calculation for the heat sink density and organic density was also introduced in Chapter 3.

The contour lines of moisture density and heat sink density in Figure 4.10(b) and 4.10(c) can explain the critical line for ignition threshold of moisture content and bulk density. Combining factors of moisture content and bulk density, it is found the higher the moisture density or the heat sink density, the lower the ignition probability of the sample. The organic density shown in Figure 4.10(d) cannot predict the critical line for ignition threshold, but it is related to the ignition and can influence the probability of ignition in many different ways including influencing the heat sink density. In mass-based ignition protocol, the higher the organic density is in samples, the more the heat produced in consuming a certain percentage of sample. In terms of heat transfer, the higher the organic density is, the better the contact of peat particles to conduct heat. In terms of oxygen supply, the higher the organic density is, the less

oxygen can penetrate to the depth of burn. These influences of the organic density need to be considered second to the heat sink density to better predict the critical line of ignition threshold.

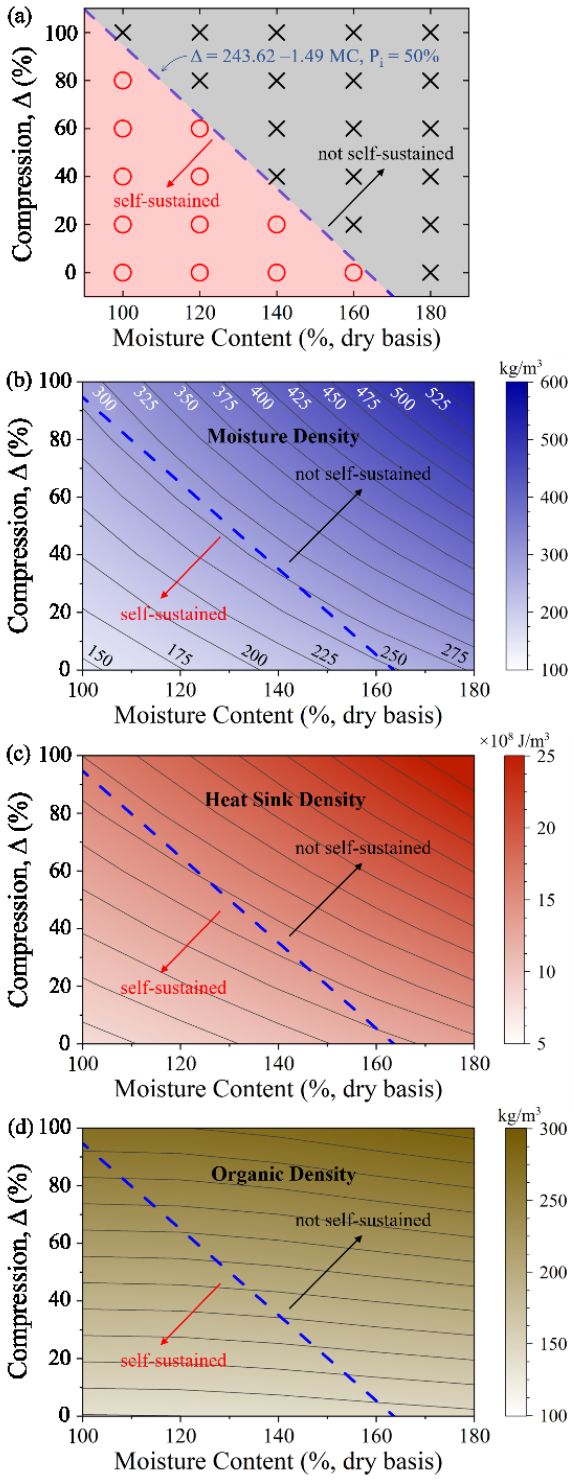

Figure 4.10 Summary of the results of experiments igniting high moisture content peat with different levels of compression. In (a), circles represent results of self-sustained smouldering

and crosses represent results of not self-sustained cases. The blue dashed line is obtained by using multiple variable logistic regression analysis for the experiment results and represents the probability of ignition to be 50%. The contour maps in (b), (c), and (d) are made by interpolating the averaged values in each soil condition.

4.3.4 Ignition signature of gas emissions

In addition, by analysing the gas emission data, it is found that the concentration of NH_3 has a surge of increase at the end of the mass-based ignition protocol in self-sustained cases (shown in Figure 4.11), indicating the ignition is strong enough to start an independent smouldering front. As shown in Figure 4.7, at the end of the original ignition protocol, mass loss can reach up to 4% when sample moisture content is above 100%. In Figure 4.11, when mass loss is increasing from 4% to 10%, the concentration of NH_3 has an obvious increase in self-sustained cases (from 0.5 ppm to 3.5 ppm for 160% moisture content and 8 ppm for 100% moisture content) indicating a stronger char oxidation process. The increase of CO_2 and CO which are also mainly emitted in the process of char oxidation can be another evidence. The concentration of CH_4 in self-sustained cases is relatively stable from 4% mass loss indicating a steady pyrolysis process, and has a tendency of deceasing when reaching 10% mass loss indicating the increasing of oxidation. The delay of emission increasing in not self-sustained case is because the mass loss is dominated by water evaporation until there is 4% mass loss.

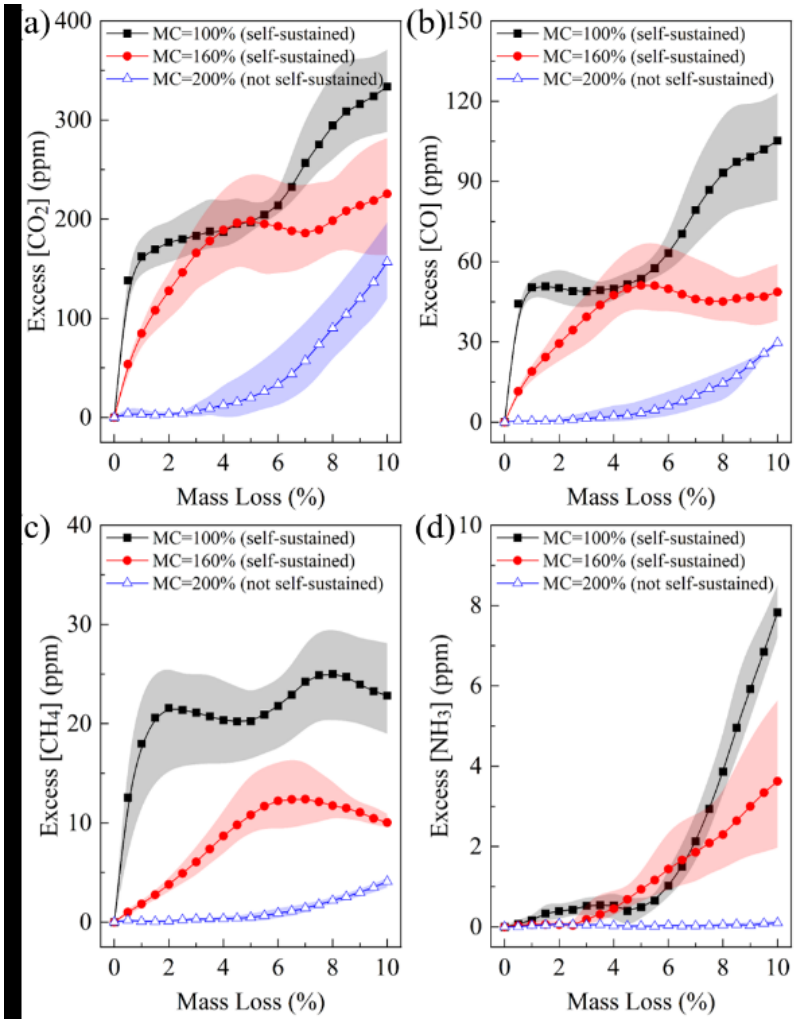

Figure 4.11 Evolutions of CO_2, CO, CH_4, and NH_3 concentrations at the duration of 10% mass loss ignition protocol. The mean values show the average of data from 5 experiments and the clouds represent the maximum and minimum values of the ranges. Background concentrations of these gases are subtracted from the results.

4.4 Conclusion

Laboratory experiments with simultaneous measurements of mass loss, temperature, and gas emissions were conducted to investigate the ignition conditions for self-sustained smouldering peat. A wide variety of soil conditions were studied, thus enabling a better understanding of the influence of moisture content and bulk density on ignition. Moisture

content plays a major role in limiting the ignition probability, meanwhile increasing density makes ignition more difficult. Along with moisture content, bulk density and inorganic content (the three most important soil conditions influencing ignition), heat sink density and organic density can be used to predict the ignition probability for different types of peat in different conditions.

By investigating peat sample temperature and mass loss, it is found that when the bottom layer thermocouple closest to the ignition source reaches 80 ℃, or the sample mass loss reaches 4% before turning off ignitor, the probability of ignition is 50%. In studying the ignition signature of gas emissions, it is found that the surge of NH_3 emission is a sign of formation of independent smouldering front. For the first time, the analysis of gas emissions at the ignition stage are focused and compared to find the ignition signature to better understand the relationship of gas emissions and ignition.

The investigation in changing ignition protocol from time-based to mass-based can contribute to the development of novel experimental methodology for better studying the ignition, spread and emissions of smouldering peat, especially field peat with different origins. These findings are valuable in understanding the initiation of smouldering combustion and contribute to the mitigation of peat fires.

Chapter 5

Influence of Density on Smouldering Dynamics and Emissions

Summary

This chapter is a short chapter presenting additional results from the previous Chapter 4, but in different topic, focusing on the influence of bulk density modified by soil compression on the smouldering spread and the associated emissions. Results show that soil compression decreases the horizontal spread rate and in-depth spread rate, and prove there is a linear correlation between the horizontal spread rate with the inverse of heat sink density (the energy required to heat the fuel in unit volume to peak temperature), and between the in-depth spread rate with the inverse of organic density (the mass of organic matter in unit volume). The experimental results also show soil compaction does not have a significant impact on the burning rate (the mass loss rate of dry peat in burning process), and the emission factors of gases. In this chapter, stages of fire evolution are defined, based on the percentage of mass loss with the range of steady stage from 20% to 80% mass loss, which will be used in the following chapters to calculate the averaged data at steady stage.

5.1 Introduction

This chapter presents additional results from experiments introduced in Chapter 4. Chapter 4 presented the influence of moisture content and bulk density (modified by compression) on ignition. Experiments were done by using Irish 2020 (H) with moisture content from 100% to 180% with compression from 0% to 100%. Results show the critical moisture content for ignition decreases when increasing the level of compression. This chapter presents the horizontal spread and in-depth spread data and emission data from the same sets of experiments studying ignition introduced in Chapter 4.

This chapter also briefly introduced the stages of fire evolution, and the method used in this thesis to define ignition, growth, steady and burnout stages. All the calculations in the following chapters followed this method.

5.2 Stages of Fire Evolution

Defining different stages of fire evolution by using the progress of mass loss can facilitate the calculation and comparisons of various experimental results. Figure 5.1 illustrates the evolution of fire dynamics and emissions in an example of smouldering experiment. Four fire evolution stages were defined with reference to the progress of mass loss: (I) ignition stage (0 to 10% mass loss), (II) growth stage (10% to 20% mass loss), (III) steady stage (20% to 80% mass loss), and (IV) burnout stage (from 80% mass loss until the end). This method of dividing stages of fire evolution agrees with the observation and emission measurements. Previous work also revealed the fire emissions are correlated with fire dynamics, but does not have clear criteria to define the stages (stages were defined visually) [39]. Chapter 5 – 8 all used this concept for data analysis.

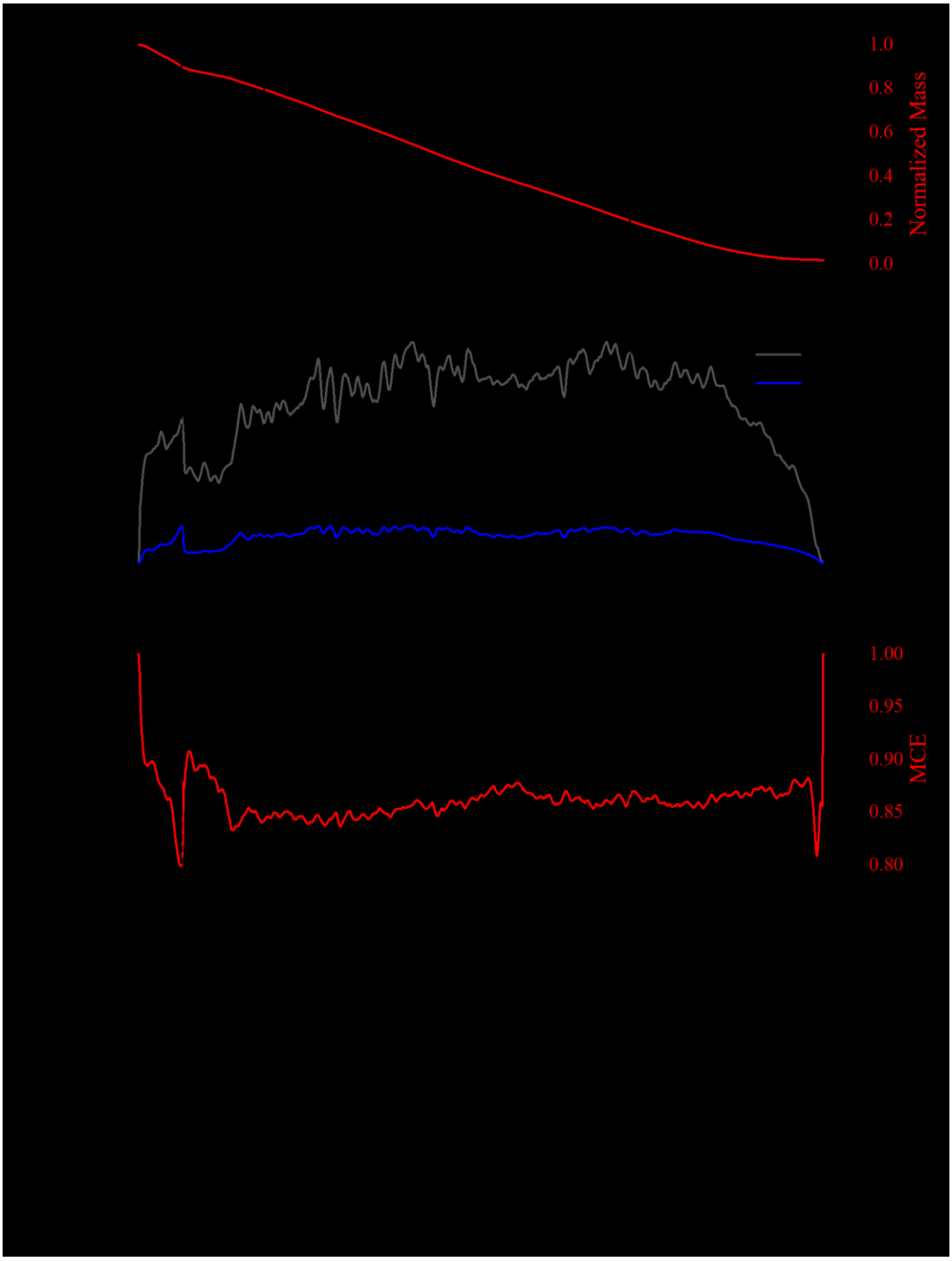

Figure 5.1 Example evolution of mass loss rate, normalized mass, CO_2 and CO concentrations (measured by FTIR), calculated emission ratio and modified combustion efficiency, PM2.5 concentration (measured by DustTrak) from the results of a smouldering experiment with 100% moisture content peat. Vertical dashed lines indicate the fire development stages: (I) ignition stage, (II) growth stage, (III) steady stage, (IV) burnout stage.

As introduced in Chapter 3, there were two experimental set-ups used in this thesis, one with emission hood and extraction fan (extraction rate of 0.035 $m^3 s^{-1}$) to collect the smoke, and the other without the emission hood set-up (open air dilution). To examine if the smoke extraction by emission hood set-up could influence the fire dynamics, experiments were done in both set-ups by using 100% moisture content peat (details introduced in Chapter 8). Figure 5.2 shows the difference in experimental setup did not have an obvious influence on the fire dynamics. All four repeats of experiments in two experimental setups finished in around 18 h. The averaged mass loss rate at steady stage was 1.24 ± 0.10 g min^{-1} in the setup with emission hood, and 1.21 ± 0.11 g min^{-1} in setup without the emission hood. The agreement in fire dynamics can help confirm the fire emissions are comparable, and the extraction rate of the set-up does not significantly influence the burning process.

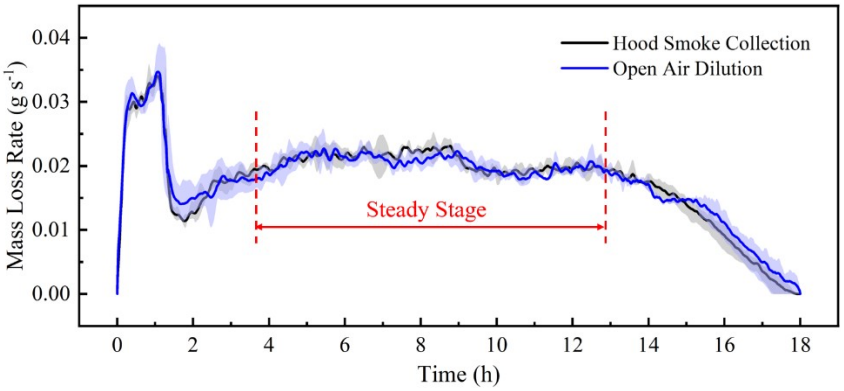

Figure 5.2 Averaged real-time mass loss rate obtained from experiments in two different experimental setups. Clouds represent the maximum and minimum ranges.

5.3 Effect of Soil Compression on Smouldering Spread

Figure 5.3 shows the data of horizontal spread and the in-depth spread measured in experiments changing bulk density of peat sample by compression. Results show soil compression decreases the horizontal spread rate and in-depth spread rate. For example, in 100%

moisture content, 80% compression decreases horizontal spread rate by 40% while decreases in-depth spread by 80%. The spread theory found in previous research [29] was proven by our experimental data. Horizontal spread rate has a high linear correlation with the inverse of heat sink density, and in-depth spread rate has a high linear correlation with the inverse of organic density. From the results, the minimum spread rates in smouldering were observed in these experiments, with 0.58 cm/h in horizontal spread rate and 0.56 cm/h in in-depth spread rate. More experiments using different peat with naturally different bulk density are presented in the following chapters.

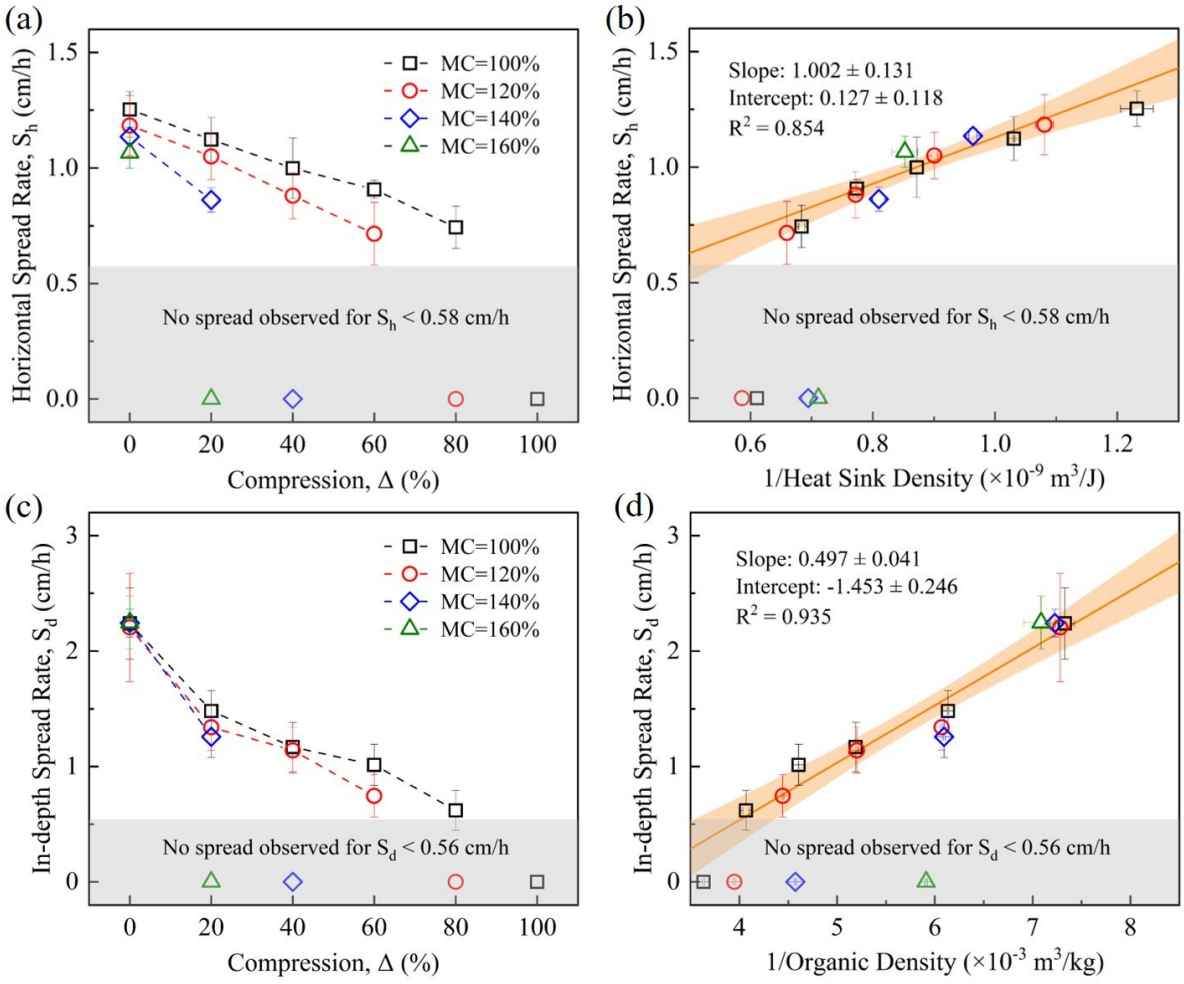

Figure 5.3 Plots of the horizontal spread and in-depth spread in the study varying bulk density by compression.

Figure 5.4 shows the summarised results of burning rate at the steady stage in the experiments of each soil condition. The results reveal that soil compaction decreases the spread rate, but does not have a significant influence on the burning rate (the mass loss rate of dry peat calculated by assuming the water evaporation rate corresponds to the moisture content of the peat). These results of spread rate and burning rate related to fire dynamics agree with previous research without the measurement of thermocouple and mass balance by using the estimation of using IR footage [29].

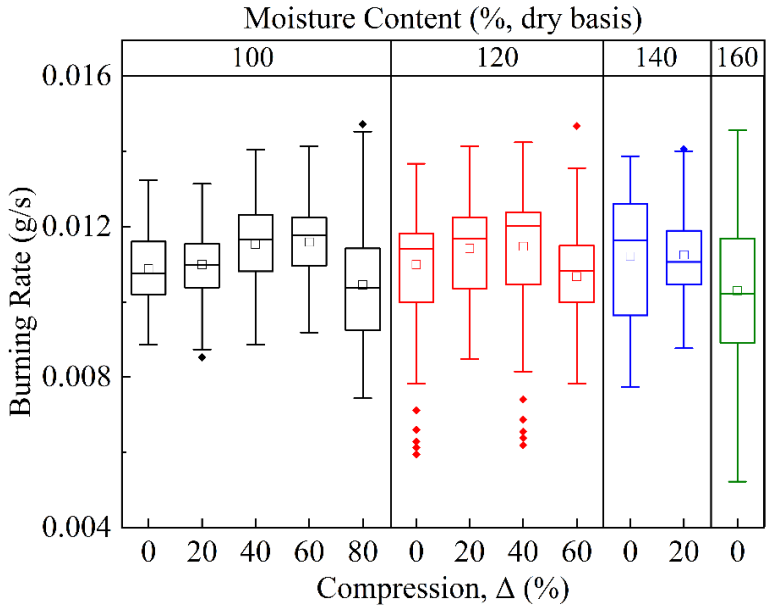

Figure 5.4 Box plots of the data of burning rate at steady stage for experiments with different soil compaction and moisture content.

5.4 Effect of Soil Compression on Emissions

Figure 5.5 shows the emission factors (EFs) of four most abundant gases emitted by peat smouldering. The results suggest the moisture content and soil compaction do not have a significant influence on the emission factors, which means burning the same amount of fuel emits the same amount of gases although the soil conditions are different in moisture content

and compression level. Figure 5.6 shows the results of modified combustion efficiency (MCE), which also suggests the moisture content and soil compaction do not have a significant influence on the MCE, an important indicator for fire regime. The MCE of burning Irish 2020 (H) is higher than the MCE range obtained in a previous literature [33], which can be because of the peat properties.

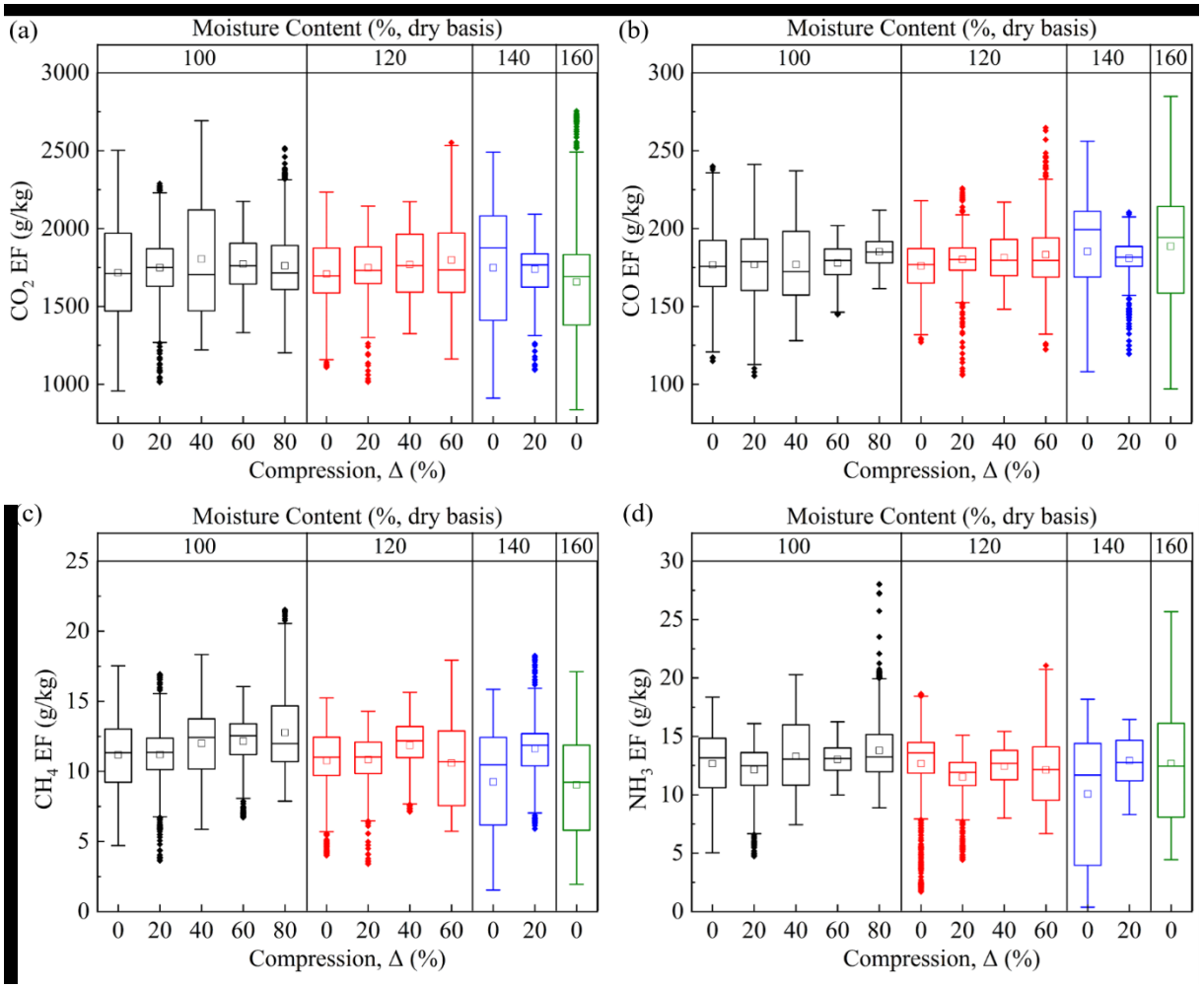

Figure 5.5 Box plots of the data of emission factors for CO_2, CO, CH_4, and NH_3 at steady stage for experiments with different soil compaction and moisture content.

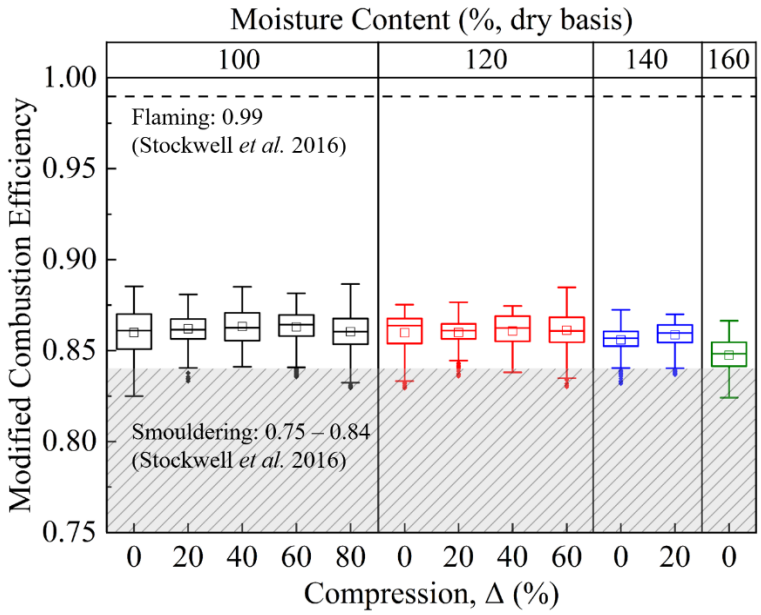

Figure 5.6 Box plots of the data of modified combustion efficiency (MCE) at steady stage for experiments with different soil compaction and moisture content.

Chapter 6

Laboratory Study of Samples from Flow Country and the Effect of Field Conditions

Summary

This chapter reported laboratory investigation of the smouldering dynamics and emissions of field peat sampled from natural peatlands, drained peatlands and peatlands under restoration in Flow Country, Scotland. In total nine samples from three sampling locations representing different field conditions and three depth ranges were studied in smouldering experiments by measuring the mass loss, temperature profile, gas and particle emissions. The results indicate high bulk density peat from long-term drained peatlands experience higher soil deterioration, and more extensive burning in terms of the amount of fuel burnt. Newly drained natural peatlands with low bulk density in drought condition are more vulnerable to fire in terms of easier ignition and faster fire spread. Samples from drained peatlands had lower averaged emission factors of CO_2, CO and NH_3, and higher averaged emission factor of CH_4 compared to samples from peatlands in natural condition and peatlands under restoration. The averaged emission factors of particles in the combustion of samples from drained peatlands and peatlands under restoration were nearly twice as high as that of peatlands in natural condition. This work contributes to linking lab-scale and field-scale fire dynamics and emission investigations, estimating fire severity and environmental impact, and developing strategies to mitigate peatland fires.

6.1 Introduction

Northern peatlands store approximately one-third of global terrestrial carbon and are important to maintain the global carbon cycle [8]. As a consequence of ongoing climate change, northern peatlands are becoming more vulnerable to fires in terms of fire frequency and severity due to drier soil and higher global atmospheric temperature [71, 86]. Smouldering is the dominant mechanism of these megafires in peatlands [3], but poorly studied in the literature.

Most of the previous laboratory peat smouldering studies used horticultural peat [15, 16, 27, 42, 78], which has a great advantage in controlling the influential factors, but has a lower bulk density because of the original usage for improving the soil structure. However, horticultural peat cannot represent the natural variation in the field and especially are not representative for higher bulk density peat sometimes found in the field, with higher carbon density and dryer conditions, for example, long term drained peatlands [87]. It is essential to understand the field conditions and apply findings in studying smouldering dynamics to the field fire management to prevent and mitigate peatland wildfires.

Scotland holds the majority of peatlands in the UK, and the blanket bog peat in Flow Country has been estimated to be the largest single expanse in Europe [88]. In May 2019, a wildfire in Flow country burned around 53.8 km^2 of peatland, causing damage to the natural soil ecosystems and deteriorating regional air quality. Six months after the fire event, we conducted a field study in burnt areas, and collected peat samples in adjacent unaffected peatlands. Samples were taken from peatlands with three different field conditions: natural peatlands, drained peatlands, and peatlands under restoration, and based on the depth of burn in the peat fire, each site in three depth ranges: shallow (0 - 10 cm), median (10 – 20 cm), and deep (20 – 30 cm). Physical and chemical properties of each sub-sample were characterised in the lab. Samples naturally dried to 100% moisture content in dry basis were ignited in an open-top reactor (internal dimension 20×20×10 cm) under controlled laboratory conditions, measuring real-time mass loss, soil temperature profile, visual and infrared signature, transient concentrations of 20 gas emission species, and mass of size-fractioned particle emissions (PM10, PM2.5 and PM1). These measurements allow quantification of the smouldering dynamics, fire severity, and emissions and provide a better understanding of how field conditions affect them.

6.2 Method

In this chapter, bench-scale experiments were conducted by using the field peat we sampled in Flow Country in Scotland to characterise the fire dynamics and emissions of the peat from different field conditions. The experiments were conducted using the emission rig developed in previous research [39], which was introduced in detail in Chapter 3. There were six types of diagnostics applied to this study to measure the real time mass loss (mass balance), temperature profile (thermocouples), visual and infrared images (Gopro and FLIR camera), gas emissions (FTIR), and particle emissions (PM cascade impactor), which were also introduced in Chapter 3. Peat samples were deposited naturally without compression in an open-top reactor with internal dimensions of 20 × 20 × 10 cm, and ignited by using a metal coil with 100 W applied (introduced in Chapter 3). Mass-based ignition protocol (turning off the ignitor when the monitored real time mass loss showed 10% sample mass loss) developed in Chapter 4 was used in this study.

There were nine peat samples named as NAT0-10, NAT10-20, NAT20-30, DRA0-10, DRA10-20, DRA20-30, RES0-10, RES10-20, and RES20-30, with NAT, DRA, and RES representing samples from peatland in natural conditions, drained peatland, and peatland under restoration, and 0-10, 10-20, and 20-30 representing samples taken from depth range of 0-10, 10-20, and 20-30 cm at each sampling site. The detailed sampling process and sample characterisation were introduced in Chapter 2, and all physical and chemical properties of these samples were summarised in Figure 2.13. These samples all had high moisture contents (218% – 1898 %, by dry mass) when taken from the field, and were naturally dried in the laboratory environment to 100% moisture content. The initial mass of each sample was weighted and a 20 g sub sample was taken from each sample to dry in an oven with 80 ℃ before drying to

calculate the initial moisture content and the mass loss of water needed to reach 100% moisture content. Before each experiment another 20 g sub sample was taken to dry in the oven with 80 ℃ to verify the moisture content. The actual moisture content obtained in this verification is within ±2% to the targeted value. In total nine experiments were conducted for these nine samples with only one experiment for each sample because of the limited quantity of these field peat. The limited replicate per condition can be a limitation of this study.

All experiments were conducted in a stable ambient laboratory environment with ambient temperature at 23.1 ± 0.8 ℃ and relative humidity at 53.7 ± 4.5 %. Each experiment was terminated when there was no further mass loss and the temperature at all thermocouples decreased to ambient temperature. The results of steady stage were the average of the data in the duration from 20% mass loss to 80% mass loss for all experiments (as described in Chapter 5).

6.3 Results and Discussion

6.3.1 Overview of the burning process

Figure 6.1 summarised the mass loss rate and normalised mass (remaining mass in reactor divided by the original mass in reactor) for all nine experiments conducted using nine different samples. These data represent the burning process of all smouldering experiments conducted in the same experimental set-up by using peat samples in the same moisture content (100%) from different field conditions. The variation of the burning process (e.g. time of ignition and burning, the variation of mass loss rate) indicates the natural variation in peat properties greatly influence the fire dynamics.

The first peak of the mass loss rate for each experiment shows the mass loss rate at the end of ignition. The time duration of ignition (to reach 10% sample mass loss) presented in Figure 6.1 ranging from 0.5 h for NAT0-10 to 2.3 h for DRA20-30 indicates the higher the bulk density is, the longer it takes at the ignition stage. Smouldering was not self-sustained in sample DRA20-30 because this peat sample has a high inherent dry bulk density, and according to the finding in Chapter 4, it also has a high heat sink density. The critical moisture content for DRA20-30 is below 100%. Chapter 7 presented another smouldering experiment conducted by using DRA20-30 in 50% moisture content of which smouldering was successfully self-sustained and the sample burned for 53.4 h.

The total burning time for these samples ranges from 7.6 h (NAT0-10) to 33.8 h (DRA10-20), which is also proportional to the dry bulk density of each sample as there are more fuels to burn. In general, samples from site NAT with lower bulk density experienced less extensive burning compared to samples from site DRA and RES (52% and 33% less on average), and samples from deeper range with higher fuel density experienced more extensive burning (e.g. 109% more in NAT20-30 than NAT0-10). Figure 6.1 also shows the mass loss rate of these field peat samples has more fluctuations at steady stage with more obvious peaks and valleys than the mass loss rate of the horticultural peat (in Chapter 5 and previous study [39]). This was because of the continuous formation and collapse of overhang [25], which can be confirmed by the visual and IR footages. The increase of fluctuation was because of the existence of large fibrous particles in field peat samples, which improved the cohesion between soil particles. Horticultural peat samples were usually milled and processed by the manufacturer to form smaller and more homogeneous soil particles.

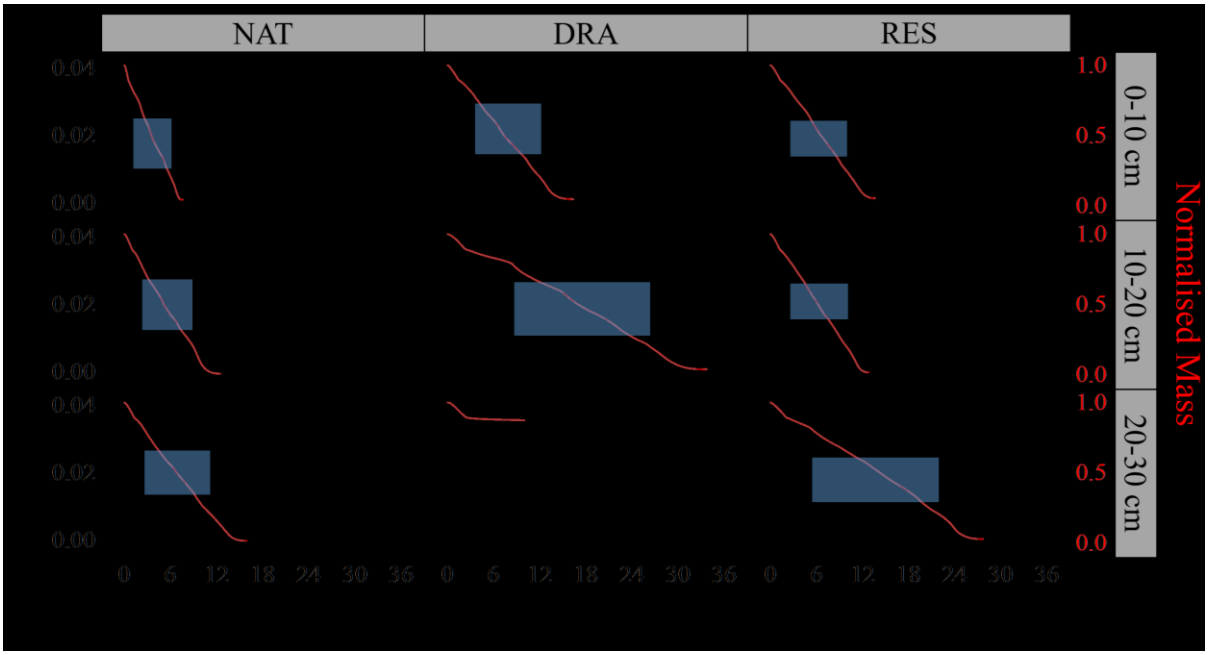

Figure 6.1 Summary of the mass loss rate and normalised mass in the burning process for all experiments. Normalised mass is calculated as the real time sample mass in the burning process divided by the initial sample mass in the reactor. The time duration of ignition (t_{ig}) and the total time duration (t_{to}) from ignition to mass loss rate decreased to 0 for each experiment are also presented in this figure. The wet bulk density (kg/m^3) of each sample is marked individually in each figure. The blue cloud marks the steady stage of each experiment. Smouldering was not self-sustained in sample DRA20-30.

Figure 6.2 shows the comparison of mass loss rate data at steady stage for all experiments. As defined in Chapter 4, we use data at the time range from 20% to 80% mass loss to represent the steady stage value. The averaged mass loss rate ranges from 0.016 to 0.020 g/s, and has a significant statistical difference ($p < 0.05$) between field samples. Potentially samples with the highest dry bulk density above 200 kg/m^3 in 100% moisture content (DRA10-20 and RES20-30), and sample with the lowest dry bulk density below 120 kg/m^3 in 100% moisture content (NAT0-10) have the lowest averaged mass loss rate. Previous research have found the burning rate of the high bulk density peat is much lower than the burning rate of low

bulk density peat and related the potential reason to chemical kinetics [82]. The difference in burning rate between different peat samples needs more studies in future to understand the influential factors for this difference in fire dynamics. Figure 6.2 also shows the comparison of the mass loss rate between field samples and horticultural samples. In general, the averaged mass loss rate of Irish horticultural peat is higher than the Scottish field peat. This difference can be originated from the difference in soil structure or the chemical kinetics.

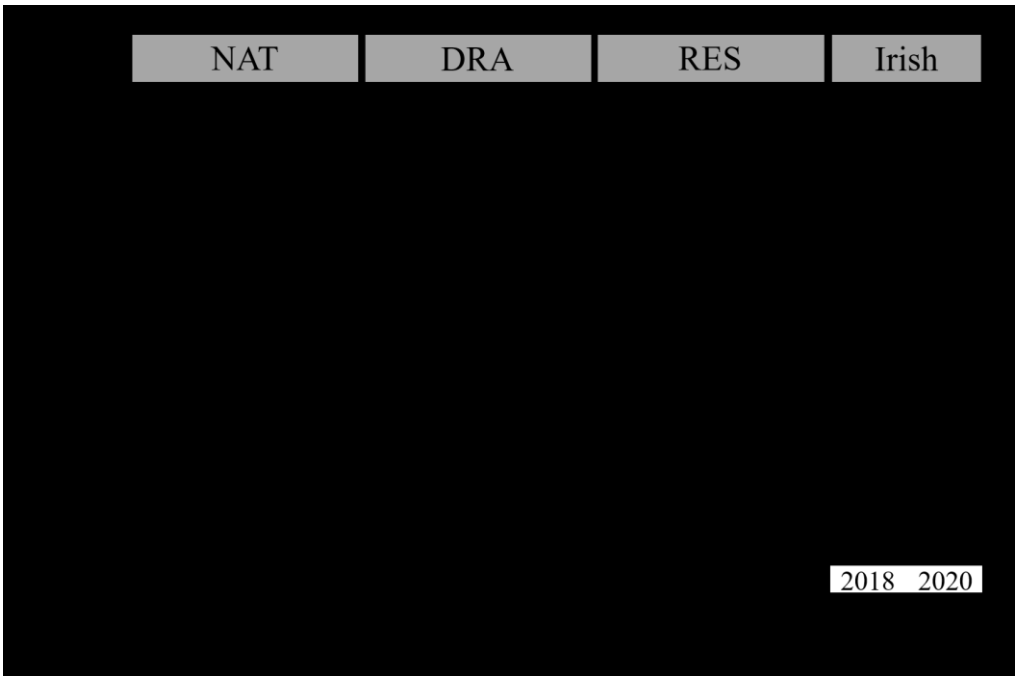

Figure 6.2 Boxplot of the mass loss rate at steady stage of all smouldering experiments. Smouldering was not self-sustained in DRA20-30, so the mass loss rate marked as 0. The whiskers of the boxplot represent the maximum and minimum values. Each box shows the lower quartile (25^{th} percentile), the median (50^{th} percentile), and the upper quartile (75^{th} percentile). The mean value is shown as a square dot. The mass loss rate data of the smouldering experiments using Irish 2018 (H) and Irish 2020 (H) in 100% moisture content are also shown in this figure for comparison (each includes three repeats).

6.3.2 Thermal residence time

Thermal residence time is the time duration above a temperature threshold at a certain location, which is an important parameter quantifying the thermal fire severity caused by smouldering [15, 18]. Previous research found thermal residence time above 300 ℃ in soil for more than 1 h leads to severe irreversible soil sterilization [18]. By analysing the temperature data obtained by thermocouples, thermal residence time of all experiments were calculated and presented in Figure 6.3. The results show the thermal residence time above 300 ℃ at all these samples exceed 1 h, which indicates smouldering wildfire can cause a severe soil sterilization in all these types of peatlands. Comparing between the results of samples from different types of peatland conditions, samples from site DRA and RES, especially at deep range, in average experienced longer thermal residence time above 300 ℃ than samples from site NAT, indicating higher severity and worse soil sterilization. Figure 6.3 also shows the peak temperature in each experiment ranging from 500 ℃ to 600 ℃, which agrees with the literature value [25, 39, 82]. A previous study mentioned the difference in peak temperature and oxidation temperature between high density peat and low density peat [82]. Figure 6.3 shows samples with higher level of bulk density (DRA10-20 and RES20-30) have higher thermal residence effect than samples with lower level of bulk density.

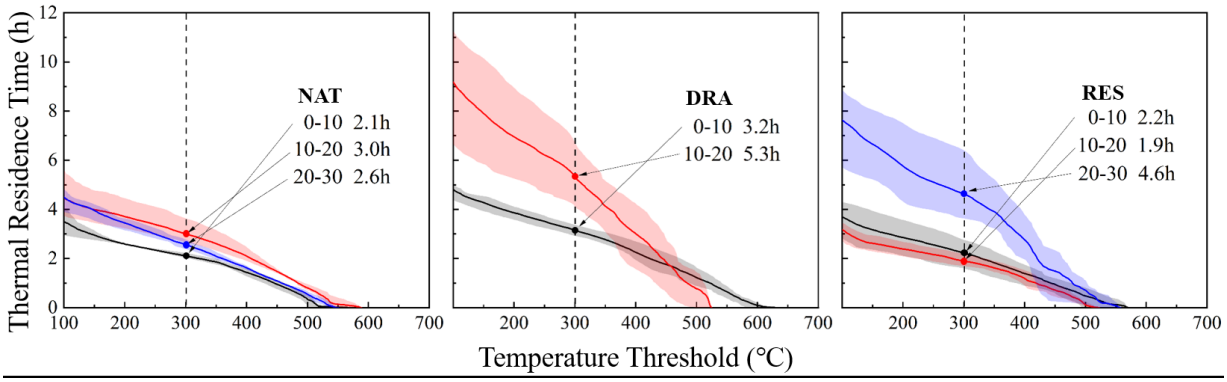

Figure 6.3 Thermal residence time at 8 cm depth during smouldering propagation. Thermal residence time is the time duration above a temperature threshold at a certain location [18]. The line represents the averaged value based on the temperature measurement of thermocouples at 8 cm depth and 7 cm, 11 cm, and 15 cm from the start location of ignition (TC10, TC11, and TC12 in Figure 3.3). The clouds represent the maximum and minimum values. The listed hours are the thermal residence times above 300 °C.

6.3.3 Smouldering spread rate

Previous research has found the linear relationship between the horizontal spread rate with the inverse of heat sink density, and the linear relationship between the in-depth spread rate with the inverse of organic density [29]. By following the calculation method introduced in Chapter 3, the heat sink density and organic density of all nine peat samples in 100% moisture content used in this study are presented in Figure 6.4. The results show samples of NAT have the lowest heat sink density and organic density, and samples of DRA have the highest heat sink density and organic density when they are both in 100% moisture content. The heat sink density and organic density also increase with the depth when they are in the same moisture content. According to the finding in Chapter 4, DRA20-30 has the highest heat sink density, which can explain the result of not self-sustained smouldering.

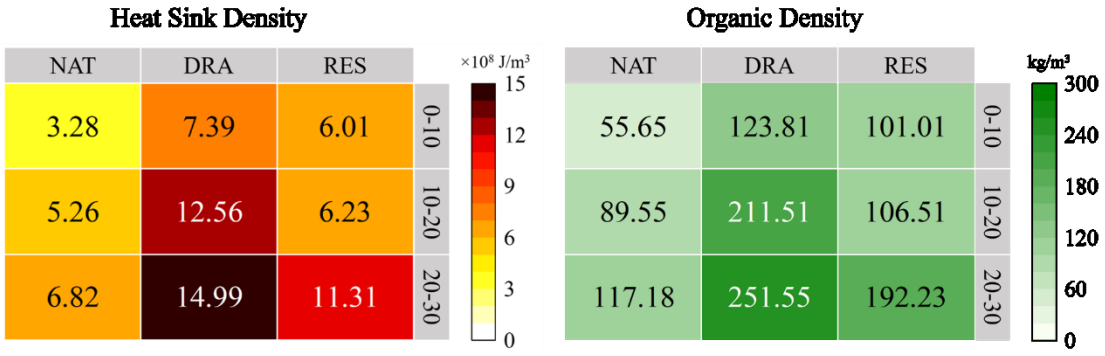

Figure 6.4 Map of heat sink density and organic density for samples used in this study.

By plotting the data of horizontal spread against the inverse of heat sink density (Figure 6.5(a)), and in-depth spread data against the inverse of organic density (Figure 6.5(b)) in this study, the spread theory developed in previous research [29] burning horticultural peat (Irish 2018(H)) with modified moisture content and bulk density in a shallow reactor was proven again by the high linearity with R^2 values of 0.96 and 0.97 in burning peat samples with naturally different bulk density with a large range. Results shows samples of NAT with lower heat sink density and organic density had the fastest smouldering spread in both horizontal and in-depth directions, and samples of DRA had the slowest spread ($p < 0.05$) when all samples were in 100% moisture content. Samples from deeper range show a slower spread in both directions even without considering the effect of oxygen supply changed by the formation of ash layer in the field condition with deep peat layer [89].

For comparison of the in-depth spread, the data from a previous research by Huang and Rein, 2017 [89] studying the in-depth spread of smouldering peat fire with the effect of moisture content and bulk density was added in Figure 6.5 (b). The in-depth spread rate in that study was from the direct measurement by thermocouples like the horizontal spread tracking thermocouple data of the smouldering front moving at the measured direction, which is the only literature reporting the experimental data of in-depth spread rate by directly tracking the

smouldering front using thermocouple data in smouldering peat. The comparison shows our method of estimating in-depth spread rate captured the trend of spread rate variation and correlated very well with the inverse of organic density. In general, the in-depth spread in our estimation is higher than the data from Huang and Rein's measurement, which can be caused by the difference in experimental configuration. Huang and Rein [89] used a column reactor with an internal dimension of 10×10×30 cm, which has a smaller burning section and deeper depth. The other in-depth spread study in literature is the work of Christensen [29] who reported the in-depth spread rate three times faster by using a shallow reactor with a depth of 1.6 cm and estimating the in-depth spread by using IR signature tracking the smouldering leading edge and trailing edge. To better understand the control parameters of horizontal and in-depth spread, the effect of scale in experiments should be considered in future research.

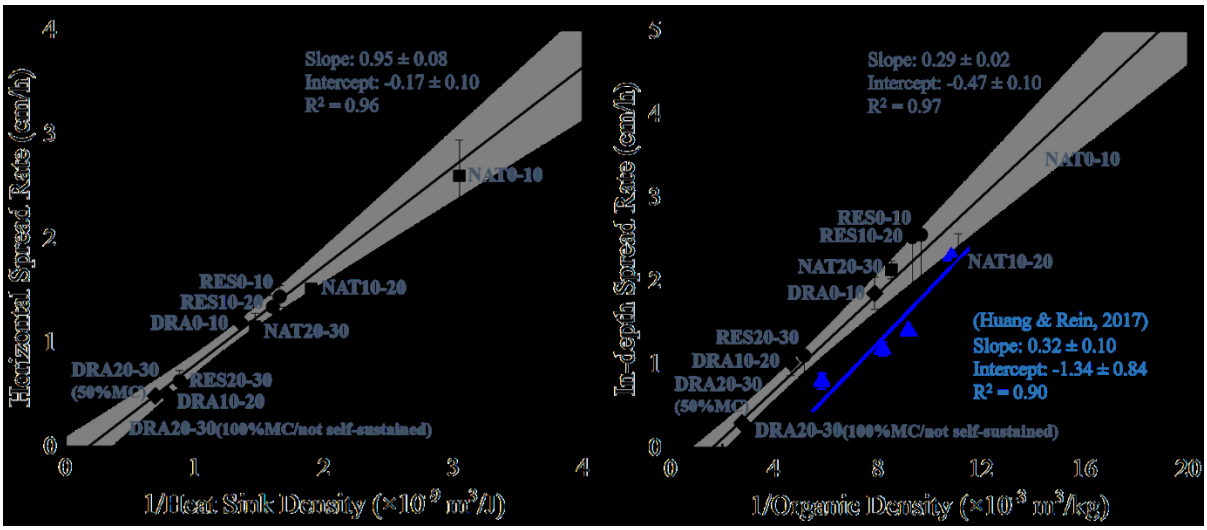

Figure 6.5 (a) The linear relationship between horizontal spread rate and the inverse of heat sink density. (b) The linear relationship between in-depth spread rate and the inverse of organic density. The data is compared with the experiments using a column reactor (10×10×30 cm) conducted by Huang and Rein, 2017 [89] (shown in blue color, only the averaged in-depth spread rate in the same depth range of 0-10 cm is plotted), which has the only reported direct measurements of in-depth spread rate of smouldering peat in controlled MC and density in

literature. The linear fit in (a) and (b) does not include the result of DRA20-30 with 100% MC which was not self-sustained and reported as 0 in both horizontal and in-depth spread. The spread rate in sample DRA20-30 with 50% MC is included in both fitting.

6.3.4 Gas emissions

Figure 6.6 shows the comparison of emission factors for the four most abundant emission gases, CO_2, CO, CH_4, and NH_3, in smouldering peat fire. The results show DRA samples had lower ($p < 0.05$) averaged emission factors of CO_2, CO and NH_3, and a higher ($p < 0.05$) averaged emission factor of CH_4 compared to samples of NAT and RES. These differences are highly related to fire dynamics and the process of smouldering. Previous research found the increase of the emission factors of CO_2, CO and NH_3 are because of the increase in the proportion of char being oxidised [39, 48], while CH_4 is mainly emitted from the decomposition of hemicellulose and cellulose in the process of peat pyrolysis [39, 48, 52, 90]. Drainage can greatly influence the peat bulk density by the effect of consolidation [87]. DRA samples from drained peatlands are in higher density and more consolidated with limited oxygen penetration, which leads to a stronger pyrolysis emitting higher amount of CH_4, and weaker oxidation emitting less CO_2, CO and NH_3. The increase of the emission factor of CH_4 also followed the trend of density increase with DRA10-20 and RES20-30 (drained peatland under restoration) showing the highest emission factors of CH_4.

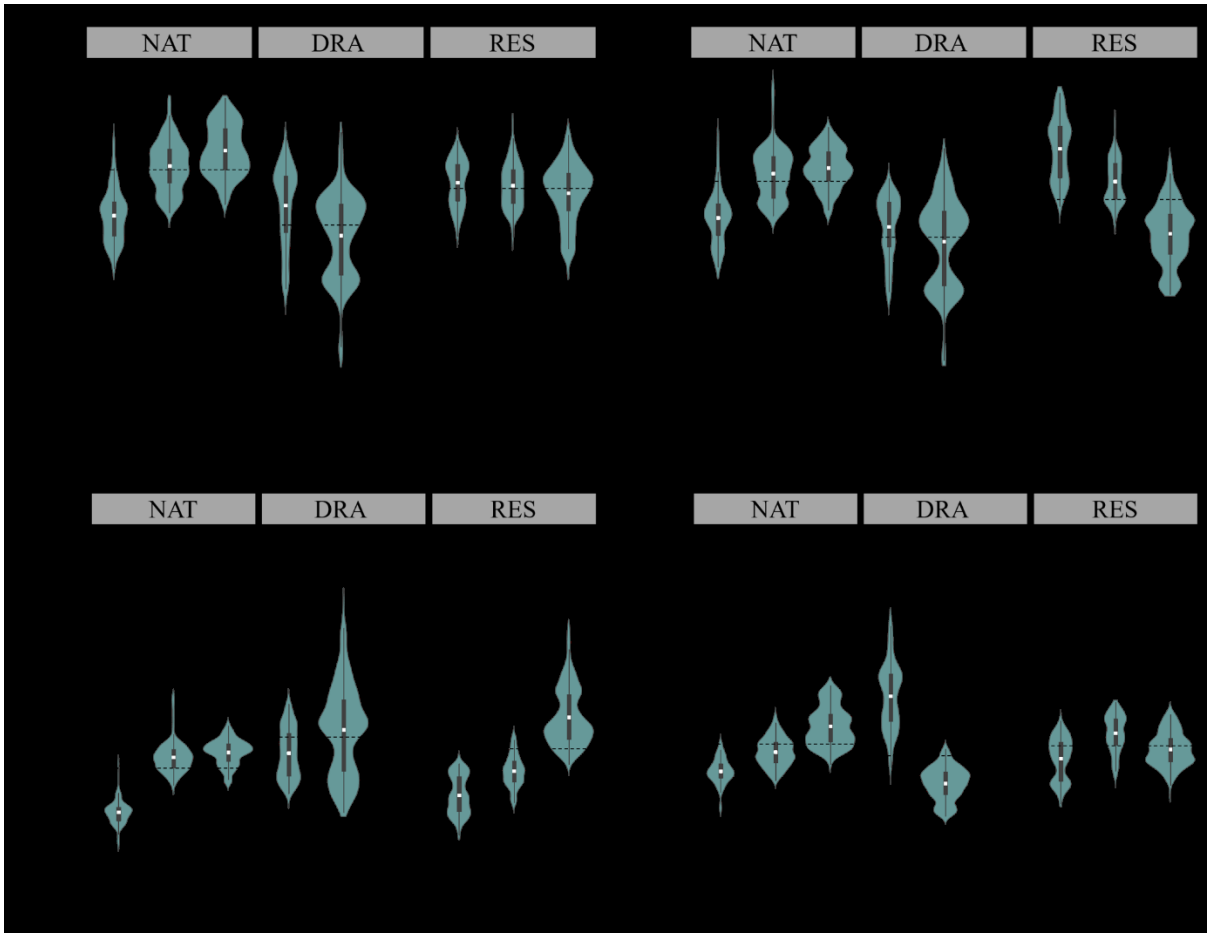

Figure 6.6 Emission factors of CO_2, CO, CH_4, and NH_3 measured by FTIR in this experimental study of samples from different field conditions. The dashed lines represent the averaged EF value of smouldering peat at different depth from the same field condition. The white squared dot represents the mean value. The black box represents the data percentage of 25% and 75%.

6.3.4 Particle emissions

There are limited number of studies investigating the particle emissions from peatland fires [4, 7]. The emission factor of particles from peat fires ranges from 5.9 g/kg [49] to 44.5 g/kg [51] in literature. Figure 6.7 summarised the emission factors of PM1, PM2.5, and PM10 in this experimental study. The results show the averaged emission factors of particles in the combustion of samples DRA and RES were nearly twice as high as that of NAT. The emission factor ranges from 25 g/kg (NAT0-10) to 55 g/kg (DRA10-20). This difference might be caused

by the chemical composition of the peat or the soil bulk density. A previous peat fire study conducted in the same experimental set-up by using Irish 2018 (H) with low bulk density reported the emission factors of 24.48 ± 1.06, 23.12 ± 1.19, and 15.04 ± 1.12 g/kg for PM10, PM2.5, and PM1, which is very similar to the results of burning NAT samples. Results of our study also show the PM2.5 (particles with aerodynamic diameters of less than 2.5 μm) dominated the particle emissions, which agrees with previous peat fire studies [39, 42].

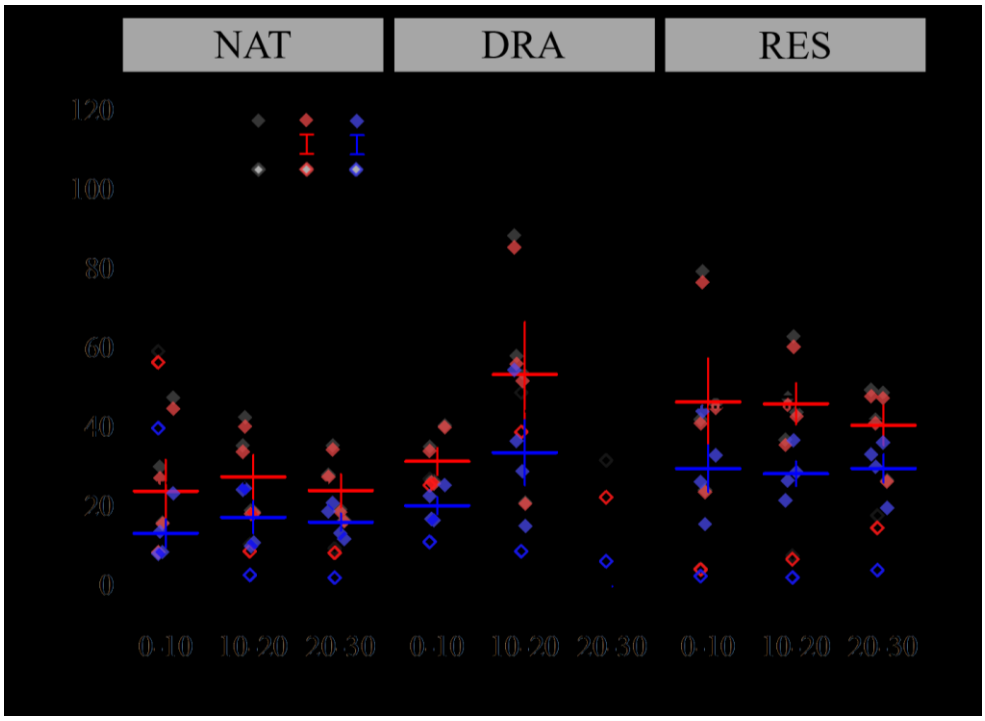

Figure 6.7 Emission factors of PM1, PM2.5, and PM10 measured by PM cascade impactor in this experimental study of samples from different field conditions. Each experiment sampled particles once at the ignition stage (when 5% mass loss) and four times at the steady stage (when 20%, 40%, 60% and 80% mass loss). Smouldering was not self-sustained in sample DRA20-30 (100% MC), so only the measurement of ignition stage was included. The dashed lines represent the averaged EF value at steady stage of the total particulate matter (TPM) for samples from the same field condition.

6.3.5 Implications to the field

Our field study was conducted six months after the fire event in that area. Although the field condition has changes compared to the condition right after the fire event, some evidences of severe burning still remained in the burnt area. Figure 6.8 shows the deepest burning observed in our field study in natural peatlands, drained peatlands and peatlands under restoration (drained previously and in the early stage of restoration), which represent the most severe fire effects on those types of peatlands in the fire event. The depth of burn (DOB) is the thickness of peat layer that is burnt in smouldering wildfire, which is an important parameter used to estimate the carbon emissions [4-6, 91]. We measured the depth of burn based on the deepest burning remained in the field, and the results are shown in Figure 6.9(b). The results show the averaged depth of burn in drained peatlands is around 25 cm, and the averaged depth of burn in natural peatlands is around 8 cm (both representing the most severe case in the fire event).

The depth of water table in peatlands limits the depth of burn in smouldering fires [92], which is an important parameter to monitor in peatland management. Figure 6.9(a) shows the variation of the depth of water table in Flow Country in the months of May, July and November from the Forsinard Flows reserve database published in [92]. In the month of our field study, the depth of water table is at its highest level in the year, which matches our field moisture content measurement. July is the month that water table at its lowest level in the year, 22 cm for natural peatlands and 33 cm for drained peatlands. In the month of fire event, the water table depth in natural peatlands is around 10 cm and in drained peatlands is around 20 cm. The difference in the depth of water table between natural and drained peatlands can explain the difference in the depth of burn shown in Figure 6.9(b). The ratio of the depth of burn over the depth of water table is higher in drained peatlands than in natural peatlands, which can be

because the water capacity in natural peatlands is better, thus higher moisture distribution above the water table.

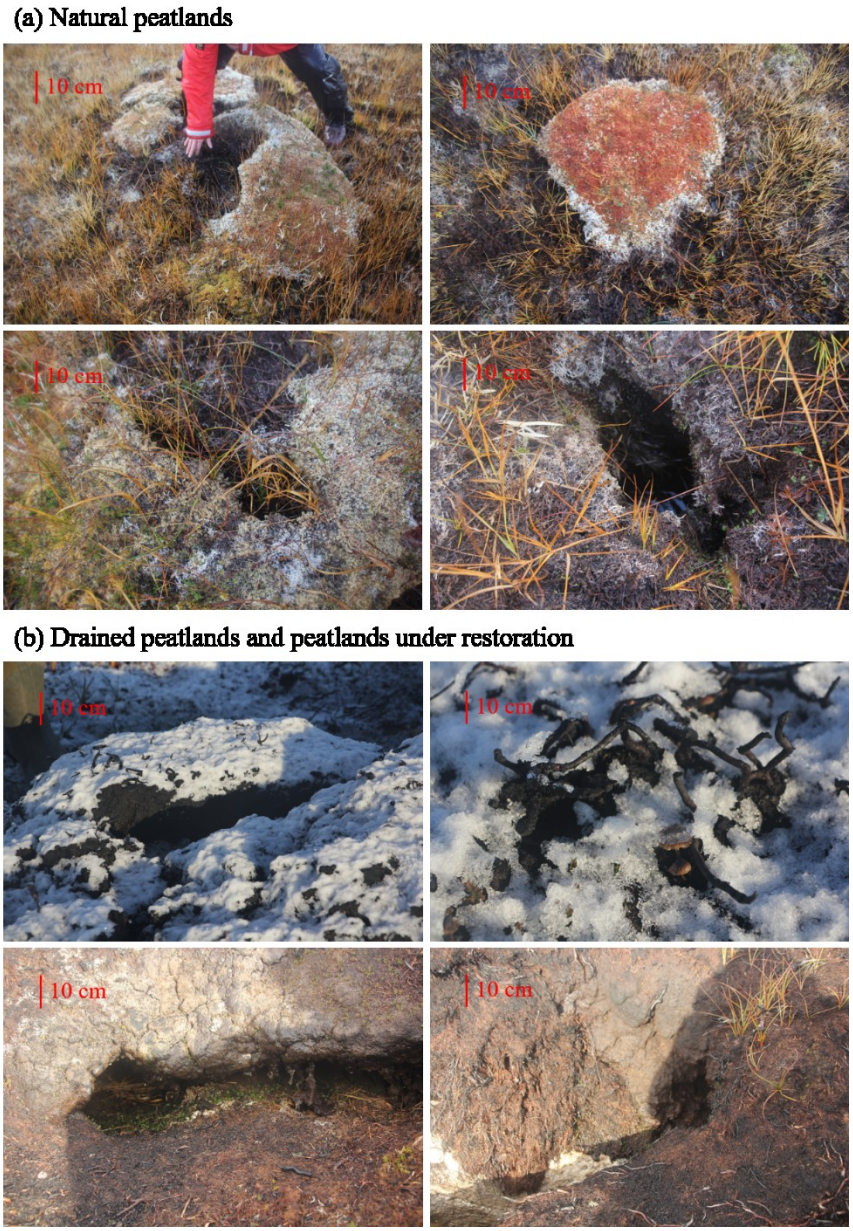

Figure 6.8 Site observations of the deepest burning remained in the field. Scales of references are added to images in red color.

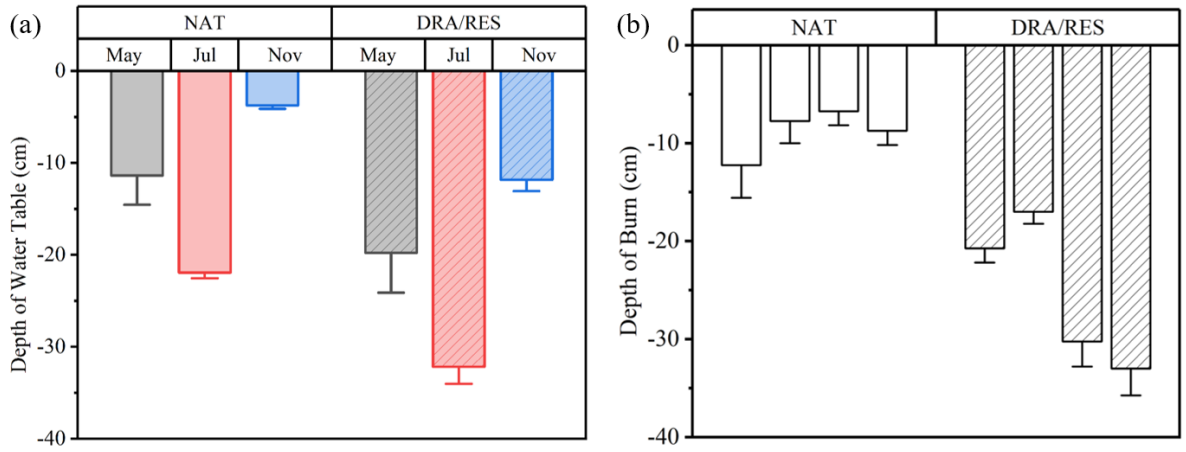

Figure 6.9 (a) Data of depth of water table in May (the month of fire event), July (the month of deepest), and November (the month of highest and the month of our field study) in natural peatlands and drained peatlands (including peatlands under restoration) in Flow Country (data from [88]). (b) Depth of burn measured in our field study in natural peatlands and drained peatlands (including peatlands under restoration) based on the most severe cases observed in the field. Four locations of the deepest burning remained in each type of peatland were chosen in the field to measure. These bar charts in (a) and (b) show the average and one standard error.

In our laboratory experiments, all peat samples were naturally dried to the same moisture content, 100%, representative field moisture content that fire can start [70] and often used in laboratory peat smouldering studies [15, 39]. However, in the field condition natural peatlands could have higher moisture content even when in drought condition, especially at deeper range. Using 100% moisture content in this study for peat samples from natural peatlands can represent the condition of newly drained natural peatlands which have experienced the shrinkage process with minor increase in bulk density, but have not experienced the consolidation process like samples from long-term drained peatlands. The experimental results of ignition and spread indicate newly drained peatlands with low bulk density in drought condition are more vulnerable to fire in terms of easier ignition and faster fire spread in both horizontal and in-depth directions.

From our laboratory results about smouldering spread in peat samples from different field conditions, we have obtained the correlation between the horizontal spread rate and the heat sink density, and the in-depth spread rate and the organic density. This correlation is very important for peatland management related to fire risk management. As heat sink density and organic density can be calculated from three very basic properties of peat, moisture content, bulk density and inorganic density, by sampling the bulk density and inorganic density of the peat in the field and monitoring the field moisture content, the probability of ignition and spread can be quantified in the peatland management, thus fire risks can be better assessed and fire prevention methods can be applied.

6.4 Conclusion

This chapter used a novel bench-scale experimental set-up to investigate the smouldering dynamics and emissions of field peat samples from natural peatlands, drained peatlands and peatlands under restoration sampled in Flow Country, Scotland. Built upon previous works on fire spread and emissions, our findings enable a better understanding of how natural variation and field conditions influence the peat properties, thus influence the fire dynamics and emissions. By analysing the burning rate, thermal residence time, horizontal and in-depth spread rate, gas and particle emissions, we provide insights into the fire risk and severity in peatlands in different field conditions. The results show high bulk density peat from long-term drained peatlands experience higher soil deterioration, and more extensive burning in terms of the amount of fuel burnt, and the amount of carbon and particle emitted. Newly drained natural peatlands with low bulk density in drought condition are more vulnerable to fire in terms of easier ignition and faster fire spread. It is remarkable that our approaches of laboratory study can contribute to the field fire management.

Chapter 7

Laboratory Study of Smouldering Multi-dimensional Spread in Samples of Different Origins

Summary

This chapter presents the laboratory study to investigate the multi-dimensional smouldering spread and the associated emissions of peat samples of different origins. Controlled laboratory conditions with diagnostics monitoring the ignition, spread, and associated emissions facilitate the investigation of different types of peat samples in smouldering. This chapter also summarised the spread data in all chapters of this thesis. The results again confirmed the spread theory showing the linear correlation between horizontal spread rate and the inverse of heat sink density, and between in-depth spread rate and the inverse of organic density in a different configuration with different types of peat. Furthermore, looking at the overall progress of multi-dimensional spread, a critical angle of spread direction (65° relative to horizontal plane) above which smouldering cannot self-sustain was found and explained by the controlling parameters and energy balance. Emissions of different types of peat in smouldering are also quantified, we broadened the range of modified combustion efficiency (MCE) for smouldering to 0.74 – 0.88, wider than values previously reported in literature, and found to be significantly dependent on the fuel composition. This study provides a better understanding on how natural variation in peat can influence the fire dynamics and emissions.

7.1 Introduction

In previous laboratory peat fire studies, horticultural peat which is mainly used as a soil improver in horticulture is the most commonly used peat [15, 19, 23, 25, 27, 42, 78, 79]. This type of peat is commercially available with good consistency between bags and already processed by peat mining company to a relatively uniform condition in soil properties, which is suitable for studying the fundamental parameters under controlled conditions and can meet

the need of experimental repeats [24]. Some studies used peat samples taken from the field [18, 80-82], which has more complexities in soil properties but close to the natural conditions. Field peat sample is more challenging to obtain and limited in quantity, which also has issues of transportation and time. Studying field peat samples is meaningful and necessary in understanding the natural variation in peat smouldering and linking the lab experiments with field measurements.

In this work, laboratory experiments were conducted with measurements quantifying the burning rate, temperature variation, horizontal and in-depth spread rate, and gas and particle emissions of smouldering peat from different origins. Summarising all the multi-dimensional spread data in this thesis, the topic of how the three most important soil properties, inorganic content, moisture content and bulk density, together influence the smouldering dynamics is better explained, which can be applied to peat with different soil conditions and of different origin.

7.2 Method

This chapter presents the bench-scale smouldering experiments conducted by using peat samples of different origins, including five types of horticultural peat, Irish 2020 (H), Irish 2018 (H), Canadian (H), Latvian Black (H) and Latvian White (H), and field peat samples of Indonesian Palangkaraya (F), Indonesian GAMBUT (F), Scottish DRA0-20 (F), and Scottish DRA20-30 (F). The origins of the samples and the characterisation of the physical and chemical properties (summarised in Table 3.1) are presented in Chapter 3. The experiments were conducted using the emission rig developed in previous research [39], which was introduced in detail in Chapter 3. There were six types of diagnostics applied to this study to measure the real time mass loss (mass balance), temperature profile (thermocouples), visual and infrared

images (Gopro and FLIR camera), gas emissions (FTIR), and particle emissions (PM cascade impactor), which were also introduced in Chapter 3. Peat samples were deposited naturally without compression in an open-top reactor with internal dimensions of 20 × 20 × 10 cm, and ignited by using a metal coil with 100 W applied. Mass-based ignition protocol (turning off the ignitor when the monitored real time mass loss showed 10% sample mass loss) developed in Chapter 4 was used in this study.

The main objective of this chapter is to study the difference of smouldering dynamics in samples of different origins, and quantify the emissions of these samples. Table 7.1 summarised all experiments conducted in this chapter by using different types of peat to achieve the objective. As not all peat types had enough quantity of sample to conduct repeated experiments, 100% moisture content was chosen to start for all types of peat because it is the most commonly used moisture content in studying smouldering peat in laboratory experiments [15, 39], and a representative moisture content for field condition that fire can be initiated [70]. Controlling samples to the same moisture content also allows the comparison of the results obtained by different types of peat, as moisture content is the most important physical parameter influencing smouldering dynamics [93]. If 100% moisture content peat can be ignited and the amount of sample was enough for more experiments, higher moisture content would be investigated to find the critical moisture content for ignition (the moisture content above which self-sustained smouldering cannot be initiated). If smouldering cannot sustain in 100% moisture content, 50% moisture content would be used. Methods of sample preparation were introduced in Chapter 3.

The results of Irish 2020 (H) included in Table 7.1 were experiments done in this thesis presented in Chapter 4 and 5, with only the results of 100%, 160% (critical moisture content), and 180% (not self-sustained case above the critical moisture content) representing the most

commonly used moisture content for comparison, and the moisture content near ignition limit. The results of Irish 2018 (H) included in Table 7.1 were experiments done in this chapter with 100%, 200%, and 220% moisture content. Irish 2018 (H) was used in previous experimental study using the same experimental set-up to investigate the effect of moisture content on fire dynamics and emissions, but with the original time-based ignition protocol (turning off ignitor in 30 min), and found 160% as the critical moisture content for ignition [42]. This chapter used the mass-based ignition protocol developed in Chapter 4 to conduct experiments using 100% moisture content and higher moisture content (200% and 220%) to find the critical ignition condition. Canadian (H) was enough for three repeats of experiment in 100% moisture content, and extra experiments using 180% and 200% to find the critical moisture content for ignition. These three horticultural peat had relatively more quantity than other types of peat used in this chapter (information summarised in Table 7.1.

All experiments in this chapter were conducted in a stable ambient laboratory environment with ambient temperature at 20.6 ± 1.9 ℃ and relative humidity at 55.5 ± 10.3 %. Each experiment was terminated when there was no further mass loss and the temperature at all thermocouples decreased to ambient temperature. The results of steady stage were the average of the data in the duration from 20% mass loss to 80% mass loss for all experiments.

7.3 Results and Discussion

7.3.1 Overview of the smouldering dynamics

Table 7.1 summarised the key indicators and results of fire dynamics for all experiments conducted using different samples. These data represent the ignition conditions and free burning process of all smouldering experiments conducted in the same experimental set-up.

The variation of the burning process indicates the natural variation in peat properties (introduced in Chapter 2 and 3) greatly influence the fire dynamics. The critical moisture content for ignition were found for three types of horticultural peat, 160% for Irish 2020 (H) (as introduced in Chapter 4), 200% for Irish 2018 (H), 180% for Canadian (H). Because of the limited quantity of other types of peat, the critical moisture content cannot be narrowed to a certain value, but the ranges were found, for Latvian Black (H) and Latvian White (H) to be above 100%, for Indonesian Palangkaraya (F) and Scottish DRA20-30 (F) to be between 50% and 100%. Smouldering in Indonesian GAMBUT (F) were initiated but not self-sustained due to the high inorganic content and the consolidated condition.

Comparing the averaged burning rate and peak temperature at steady stage between the results at the critical moisture content for ignition and 100% moisture content, it is found that at the critical moisture content, there was a significant decrease ($p < 0.05$) in burning rate and peak temperature in all these three types of peat, because smouldering was hardly sustained at the limit and the propagation was not stable with a lot of interruptions from the collapse of overhang, which is also confirmed by the visual and IR footages. This finding agrees with the finding in Chapter 5 that the burning rate and peak temperature do not have significant changes when increasing moisture content from 100% to 140%, but with an obvious drop at 160% moisture content. The results show the drop of burning rate and peak temperature is more significant in Irish 2018 (H) and Canadian (H) at the critical moisture content than Irish 2020 (H). Table 7.1 also includes the result of spread rate, which will be discussed in 7.3.2.

Table 7.1 Summary of the smouldering dynamics of all experiments

Peat Type	MC (%)	Num. of exp.	Burning rate[a] (g/min)	Peak temperature[b] (°C)	Spread rate	
					S_h (cm/h)	S_d (cm/h)
Irish 2020 (H)	100	10	0.65 ± 0.05	579 ± 36	1.25 ± 0.08	2.24 ± 0.31
	160*	5	0.60 ± 0.12	468 ± 125	1.07 ± 0.07	2.25 ± 0.23
	180	5	Not self-sustained			
Irish 2018 (H)[c]	100	3	0.80 ± 0.09	578 ± 20	2.22 ± 0.44	2.43 ± 0.86
	200*	2	0.31 ± 0.14	311 ± 43	1.22 ± 0.34	2.31 ± 1.00
	220	1	Not self-sustained			
Canadian (H)	100	3	0.74 ± 0.11	509 ± 87	3.40 ± 0.49	4.51 ± 0.41
	180*	1	0.48 ± 0.13	339 ± 137	1.71 ± 0.55	3.68 ± 0.44
	200	2	Not self-sustained			
Latvian Black (H)	100	1	0.63 ± 0.08	613 ± 12	1.56 ± 0.22	1.92 ± 0.76
Latvian White (H)	100	1	0.67 ± 0.08	559 ± 12	2.59 ± 0.40	3.03 ± 0.33
Indonesian Palangkaraya (F)	100	1	Not self-sustained			
	50	3	1.08 ± 0.24	647 ± 5	0.83 ± 0.33	0.54 ± 0.14
Indonesian GAMBUT (F)	100	3	Not self-sustained			
	0	3	Not self-sustained			
Scottish DRA0-20 (F)	100	1	0.53 ± 0.11	555 ± 34	0.74 ± 0.01	1.54 ± 0.55
Scottish DRA20-30 (F)	100	1	Not self-sustained			
	50	1	0.48 ± 0.10	585 ± 7	0.49 ± 0.02	0.30 ± 0.06

*Critical moisture content for ignition is the moisture content threshold above which self-sustained smouldering cannot be initiated in the peat sample. The critical moisture content for ignition were found for Irish 2020 (H), Irish 2018 (H), and Canadian (H) to be 160%, 200%, and 180%. The other samples used in this study all have limited quantity and cannot have more experiments to narrow the critical moisture content value, but the results indicate the critical moisture content for Latvian Black (H) and Latvian White (H) should all be above 100%, for Indonesian Palangkaraya (F) and Scottish DRA20-30 (F) should be between 50% and 100%.

[a]Burning rate is the mass loss rate of dry peat which was calculated by using the mass loss data extracting the mass loss of water assuming a constant drying process.

[b]Peak temperature is the highest temperature value measured by thermocouples at the 8 cm depth.

[c]The results of Irish 2018 (H) in 100% moisture content agree with previous study [39] using the same peat and experimental set-up.

7.3.2 Spread rate and spread direction

Smouldering has multi-dimensional spread as shown in Figure 7.1. The horizontal spread rate and in-depth spread rate in all smouldering experiments for different types of peat are presented in Table 7.1. The results of spread in different types of peat in this chapter again confirm the linear relationship between the horizontal spread rate and the inverse of heat sink density, and the in-depth spread rate and the inverse of organic density, which was also shown in Chapter 5, Chapter 6, and previous study first reported this theory [29]. Figure 7.2 plotted all data of horizontal spread and in-depth spread in this thesis, including the data in Chapter 5 studying the influence of moisture content and modified bulk density by compression on smouldering spread by using Irish 2020 (H), the data in Chapter 6 studying the influence of field conditions on smouldering spread by using field peat samples from Flow Country, Scotland, and data of experiments done in this chapter with more results from peat samples of different origins. The high linearity with R^2 values of 0.86 and 0.88 in such a great variety of sample conditions and origins confirm again the theory developed previously [29] to show the control parameters for horizontal spread and in-depth spread are the heat sink density and organic density.

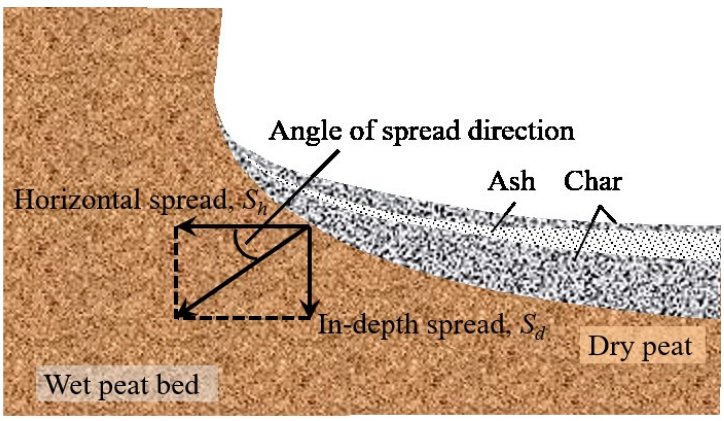

Figure 7.1 Illustration to show smouldering multi-dimensional spread. (Figure revised from the illustration in [25]).

The linear fitting line of data from the whole thesis of Christensen [29], including the studies of the effect of moisture content, inorganic content, and bulk density on smouldering spread in a shallow reactor (1.6 cm depth), is also plotted in Figure 7.2 for comparison. It is noticed that the slopes of the fitting lines for both horizontal spread rate with the inverse of the heat sink density (3.28), and in-depth spread rate with the organic density (0.67) in Christensen's thesis [29], are all around three times bigger than the slopes of fitting lines of the data from this thesis (0.97 and 0.23). This indicates the scale of the experimental set-up, especially the depth and the length of the reactor, can influence the smouldering spread by limiting the heat transfer regime in smouldering propagation when the smouldering front reaching the insulated boundary. Future research can investigate the scale effect on this spread theory and conduct sensitivity study for the size of the reactor.

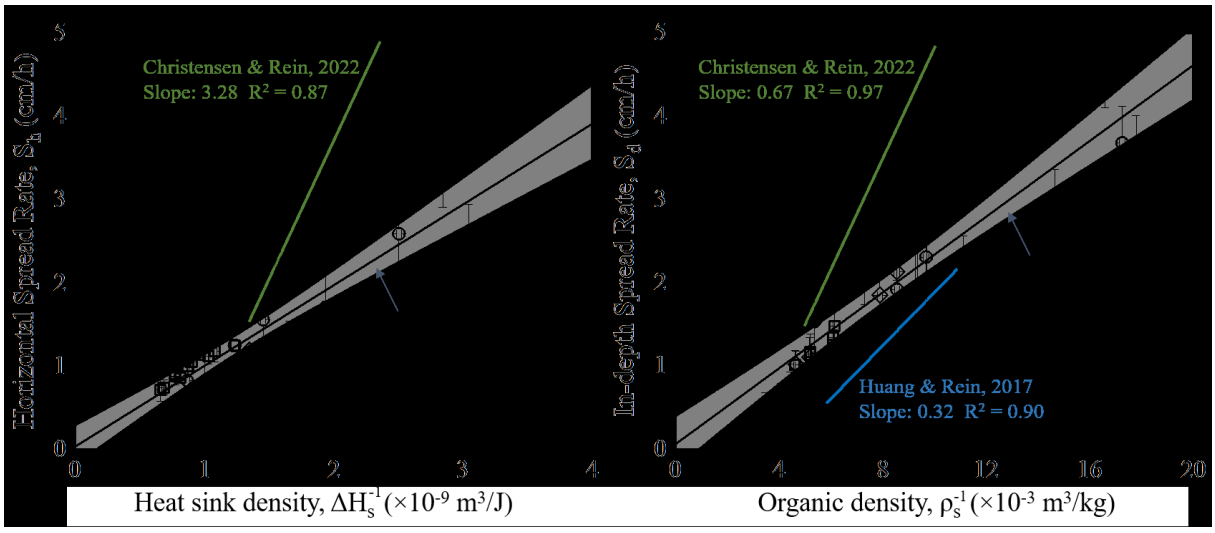

Figure 7.2 (a) The linear relationship between horizontal spread rate and the inverse of heat sink density. (b) The linear relationship between in-depth spread rate and the inverse of organic density. All data points in these figures are from the results of all experiments done in this thesis. The linear fit in (a) and (b) does not include the result of not self-sustained cases. The fitting lines concluded in Christensen's thesis [24] are also presented in these figures for comparison. (b) includes the fitting line obtained from the in-depth spread data in Huang and

Rein, 2017 [89] (only the averaged in-depth spread rate in the same depth range of 0-10 cm is plotted), which has the only reported direct measurements of in-depth spread rate of smouldering peat in controlled MC and density in literature.

The spread theory firstly presented in Christensen's thesis [24], showing the horizontal spread and in-depth spread are controlled by two different parameters, heat sink density and organic density, is examined in the experiments of this thesis. Christensen's thesis explained the difference of the controlling mechanism can be explained by the oxygen supply to the direction of spread [24]. In-depth spread is forward spread with oxygen supply in the same direction of smouldering spread, and oxygen cannot penetrate deeper without a certain depth of char layer consumed or oxidised [93, 94], so with the increase of organic density, the amount of char needed to be consumed for in-depth spread to continue is also increased. Horizontal spread is perpendicular to the direction of oxygen supply, which is more limited by heat sink effect, because the drying and pyrolysis front can propagate independently without oxygen supply if the endothermic process can continue [95]. Christensen's thesis [29] concluded the rate of char formed (drying and pyrolysis) has to be faster than the rate of char consumed (oxidation), so the horizontal spread has to be faster than the in-depth spread to have smouldering sustain. This conclusion explained the controlling parameters of horizontal spread and in-depth spread well, but overlooked some factors influence the calculation of horizontal spread and in-depth spread. Chapter 3 presented the expansion effect in Figure 3.2 when adding moisture to dry peat, the volume can expand to twice of the volume when increasing moisture. The in-depth spread rate was not only calculated from the effect of the consumption of char, but also the surface regression when drying front propagates. Drying front is also propagate horizontally, but due to the gravity, surface regression is only happening to the direction of in-depth spread, which accelerates the in-depth spread rate. In conclusion, the in-depth spread rate

is possible to be higher than horizontal spread rate, but because of the controlling mechanisms, there is a limit in the ratio.

Figure 7.3 plotted all horizontal spread and in-depth spread data in this thesis including many of the cases near ignition limit. A critical angle of spread is found to be around 65° (relative to the horizontal plane) above which smouldering cannot be self-sustained. The not self-sustained cases, for example, Irish 2020 (H) in 180% MC, Irish 2018 (H) in 220% MC, Canadian (H) in 200% MC, and Scottish DRA20-30 (F) in 100% MC, all showed 0 in spread rate, but by using the correlation found linking to the heat sink density and organic density to calculate the spread rate, the derived spread angles are all above 65°. This critical angle of spread is related to the ratio of horizontal spread rate and in-depth spread rate, which is further related to the ratio of the correlation of heat sink density and the correlation of organic density. Heat sink density is the energy needed to heat peat to smouldering temperature, while organic density is proportional to energy produced in peat combustion, so the physical meaning of this critical angle is the heat produced in smouldering combustion has to be larger than the heat needed to reach smouldering temperature, which perfectly defined the mechanism of self-sustained smouldering. As 65° is close to the degree of polar circle (66.6°), we name this theory as polar circle theory for critical angle of spread direction.

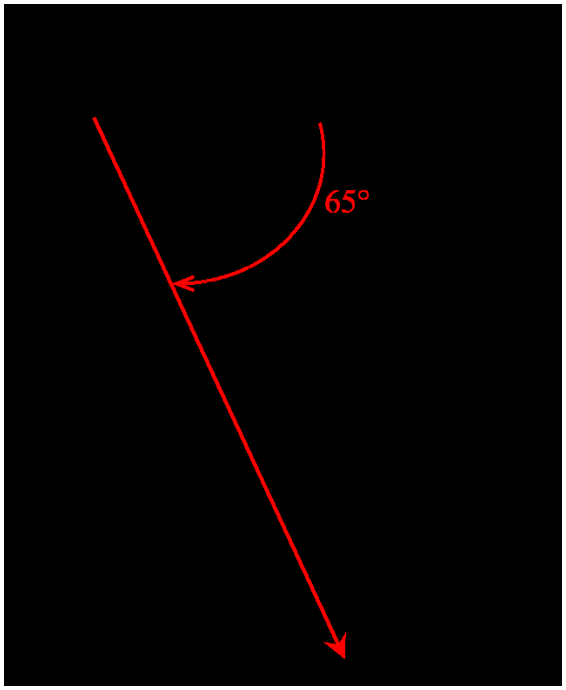

Figure 7.3 Plots of horizontal and in-depth spread data from all experiments in this thesis. A critical angle of spread direction above which smouldering cannot be self-sustained is found to be around 65˚ (shown as red arrow in this figure).

7.3.3 Gas and particle emissions

Table 7.2 summarised the modified combustion efficiency (MCE) and the emission factors (EF) of PM1, PM2.5, and PM10 for all smouldering experiments conducted using different samples. MCE is an important parameter widely used in atmosphere science and remote sensing to indicate combustion regime [33, 52, 83]. Previous research found flaming has a high MCE around 0.99, while the range of smouldering is 0.75 - 0.84. Our measurements for different types of peat at smouldering steady stage show the range of MCE can be broadened to 0.74 - 0.88. It is found that MCE is significantly dependent on the chemical composition of the fuel (MCE data has significant differences between different types of peat with p value all below 0.05), with a potential increase with the increase of the decomposition rate of the peat, for example, Irish 2020 (H) has a higher decomposition rate than Irish 2018 (H), and Latvian

Black (H) has a higher decomposition rate than Latvian White (H). The emission factors of particles are within the range of particle emissions reported in literature [7]. The difference between different types of peat can be also generated by the fuel composition, which still requires more investigations.

Table 7.2 Summary of the results of gas and particle emissions of all experiments

Peat Type	MC (%)	MCE	EF PM (g/kg)		
			PM1	PM2.5	PM10
Irish 2020 (H)	100	0.86 ± 0.01	11.87 ± 1.47	18.09 ± 2.23	19.49 ± 2.43
Irish 2018 (H)	100	0.74 ± 0.01	15.04 ± 1.12	23.12 ± 1.19	24.48 ± 1.06
Canadian (H)	100	0.80 ± 0.01	38.11 ± 8.39	56.40 ± 13.03	58.35 ± 13.58
Latvian Black (H)	100	0.88 ± 0.01	32.23 ± 6.61	53.13 ± 9.88	56.09 ± 10.7
Latvian White (H)	100	0.77 ± 0.01	25.49 ± 5.96	41.28 ± 6.71	45.17 ± 7.61
Indonesian Palangkaraya (F)	50	0.79 ± 0.02	8.63 ± 1.13	11.00 ± 1.40	11.25 ± 1.38
Scottish DRA0-20 (F)	100	0.79 ± 0.01	22.07 ± 6.1	37.41 ± 5.32	41.59 ± 3.93
Scottish DRA20-30 (F)	50	0.78 ± 0.01	36.76 ± 9.75	54.34 ± 14.13	57.67 ± 15.54

Figure 7.3 shows the particle mass concentration ratios derived from measurements of experiments conducted in this thesis. The measurement results have shown there is negligible amount of particles with aerodynamic diameters of larger than 10 μm emitted from smouldering peat, which agrees with literature [28, 39]. Three ranges of aerodynamic diameter for particle emissions were divided by referencing to the measurement methods: 0 - 1, 1 - 2.5, and 2.5 - 10 μm. The particle emission ratio is defined as the mass concentration at each range divided by the mass concentration at the total range. Ternary plot in Figure 7.4 shows distinctive groups of the particle emission ratio for the ignition stage and steady stage of the smouldering experiments, which agrees with the previous finding [39]. Data from previous research [42] measuring the particle emissions from a mixing of smouldering and flaming in

peat is also plotted for comparison. The results show the ratio of particle emitted at the range of 0 - 1 μm is above 80% when flaming is also happening in peatland fires, between 40% and 80% at steady stage of smouldering free propagation, and below 40% at the ignition stage. Smouldering at steady stage has a higher ratio at the range of 1 - 2.5 μm than flaming, and both smouldering at steady stage and flaming have very low ratio of the range 2.5 - 10 μm. This distinct difference is caused by the difference in combustion mechanisms. Ignition stage of smouldering has a higher ratio of the range 2.5 - 10 μm, which can be because of the soil performing as filters to filter much finer particles.

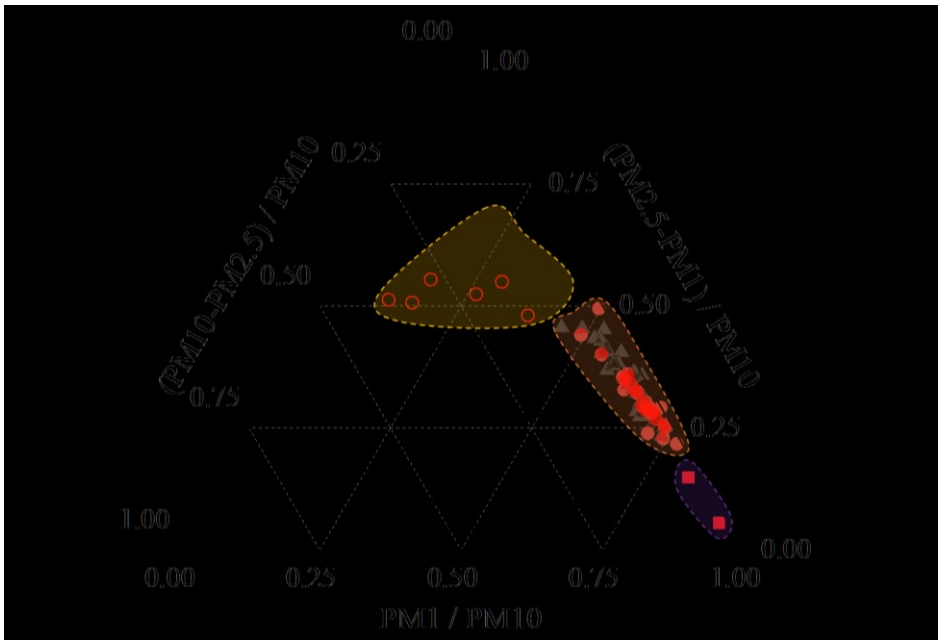

Figure 7.4 Ternary plot with the mass concentration ratios of (PM10-PM2.5) / PM10, (PM2.5-PM1) / PM10, and PM1 / PM10 measured in experiments in this thesis showing the difference between the ignition stage and steady stage of peat smouldering, and the mixing of flaming and smouldering in peat from literature values [42] for comparison. Symbols with red color represent the results of horticultural peat and symbols with black color represent the results of field peat. Data from different combustion stages are grouped in the figure.

7.4 Conclusion

This chapter presented the experimental results of burning peat samples of different origins in controlled laboratory conditions with diagnostics of monitoring mass loss, temperature profile, gas and particle emissions. The results confirmed the spread theory showing the linear correlation between horizontal spread rate and the inverse of heat sink density, and between in-depth spread rate and the inverse of organic density. The controlling mechanisms in both horizontal spread and in-depth spread were well explained by oxygen supply and heat transfer in different process of smouldering. One fundamental but most neglected fact related to the bulk density change in varied moisture content was recapped to explain the effect of drying in in-depth spread measurement. Furthermore, smouldering has multi-dimensional spread and a polar circle theory of the critical angle of spread direction (65° relative to horizontal plane) above which smouldering cannot self-sustain was proposed. Peat samples of different origins used in this study can represent the natural variation in peat properties and they share the same rule of determining the multi-dimensional spread. This chapter also help to advance the understanding of how natural variation in peat properties can influence fire dynamics and emissions, thus contribute to apply the fundamental knowledge of smouldering in field peat fire management and mitigation.

Chapter 8

Laboratory Benchmark of Low-Cost Portable Gas and Particle Analysers for the Field Measurements

Summary

Smouldering peat fires emit large amounts of carbon, toxic gases and PM, posing health and environmental hazards. It is challenging to conduct field measurements on peatland wildfire emissions, and the available instruments are always in high cost and low mobility. Here we studied three commercial low-cost and portable air quality analysers (KANE101, SDS011 and FLOW) and compared them to research-grade instrumentations (FTIR, PM Cascade Impactor and DustTrak). A series of laboratory experiments of peat smouldering were conducted including the stages of ignition, spread and burnout. The gas analyser KANE101 accurately measured CO2 and allowed accurate calculation of modified combustion efficiency (MCE). The FLOW air pollution sensor was found not suitable for PM measurements near fire source because of the small range. FLOW captured the variation of VOCs (volatile organic compounds), but did not correlate well in NO_2 compared to the FTIR results. The PM sensor SDS011 responded well in measuring PM10, but underestimated PM2.5 by 50%. KANE101 and SDS011 can be used in the field after calibration. This work provides a better understanding of how low-cost and portable emission sensors can be of use for wildfire measurements in the field.

8.1 Introduction

The emissions of peatland wildfires which are called haze have adverse effects on human health, local environment and economy, and climate [4, 40, 41]. However, literatures with regard to the field measurement quantifying the emissions of peat fires are scarce, which is mainly due to the challenging situation in the field and the limitations of instruments in cost and mobility. Field experiments measure results directly from real fires providing the most representative data, while laboratory experiments can control the variables to provide the

fundamental understanding of fire dynamics and emissions and test the hypotheses from field observations [24]. Both field and laboratory studies in peat fires are vital in understanding wildfires.

Chapter 3 has a review of devices used in 27 literatures in the past 20 years studying peat fire emissions in laboratory and field. It is found that all devices used in literature measuring gases and particles are in relatively high price and mostly with low and medium mobility. It is important to develop cost-effective air quality sensors to meet the requirement of high spatial and temporal measurements, and to be applied in facilitating the peat fire detection, validating remote sensing models, and estimating the health risks for residents or fire fighters exposed to peat fire emissions. With the development of sensor technologies and the application of commercial air quality sensors, the reliability of these air quality sensors in measuring wildfire smoke is an important topic to study.

In this chapter, three low-cost portable air quality sensors which are representative of similar sensors in the market were evaluated in controlled laboratory conditions in measuring peat fire emissions against research grade and calibrated instruments (FTIR, PM Cascade Impactor, and DustTrak). The objective of this study contributes towards the development of air quality diagnostics for field peat fire measurements.

8.2 Method

In this experimental study, Irish horticultural peat (Irish 2020 (H)) is used. Peat samples deposited in an open-top reactor with an internal dimension of 20 × 20 × 10 cm^3 (built by mineral fibre boards) were ignited by using a helical ignition coil (length of 18 cm, diameter of 1 cm) mounted at one side board (5 cm from the top surface) by following the reactor and

ignitor design of previous research [25, 39]. At the ignition stage, the ignition coil had a constant power supply of 100 W, and was turned off when the sample had 10% mass loss. To monitor the smouldering dynamics, a mass balance was used to record the real time mass loss; twelve thermocouples were inserted into the reactor to measure the soil temperature profile (3 rows and 4 columns); Gopro and FLIR camera were installed to record the visual and infrared signature of the experiments (shown in Figure 8.1).

Devices used to measure the gas and particle emissions in this study are shown in Figure 8.1. The basic specifications of these devices are presented in Table 8.1 and the photos are shown in Figure 8.2. Three low-cost sensors (KANE101, SDS011, and FLOW) were evaluated against research-grade reference instruments (FTIR, PM Cascade Impactor, and DustTrak).

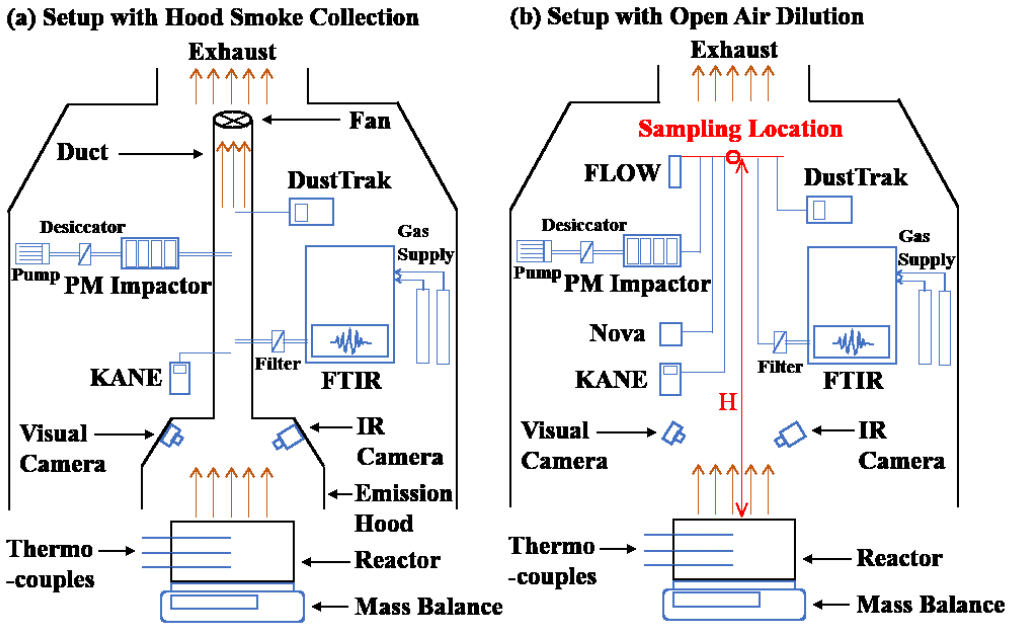

Figure 8.1 Schematics of the experimental setups. (a) experimental setup with hood smoke collection (devices are sampling the well-mixed flow inside the duct); (b) experimental setup with open air dilution (devices are sampling at the same height with inlet apart from each other for more than 2 cm, but less than 5 cm).

Figure 8.2 Photos of the devices used in this study. (a) Thermo Scientific Nicolet iG50 Fourier-transform infrared spectroscopy (FTIR). (b) Dekati 4-stage PM cascade impactor. (c) TSI DustTrak DRX handheld aerosol monitor. (d) KANE101 indoor air quality analyser. (e) Plume Labs FLOW 2 air pollution sensor. (f) Nova SDS011 PM sensor. The unit sizes of all devices are listed in Table 8.1.

Table 8.1 Specifications of the devices used in this study

	Approximate Cost (in 2021 UK) (£)	Dimension (cm^3)	Power Supply	Data Logging	Measurement	Range
FTIR	62,000	60×50×100	Cable to power (100-240 VAC)	Software	CO_2, CO, CH_4, NH_3, C_2H_2, C_2H_4, C_2H_6, C_3H_6, C_3H_8, C_4H_{10}, CH_3OH, CH_2O, NO, NO_2, HCN, CH_3COOH, CH_4O, CH_2O_2, HCl, SO_2	Depend on spectral range

PM Cascade Impactor	15,000	8×8×20	Cable to power (110-230 VAC)	By hand	PM1, PM2.5, PM10	< 1 mg/stage, depends on the aerosol
DustTrak DRX	9,000	13×12×32	Rechargeable battery	On-board memory	PM1, PM2.5, PM10	1 - 1.5×10^5 μg/m^3
KANE101	500	9×5×20	Rechargeable battery	By hand	CO_2	200 - 4,000 ppm
					CO	0 - 1,000 ppm
FLOW	200	4×2×9	Rechargeable battery	Wireless	PM1	0 - 200 μg/m^3
					PM2.5	
					PM10	
					VOCs	0 - 10 ppm
					NO_2	0 - 0.3 ppm
SDS011	12	7×2×7	USB to external source	Built-in SD card	PM2.5	0 - 1,000 μg/m^3
					PM10	0 - 2,000 μg/m^3

Fourier-transform infrared (FTIR) spectroscopy (Thermo Scientific Nicolet iG50) was used as the reference instrument for gas emissions. This instrument was calibrated and used in previous peat fire emission studies [28, 39, 42] to record the real-time concentrations of around 20 gas species. Before and after each experiment, the FTIR system was purged by pure nitrogen thoroughly. When measuring the concentrations of gases, all ducts of the FTIR system are heated to 100 ℃ to avoid gas condensation [39].

There were two reference devices for particle measurements in the experiments representing two commonly-used principles: gravimetric method and optical method. Dekati 4-stage PM cascade impactor (gravimetric method) was used to collect size-fractioned particles ($D \leq 1$ μm, 1 μm $\leq D \leq$ 2.5 μm, 2.5 μm $\leq D \leq$ 10 μm, $D \geq$ 10 μm) onto the filters in each of the stages of the cascade impactor, which was also used in previous peat fire particle measurements [39, 42]. The sampling flow rate was set to be 0.0005 m^3 s^{-1} ± 5.0% by adjusting

the setup of the pump, leading to an accuracy of ± 2.8% for the size of particles. The sampling duration was 10 min each time, and in each experiment the sampling was conducted five times, one at ignition stage (at the time of 5% mass loss), and four at steady stage (at the time of 20%, 40%, 60%, and 80% mass loss). The filters were weighed immediately after sampling by using a Sartorius balance (resolution 0.01 mg). The PM1, PM2.5 and PM10 were calculated by the measured mass gain of filters at each stage of the impactor.

The other reference device for particle measurements was DustTrak DRX aerosol monitor (optical method), which can provide real-time mass fraction concentrations including PM1, PM2.5 and PM10. This device has been used in laboratory studies on particle emissions of peat fires [43] and smouldering and flaming fuels [96]. This light-scattering laser photometer has a portable version that can be used in the field measurements with a high aerosol concentration range up to 150 mg m^{-3}. Due to the protocol of calibration in factory using coarser particles than particles emitted by biomass burning, this device was calibrated again in experiments for peat fire particles by using gravimetric method [59, 97]. The sampling flow rate of DustTrak in experiments was set to be 3 L min-1 with a data recording frequency of 1 Hz.

A portable gas analyser KANE101 measuring the concentration of CO_2 and CO (two most abundant gas species emitted by peat fires) was evaluated in experiments by using the data obtained by FTIR. The principle for CO_2 measurement is NDIR (non-dispersive infrared) sensor and for CO measurement is electrochemical sensor. This device has a reported accuracy of ± 10% and resolution of 1 ppm for both CO_2 and CO after calibration, and has a wide range up to 5000 ppm for CO_2 and 1000 ppm for CO. The version of KANE101 in our assessment can measure the real-time CO_2 and CO concentrations, but cannot record the data. In each

experiment the values of measurement were recorded by hand five times at the same mass loss intervals described above.

A portable air quality monitor named FLOW from Plume Labs was assessed in experiments. This device can measure real-time concentrations of PM1, PM2.5, PM10, NO_2, and VOCs, and can update the air quality index via a smartphone app in real-time. The measurement ranges are 0 – 200 μg m^{-3} for PM, 0 – 300 ppb for NO_2, and 0 – 10 ppm for VOCs. This device can represent similar commercial air pollution sensors developed in recent years for monitoring personal exposure to air pollutions, and is popular in citizen science projects mapping the air pollutions of urban areas [98].

A particle sensor SDS011 (Arduino-based) that can measure real-time concentrations of PM2.5 and PM10 was studied in experiments. This PM sensor containing a small fan and a fine laser beam for light scattering is an improved version of similar sensors in market. It can provide real-time reading (frequency of 1 Hz) of the environmental particle concentration, and has a relatively larger range of 0 – 1000 μg m^{-3} for PM2.5 and 0 – 2000 μg m^{-3} for PM10.

There are two experimental setups, hood smoke collection and open air dilution, used for this study. The experimental setup with hood smoke collection shown in Figure 8.1(a) was used in previous research studying transient gas and particle emissions of peat fires [39, 42]. In this setup, an emission hood connected with a duct to an adjustable fan collects smoke produced by controlled peat fire. The setup was calibrated previously [39] to set the duct flow rate to 2 m s^{-1} and the skirt free height (the distance between the hood and the reactor) to be 2 cm. This allows the smoke produced to be completely collected in the hood and well mixed in the duct, while the impact of experimental setup to fire dynamics is reduced to the minimum. A preliminary experiment was conducted by using this setup with all six devices measuring

emissions inside the duct to test their ranges and capacities. The results indicated that the PM concentration in the setup of hood smoke collection was higher than the measurement range of FLOW and SDS011. Then three experiments were conducted (Exp. 1, 2 and 3) in this setup by using FTIR, PM Impactor, DustTrak, and KANE for emission measurements. The other experimental setup with open air dilution shown in Figure 8.1(b) did not use the emission hood to collect emission gases and particles. The smoke released by smouldering peat was naturally diluted inside the combustion fume hood (1.2 × 1.2 × 3 m^3) connecting to exhaust. The averaged velocity across the section of the fume hood is 0.6 m s-1. A metal structure was built to lift the inlet of all devices to the same sampling height (H). Two sampling heights 1.5 m and 2 m were chosen in experiments, and two experiments were done at each sampling height (Exp. 4 and 5 at 1.5 m, and Exp. 6 and 7 at 2 m). Experiments were conducted in a relatively stable ambient condition with temperature at 21.4 ± 1.5 ℃ and relative humidity at 33.3 ± 4.5 %.

8.3 Results and Discussion

8.3.1 Performance of FLOW and SDS011 for PM measurements

The standard factory calibration for DustTrak uses Arizona Road Dust which is coarser than particles emitted by biomass burning, so it is important to recalibrate the device for different particles in experiments by using gravimetric method. Figure 8.3 shows the derivation of the linear recalibration factor for the PM concentration data of DustTrak. The derived recalibration factors for the mass concentration of PM10 and PM2.5 measured by DustTrak are 0.368 ± 0.036 and 0.364 ± 0.036. These factors are the first reported recalibration factors for DustTrak in controlled laboratory environment measuring peat fire emissions. These factors are lower than the recalibration factor of 0.5 ± 0.01 derived in a field peat fire study [59], and very close to the recalibration factor of 0.37 for wood smoke measurement in laboratory

conditions [99]. The difference can be originated from the difference in burning fuel or the environmental uncertainties, and valuable for future studies to compare.

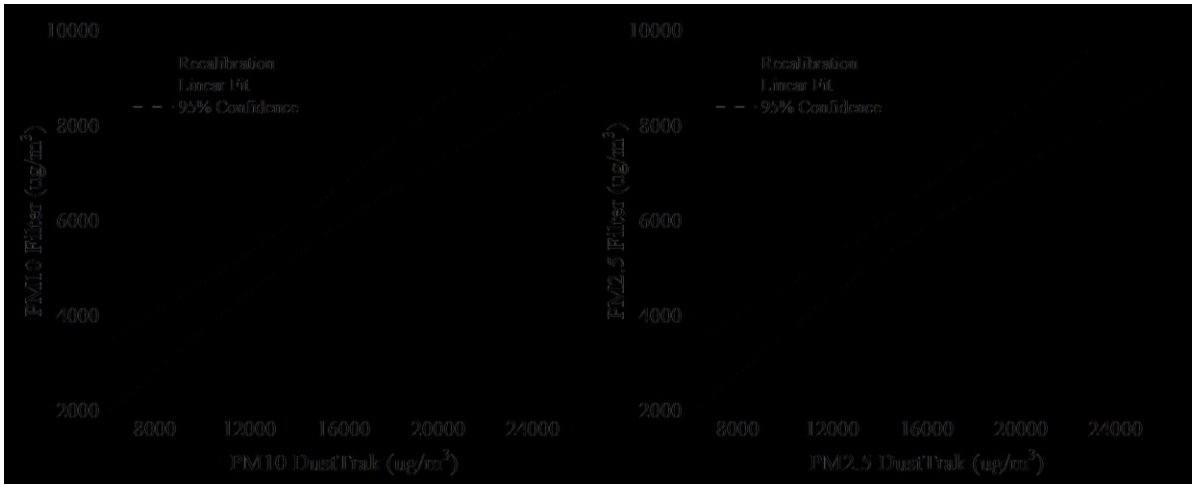

Figure 8.3 Derivation of the recalibration factor for the data of DustTrak in measuring the mass concentration of PM10 and PM2.5 in peat fire emissions.

Figure 8.4 shows the particle measurements by three different devices (DustTrak, SDS011, and FLOW) in one experiment (Exp. 7). Comparing to the reference device DustTrak, SDS011 captured the variation of data at all stages of fire evolution and responded relatively well in PM10 measurement, while the PM2.5 measurement at steady stage was nearly 50% lower than the reference. This was because of the limited capability of SDS011 in differentiate the particle sizes. Figure 8.5 shows the high correlation ($R^2 \in [0.79, 0.97]$) between the PM10 measurements of SDS011 and DustTrak. The mean absolute error (MAE) and root mean squared error (RMSE) of PM10 measurements are 39.8 μg m^{-3} and 60.2 μg m^{-3} for Exp. 6, and 92.1 μg m^{-3} and 117.5 μg m^{-3} for Exp. 7 with 18 h measurements for each experiment.

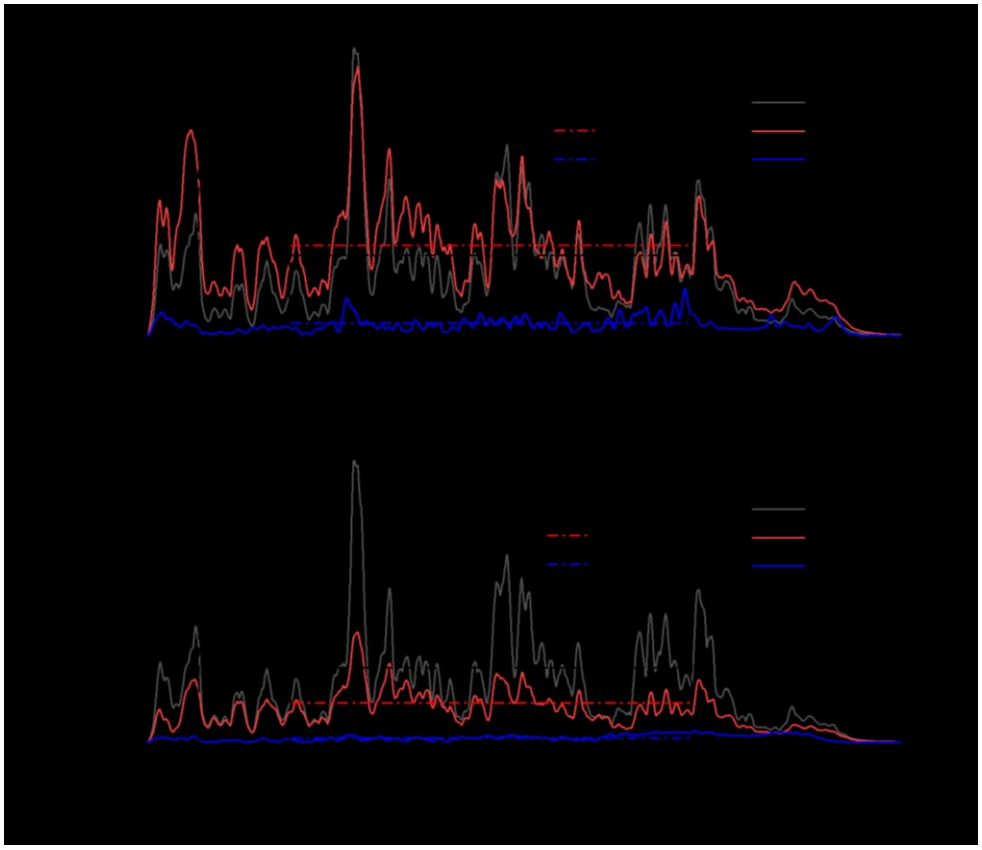

Figure 8.4 Comparisons of the PM measurement results from different devices in one experiment (Exp. 7). (a) and (b) show the results of PM10 and PM2.5 measurements. The dash-dot lines in both figures indicate the averaged values at the steady stage.

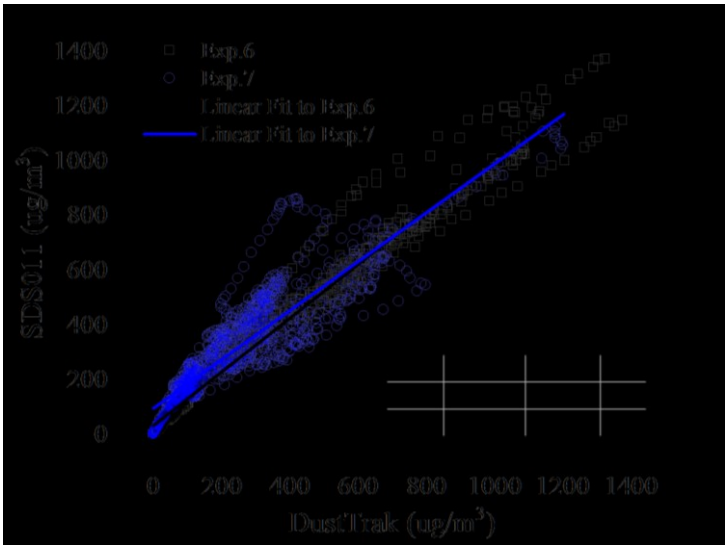

Figure 8.5 Scatter plots of the readings of Nova SDS011 against the readings of the reference device DustTrak in Exp. 6 and 7 sampling at the height of 2 m with open air dilution.

The averaged PM concentration measured by FLOW was out of its range (200 μg m^{-3}), but the data did not show a cut-off. This device was not designed for PM concentration as high as what wildfire emits, and can only be used for air pollution away from the fire. SDS011 showed cut-off at the range limits of PM10 2000 μg m^{-3} and PM2.5 1000 μg m^{-3}, so it is more reliable to be used to measure wildfire smoke with calibration and noticing the range limits.

The results of PM mass concentration depend on many factors, including the scale of burning and the distance of measurement. Reporting the in-plume measurement near fire source can help quantify the emission factor of particles, while out-of-plume results can help study the health impact of peat fires. The choice of PM measurement ranges in peat fire field study need to consider the objective. WHO (World Health Organization) global air quality guidelines stated that exposure to the 24 h concentrations of PM10 exceeding 50 μg m^{-3} and PM2.5 exceeding 25 μg m^{-3} can have negative health outcomes to human [100]. The measurement range of up to 100 - 500 μg m^{-3} which can cover the range in WHO guidelines by most of the air quality analysers similar to FLOW in consumers' market is suitable to monitor the ambient PM exposure resulted by emissions in urban environments like transportation, but not suitable for the measurement of peat fire emissions. A previous field study conducted in Sumatra, Indonesia during a peat fire showed the mass concentration of PM2.5 in the plume 100 m from the peat fire was 1600 ± 400 μg m^{-3}, and around 60 km downwind direction from the peat fire was 600 ± 420 μg m^{-3} [64]. Another field measurement on peat fires in Sumatra, Indonesia with in-plume measurements showed the PM2.5 concentration was as high as 7120 ± 3620 μg m^{-3} [65]. To the best knowledge of authors, there is no low-cost PM sensors in market that can measure PM concentrations higher than 2000 μg m^{-3} (range limit of SDS011). Dilutors which are widely used in laboratory research were not used in this study since the focus of this study

is to evaluate devices for field use, while dilutors are reducing the portability of devices for field works.

After finishing all experiments, two DustTrak devices failed functioning due to the fine particle contamination to the optic system, while the SDS011 continued working effectively. This indicates that the compatibility with measurement conditions should be considered when choosing devices for long-term field monitoring. Sophisticated instruments require higher maintenance costs and more technical support, while low-cost sensors with promising data accuracy can fulfil the demands of large spatial and temporal field monitoring.

8.3.2 Performance of KANE101 and FLOW for gas measurements

Figure 8.6 shows the high linear correlation ($R^2 = 0.98$) between KANE101 and FTIR measuring the CO_2 concentration, and the moderate correlation ($R^2 = 0.56$) for CO concentration. The MAE and RMSE are 21.19 ppm and 28.88 ppm for CO_2 measurement, and 4.01 ppm and 5.30 ppm for CO measurement, which are all within the accuracy (±10%) reported by the manufacturer. The MCE at steady stage calculated by KANE101 is 0.8549 ± 0.0147, which is very close to the value of 0.8542 ± 0.0125 obtained by FTIR (nearly 10 h steady stage measurement and three experiments). In general, KANE101 performed very well in measuring the concentrations of CO_2 and CO.

Figure 8.6 Scatter plots of the readings of KANE101 against the readings of the reference instrument FTIR in Exp. 1, 2, and 3 sampling with hood smoke collection. The error bars represent the correlated standard deviation.

The measurement of VOCs and NO2 by FLOW were evaluated using the data from FTIR. There are a diverse number of gases belonging to the category of VOCs. The VOCs gases that FLOW measures are unfortunately not reported by its manufacturer. The VOCs concentration obtained by our FTIR is the sum of the concentrations of Acetylene, Ethylene, Propylene, Propane, Methanol, Butane, Formaldehyde, Acetaldehyde, and Formic Acid and are calibrated. Some VOCs species in small amounts reported in previous peat fire studies [34, 101] include Chloromethane and Benzene, but these were not part of the FTIR because lack of calibration. The comparison of FTIR and FLOW is in Figure 8.7 and indicates FLOW underestimated the concentration of VOCs at steady stage. In terms of NO_2, FLOW showed a value of 0 at steady stage, while FTIR averaged at 0.6 ppm which indicated that the sensor of NO_2 in FLOW is not sensitive enough for this application.

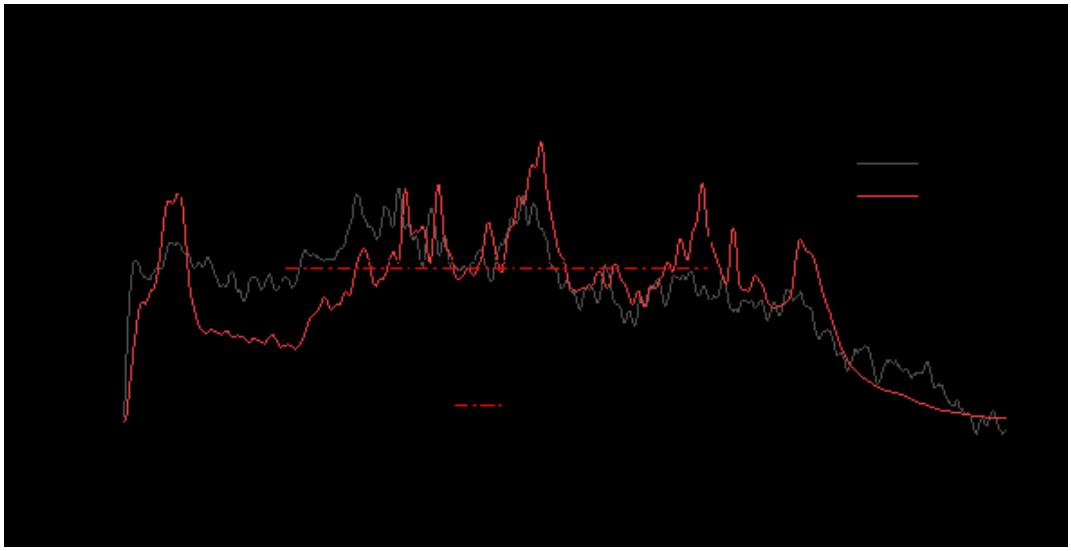

Figure 8.7 Comparisons of the VOCs estimation from FTIR and FLOW in preliminary experiment. The dash-dot lines in both figures indicate the averaged values at the steady stage.

8.3.3 Calculating emission factors

Figure 8.8 shows the comparisons of EF results for the 4 most abundant species (CO_2, CO, CH_4, NH_3). It is found that in general the carbon balance method underestimated the emission factors of CO_2, CO, CH_4, NH_3 by 10.6%, 8.9%, 22.1% and 11.4% compared to the mass loss method, which is different with the finding in previous work [39]. The uncertainty of EF quantification in the field measurement is unavoidable [44] since the calculation is highly dependent on the result of combustion efficiency and emission ratios of measured gases, the estimation of the fuel carbon content (F_c), and environmental conditions (e.g. the wind conditions). Therefore, it is necessary to also conduct controlled laboratory experiments to compare the results with field measurement to improve the estimation of EF.

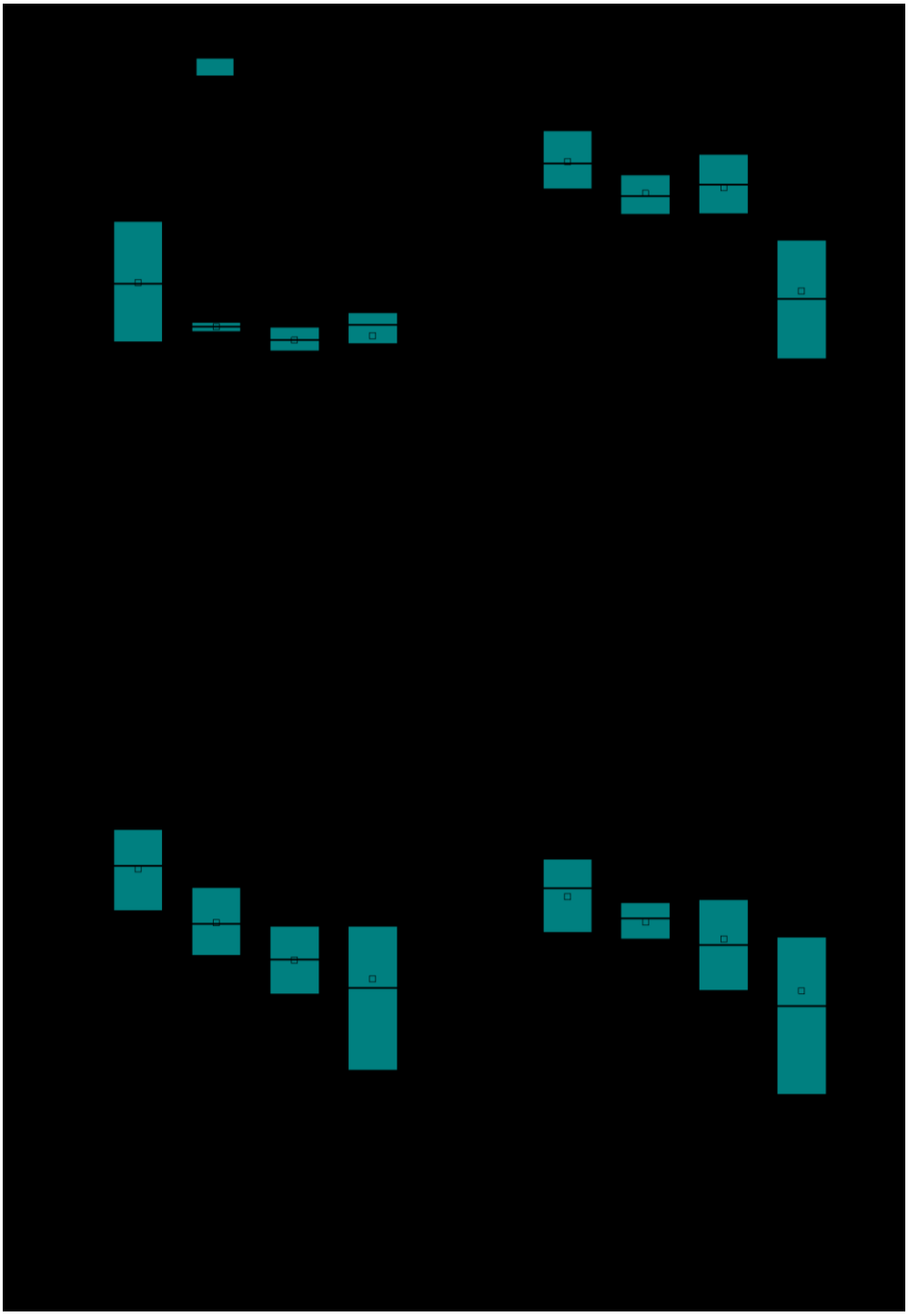

Figure 8.8 Comparisons of emission factors at steady stage calculated by different methods in different experimental setups. EF calculated with hood smoke collection averaged results of Exp. 1, 2, and 3. EF calculated with open air dilution at the sampling height of 1.5 m averaged results of Exp. 3 and 4. EF calculated with open air dilution at the sampling height of 2 m averaged results of Exp. 5 and 6.

8.4 Conclusions

In this work, we study the validity and accuracy of three commercially available air quality sensors, KANE101, SDS011, and FLOW, for smouldering peat fire emissions. We conducted controlled laboratory-scale experiments measuring the particulate matter and gas emissions from smouldering Irish horticultural peat. Sensors were evaluated against research-grade reference instruments (FTIR, PM Cascade Impactor, and DustTrak).

KANE101 gave accurate CO_2 concentration measurements, and allowed accurate calculation of the MCE. SDS011 underestimated PM2.5 measurements concentrations and gave relatively accurate PM10 measurements. The average experimental PM concentration was out of the range of FLOW (200 μg m^{-3}). FLOW is not valid for field-scale wildfire PM concentrations; field studies of peat fire episodes in Indonesia have measured PM2.5 concentrations as high as 1600 μg m^{-3} [64] and 7120 μg m^{-3} [65]. Compared to the sum of selected relevant VOCs concentrations measured by the reference instrument FTIR, FLOW underestimated the concentration of VOCs. Furthermore, the FLOW NO_2 sensor did not detect NO_2 in heavy smoke and high particle concentration conditions.

The emission factor (EF) was calculated with two methods. By calculating the EF of CO_2, CO, CH_4, NH_3, we found the carbon balance method underestimated the emission factor compared to the mass loss method. It is very important to conduct this study for research purpose of quantifying the emissions of peat fires, and also the general application in people's health monitoring. This work provides a better understanding of how low-cost and portable emission sensors can be of use for wildfire measurements in the field.

Chapter 9

Conclusions of this Thesis

Tackling peatland wildfires, the largest fires on Earth in terms of fuel consumption, is an emerging combustion topic in the context of climate change. Dominated by smouldering, peat fires destroy important natural habitats and soil ecosystems, releasing ancient carbon to the atmosphere, and creating regional haze episodes of severe and extensive impacts on human health. The understanding of fundamental smouldering dynamics and their application to peatlands are essential to mitigation methodologies development. This thesis conducted field sampling and laboratory experiments to investigate the ignition and spread of smouldering in peat of different origins with different soil conditions, and quantify the correlated gas and particle emissions. Figure 9.1 shows all different types of peat studied in this thesis.

Smouldering peat fire is still an emerging topic and requires more research investigations in experimental study and in computational study, in the lab and in the field. There are still many aspects in this topic not well understood. Here some suggestions for future study are listed. This thesis found the configuration of reactor can impact the results of fire dynamics, which is also a limitation of this thesis and many lab-scale experimental study. The horizontal reactor used in this thesis has insulations at the bottom and four boundary walls of the reactor, of which the depth and length of the reactor have impacts in altering the heat transfer when smouldering reaching the bottom and the end wall of the boundary, thus limit the multi-dimensional spread. More experimental works can be done to study how the scale of the configuration can influence the fire dynamics, which is important in applying results found in the lab scale to the field. More field works are needed to examine findings obtained in laboratory studies in the real field scale. More diagnostics that can facilitate the field measurements need to be developed and assessed. The understanding of gas and particle emissions from peat fires is still very limited. This thesis has found the differences in gas and

particle emissions in different types of peat, but the basic mechanisms leading to these differences and how are they related to combustion dynamics still need more investigations.

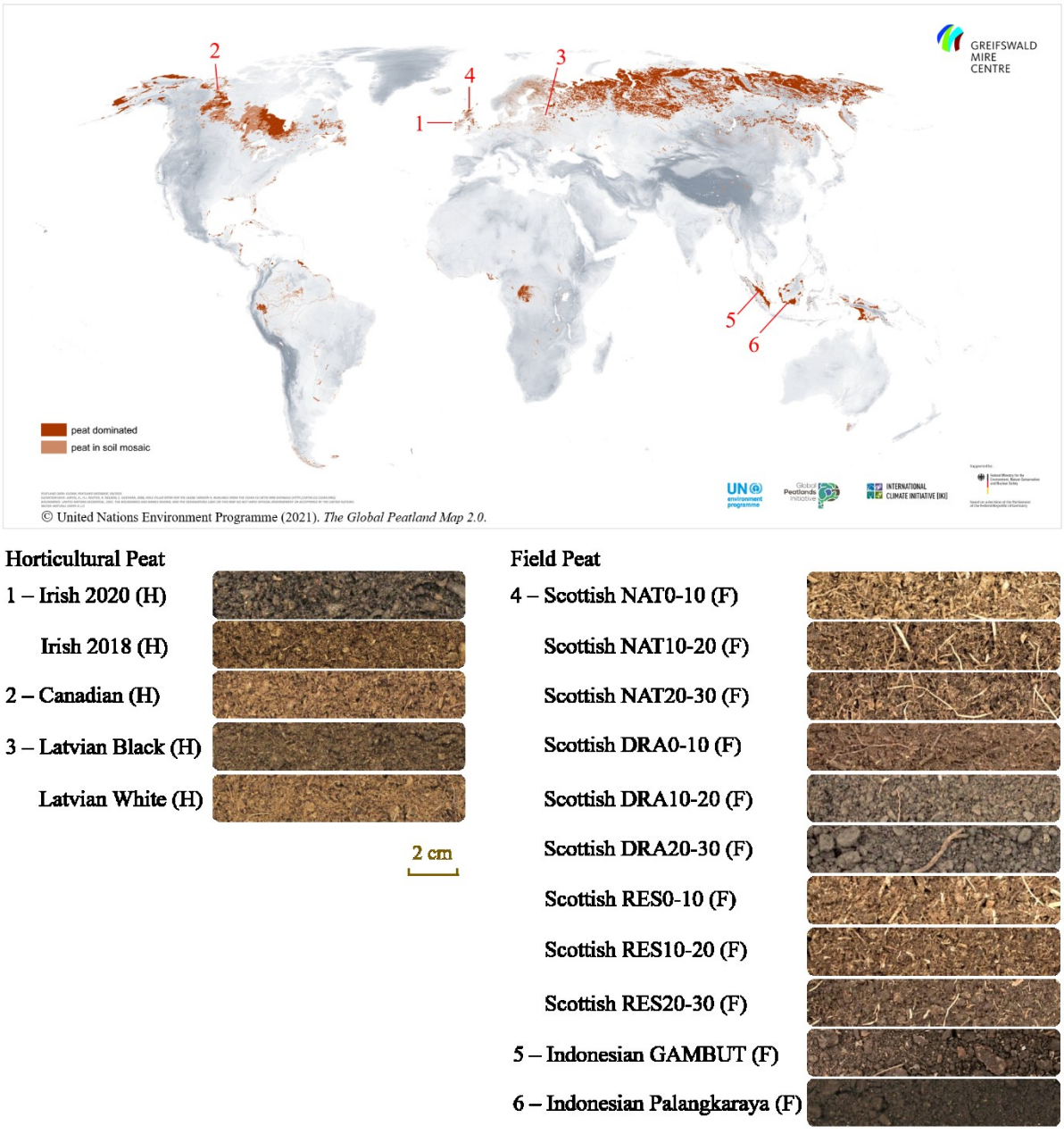

Figure 9.1 Peat samples of different origins studied in this thesis, including horticultural peat samples from Ireland, Canada, and Latvia, and field peat samples from Scotland and Indonesia. The origins of countries are marked in global peatland map made by the United Nations Environmental Programme.

This thesis investigated the ignition and spread of smouldering in peat samples from different origins with different bulk density, and also quantified the associated emissions. The key findings are presented here.

1. The understanding of the basic mechanisms of ignition of peat to initiate self-sustained smouldering is essential in the development of mitigation technologies and strategies, but not well studied yet in the literature. In this research, laboratory experiments were conducted to improve the understanding of how peat conditions (moisture content and bulk density) and ignition protocols influence the ignition probability. A modified ignition protocol was developed by stopping the heat source when 10% mass of the sample is lost. This mass-based ignition protocol was found to be robust to initiate self-sustained smouldering in peat samples for a wide range of soil conditions. The investigation in changing ignition protocol from time-based to mass-based can contribute to the development of novel experimental methodology for better studying the ignition, spread and emissions of smouldering peat, especially field peat with different origins across a great range of bulk density. Results show that although the moisture content plays a major role in the ignition probability, bulk density is also important. Increasing density decreases the critical moisture content by increasing the mass of water in a unit volume. This increase of heat sink makes the ignition more difficult. Heat sink density and organic density can be used to predict the ignition probability by summarising the effect of the three most important soil properties, inorganic content, moisture content and bulk density. This thesis provided a systematic framework for the first time studying the topic of ignition to initiate self-sustained smouldering in peat with a great variety of soil properties and of different origins.

2. This thesis also provided a comprehensive framework in field peat sampling, which is an important step linking the laboratory study with the field study. Laboratory studies using

peat samples from Flow Country, Scotland help greatly in understanding how field conditions and natural variation impact on the fire dynamics and emissions. Results revealed that high bulk density peat from long-term drained peatlands experience higher soil deterioration, and more extensive burning in terms of the amount of fuel burnt. Newly drained natural peatlands with low bulk density in drought condition are more vulnerable to fire in terms of easier ignition and faster fire spread. Samples from drained peatlands had lower averaged emission factors of CO_2, CO and NH_3, and higher averaged emission factor of CH_4 compared to samples from peatlands in natural condition and peatlands under restoration. As CO_2, CO and NH_3 are mostly emitted from the process of char oxidation and CH_4 is mostly emitted from the process of pyrolysis, the difference in results might be generated from the soil structure of which drained peatlands have more consolidated condition with higher bulk density. The averaged emission factors of particles in the combustion of samples from drained peatlands and peatlands under restoration were nearly twice as high as that of peatlands in natural condition. This difference might be caused by the chemical composition of the peat or the soil bulk density.

3. Most of the previous laboratory smouldering studies used horticultural peat which has a great advantage in controlling the influential factors, but has lower bulk density, and is not representative of higher bulk density peat sometimes found in the field, with higher carbon density and dryer conditions. In this thesis, a series of laboratory experiments were conducted to investigate the critical ignition conditions and governing fire spread parameters for smouldering peat of various origins, and to quantify the associated emissions. The results confirmed the spread theory showing the linear correlation between horizontal spread rate and the inverse of heat sink density, and between in-depth spread rate and the inverse of organic density. The controlling mechanisms in both horizontal spread and in-depth spread were well explained by oxygen supply and heat transfer in different process of smouldering. One

fundamental but most neglected fact related to the bulk density change in varied moisture content was recapped to explain the effect of drying in in-depth spread measurement. Furthermore, smouldering has multi-dimensional spread and a polar circle theory of the critical angle of spread direction (65° relative to horizontal plane) above which smouldering cannot self-sustain was proposed and explained by the controlling parameters and energy balance. Peat samples of different origins used in this study can represent the natural variation in peat properties and they share the same rule of determining the multi-dimensional spread. This thesis also quantified emissions of different types of peat in smouldering. We broadened the range of modified combustion efficiency (MCE) for smouldering to 0.74 – 0.88, wider than the values reported in literature, and found to be significantly dependent on the fuel composition. This chapter also help to advance the understanding of how natural variation in peat properties can influence fire dynamics and emissions, thus contribute to apply the fundamental knowledge of smouldering in field peat fire management and mitigation.

This thesis coupled laboratory studies with field sampling, and conducted smouldering peat experiments by using peat samples of various origins with a large range of inherent bulk density. Findings from previous research by using one type of horticultural peat were linked to different types of peat. The understanding of multi-dimensional spread of smouldering is improved comparing to previous research mainly looking at one dimension of spread. The correlations found between the horizontal spread and the heat sink density, between the in-depth spread and the organic density, and the critical angle of spread direction found related to these parameters can help to improve the peatland wildfire management by monitoring the three basic soil properties, inorganic content, moisture content and bulk density to predict the fire risks and find potential prevention strategies. The findings in ignition, spread, and emissions of the smouldering experiments by using different types of peat are important to link

the findings in the lab to the field. This thesis provides a better understanding of how smouldering wildfires start and spread in different types of peat and the associated emissions, thus contributing to prevention and mitigation.

References

[1] K.K. McLauchlan, P.E. Higuera, J. Miesel, B.M. Rogers, J. Schweitzer, J.K. Shuman, A.J. Tepley, J.M. Varner, T.T. Veblen, S.A. Adalsteinsson, J.K. Balch, P. Baker, E. Batllori, E. Bigio, P. Brando, M. Cattau, M.L. Chipman, J. Coen, R. Crandall, L. Daniels, N. Enright, W.S. Gross, B.J. Harvey, J.A. Hatten, S. Hermann, R.E. Hewitt, L.N. Kobziar, J.B. Landesmann, M.M. Loranty, S.Y. Maezumi, L. Mearns, M. Moritz, J.A. Myers, J.G. Pausas, A.F.A. Pellegrini, W.J. Platt, J. Roozeboom, H. Safford, F. Santos, R.M. Scheller, R.L. Sherriff, K.G. Smith, M.D. Smith, A.C. Watts, Fire as a fundamental ecological process: Research advances and frontiers, Journal of Ecology 108 (2020) 2047-2069.

[2] D.M.J.S. Bowman, J.K. Balch, P. Artaxo, W.J. Bond, J.M. Carlson, M.A. Cochrane, C.M. D'Antonio, R.S. DeFries, J.C. Doyle, S.P. Harrison, F.H. Johnston, J.E. Keeley, M.A. Krawchuk, C.A. Kull, J.B. Marston, M.A. Moritz, I.C. Prentice, C.I. Roos, A.C. Scott, T.W. Swetnam, G.R.v.d. Werf, S.J. Pyne, Fire in the Earth System, Science 324 (2009) 481-484.

[3] G. Rein, Smouldering Fires and Natural Fuels, Fire Phenomena and the Earth System2013, pp. 15-33.

[4] G. Rein, X. Huang, Smouldering wildfires in peatlands, forests and the arctic: Challenges and perspectives, Current Opinion in Environmental Science & Health 24 (2021) 100296.

[5] M.R. Turetsky, B. Benscoter, S. Page, G. Rein, G.R. van der Werf, A. Watts, Global vulnerability of peatlands to fire and carbon loss, Nature Geoscience 8 (2014) 11-14.

[6] S.E. Page, F. Siegert, J.O. Rieley, H.-D.V. Boehm, A. Jaya, S. Limin, The amount of carbon released from peat and forest fires in Indonesia during 1997, Nature 420 (2002) 61-65.

[7] Y. Hu, N. Fernandez-Anez, T.E.L. Smith, G. Rein, Review of emissions from smouldering peat fires and their contribution to regional haze episodes, International Journal of Wildland Fire 27 (2018) 293-312.

[8] Z.C. Yu, Northern peatland carbon stocks and dynamics: a review, Biogeosciences 9 (2012) 4071-4085.

[9] J. Xu, P.J. Morris, J. Liu, J. Holden, PEATMAP: Refining estimates of global peatland distribution based on a meta-analysis, CATENA 160 (2018) 134-140.

[10] M.A. Santoso, X. Huang, N. Prat-Guitart, E. Christensen, Y. Hu, G. Rein, Smouldering fires and soils, Fire effects on soil properties, CSIRO, Australia, 2019.

[11] S.E. Page, J.O. Rieley, C.J. Banks, Global and regional importance of the tropical peatland carbon pool, Global Change Biology 17 (2011) 798-818.

[12] X.J. Walker, J.L. Baltzer, S.G. Cumming, N.J. Day, C. Ebert, S. Goetz, J.F. Johnstone, S. Potter, B.M. Rogers, E.A.G. Schuur, M.R. Turetsky, M.C. Mack, Increasing wildfires threaten historic carbon sink of boreal forest soils, Nature 572 (2019) 520-523.

[13] T.J. Ohlemiller, Modeling of smoldering combustion propagation, Progress in Energy and Combustion Science 11 (1985) 277-310.

[14] M.A. Santoso, E.G. Christensen, J. Yang, G. Rein, Review of the Transition From Smouldering to Flaming Combustion in Wildfires, Frontiers in Mechanical Engineering 5 (2019).

[15] M.A. Santoso, W. Cui, H.M.F. Amin, E.G. Christensen, Y.S. Nugroho, G. Rein, Laboratory study on the suppression of smouldering peat wildfires: effects of flow rate and wetting agent, International Journal of Wildland Fire 30 (2021) 378-390.

[16] S. Lin, Y.K. Cheung, Y. Xiao, X. Huang, Can rain suppress smoldering peat fire?, Science of The Total Environment 727 (2020) 138468.

[17] D.M.J. Purnomo, Cellular Automata Simulations of Field-Scale Flaming and Smouldering Wildfires in Peatlands, Imperial College London, 2022.

[18] G. Rein, N. Cleaver, C. Ashton, P. Pironi, J.L. Torero, The severity of smouldering peat fires and damage to the forest soil, CATENA 74 (2008) 304-309.

[19] R.M. Hadden, G. Rein, C.M. Belcher, Study of the competing chemical reactions in the initiation and spread of smouldering combustion in peat, Proceedings of the Combustion Institute 34 (2013) 2547-2553.

[20] W.H. Frandsen, Ignition probability of organic soils, Canadian Journal of Forest Research 27 (1997) 1471-1477.

[21] J. Reardon, K. Ryan, Factors affecting sustained smouldering in organic soils from pocosin and pond pine woodland wetlands, International Journal of Wildland Fire 16 (2007).

[22] R. Hartford. Smoldering combustion limits in peat as influenced by moisture mineral content and organic bulk density. In: editor^editors. 1993. p.

[23] F. Restuccia, X. Huang, G. Rein, Self-ignition of natural fuels: Can wildfires of carbon-rich soil start by self-heating?, Fire Safety Journal 91 (2017) 828-834.

[24] E. Christensen, Y. Hu, F. Restuccia, M.A. Santoso, X. Huang, G. Rein, Experimental Methods and Scales in Smouldering Wildfires, in: P. Pereira, J. Mataix-Solera, X. Ubeda, G. Rein, A. Cerdà (Eds.), Fire effects on soil properties, Commonwealth Scientific and Industrial Research Organisation (CSIRO), Melbourne, Australia, 2018, pp. 267-280.

[25] X. Huang, F. Restuccia, M. Gramola, G. Rein, Experimental study of the formation and collapse of an overhang in the lateral spread of smouldering peat fires, Combustion and Flame 168 (2016) 393-402.

[26] W.H. Frandsen, The influence of moisture and mineral soil on the combustion limits of smoldering forest duff, Canadian Journal of Forest Research 17 (1987) 1540-1544.

[27] N. Prat-Guitart, G. Rein, R.M. Hadden, C.M. Belcher, J.M. Yearsley, Propagation probability and spread rates of self-sustained smouldering fires under controlled moisture content and bulk density conditions, International Journal of Wildland Fire 25 (2016) 456-465.

[28] Y. Hu, W. Cui, G. Rein, Haze emissions from smouldering peat: The roles of inorganic content and bulk density, Fire Safety Journal 113 (2020) 102940.

[29] E.G. Christensen, Experimental investigation of the effects of soil and environmental conditions on smouldering wildfires, Mechanical Engineering, Imperial College London, 2020.

[30] W. Cui, Laboratory Investigation of the Ignition and Spread of Smouldering in Peat Samples of Different Origins and the associated Emissions, Imperial College London, London, 2022.

[31] S.N. Koplitz, L.J. Mickley, M.E. Marlier, J.J. Buonocore, P.S. Kim, T. Liu, M.P. Sulprizio, R.S. DeFries, D.J. Jacob, J. Schwartz, M. Pongsiri, S.S. Myers, Public health impacts of the severe haze in Equatorial Asia in September–October 2015: demonstration of a new framework for informing fire management strategies to reduce downwind smoke exposure, Environmental Research Letters 11 (2016) 094023.

[32] A. Heil, J. Goldammer, Smoke-haze pollution: a review of the 1997 episode in Southeast Asia, Regional Environmental Change 2 (2001) 24-37.

[33] C.E. Stockwell, T. Jayarathne, M.A. Cochrane, K.C. Ryan, E.I. Putra, B.H. Saharjo, A.D. Nurhayati, I. Albar, D.R. Blake, I.J. Simpson, E.A. Stone, R.J. Yokelson, Field measurements of trace gases and aerosols emitted by peat fires in Central Kalimantan, Indonesia, during the 2015 El Niño, Atmos. Chem. Phys. 16 (2016) 11711-11732.

[34] I.J. George, R.R. Black, C.D. Geron, J. Aurell, M.D. Hays, W.T. Preston, B.K. Gullett, Volatile and semivolatile organic compounds in laboratory peat fire emissions, Atmospheric Environment 132 (2016) 163-170.

[35] T.R. Muraleedharan, M. Radojevic, A. Waugh, A. Caruana, Chemical characterisation of the haze in Brunei Darussalam during the 1998 episode, Atmospheric Environment 34 (2000) 2725-2731.

[36] L. Kiely, D.V. Spracklen, C. Wiedinmyer, L. Conibear, C.L. Reddington, S.R. Arnold, C. Knote, M.F. Khan, M.T. Latif, L. Syaufina, H.A. Adrianto, Air quality and health impacts of vegetation and peat fires in Equatorial Asia during 2004–2015, Environmental Research Letters 15 (2020) 094054.

[37] R. Burnett, H. Chen, M. Szyszkowicz, N. Fann, B. Hubbell, C.A. Pope, J.S. Apte, M. Brauer, A. Cohen, S. Weichenthal, J. Coggins, Q. Di, B. Brunekreef, J. Frostad, S.S. Lim, H. Kan, K.D. Walker, G.D. Thurston, R.B. Hayes, C.C. Lim, M.C. Turner, M. Jerrett, D. Krewski, S.M. Gapstur, W.R. Diver, B. Ostro, D. Goldberg, D.L. Crouse, R.V. Martin, P. Peters, L. Pinault, M. Tjepkema, A.v. Donkelaar, P.J. Villeneuve, A.B. Miller, P. Yin, M. Zhou, L. Wang, N.A.H. Janssen, M. Marra, R.W. Atkinson, H. Tsang, T.Q. Thach, J.B. Cannon, R.T. Allen, J.E. Hart, F. Laden, G. Cesaroni, F. Forastiere, G. Weinmayr, A. Jaensch, G. Nagel, H. Concin, J.V. Spadaro, Global estimates of mortality associated with long-term exposure to outdoor fine particulate matter, Proceedings of the National Academy of Sciences 115 (2018) 9592-9597.

[38] S.C. Emmanuel, Impact to lung health of haze from forest fires: The Singapore experience, Respirology 5 (2000) 175-182.

[39] Y. Hu, E. Christensen, F. Restuccia, G. Rein, Transient gas and particle emissions from smouldering combustion of peat, Proceedings of the Combustion Institute 37 (2019) 4035-4042.

[40] J.S. Reid, R. Koppmann, T.F. Eck, D.P. Eleuterio, A review of biomass burning emissions part II: intensive physical properties of biomass burning particles, Atmos. Chem. Phys. 5 (2005) 799-825.

[41] M.R. Turetsky, W.F. Donahue, B.W. Benscoter, Experimental drying intensifies burning and carbon losses in a northern peatland, Nature Communications 2 (2011) 514.

[42] Y. Hu, E.G. Christensen, H.M.F. Amin, T.E.L. Smith, G. Rein, Experimental study of moisture content effects on the transient gas and particle emissions from peat fires, Combustion and Flame 209 (2019) 408-417.

[43] J.G. Watson, J. Cao, L.W.A. Chen, Q. Wang, J. Tian, X. Wang, S. Gronstal, S.S.H. Ho, A.C. Watts, J.C. Chow, Gaseous, PM2.5 mass, and speciated emission factors from laboratory chamber peat combustion, Atmos. Chem. Phys. 19 (2019) 14173-14193.

[44] T.E.L. Smith, Evaluation and Application of FTIR spectroscopy for field study of biomass burning emissions, King's College London, London, 2013.

[45] C.E. Stockwell, R.J. Yokelson, S.M. Kreidenweis, A.L. Robinson, P.J. DeMott, R.C. Sullivan, J. Reardon, K.C. Ryan, D.W.T. Griffith, L. Stevens, Trace gas emissions from combustion of peat, crop residue, domestic biofuels, grasses, and other fuels: configuration and Fourier transform infrared (FTIR) component of the fourth Fire Lab at Missoula Experiment (FLAME-4), Atmos. Chem. Phys. 14 (2014) 9727-9754.

[46] T.J. Christian, B. Kleiss, R.J. Yokelson, R. Holzinger, P.J. Crutzen, W.M. Hao, B.H. Saharjo, D.E. Ward, Comprehensive laboratory measurements of biomass-burning emissions: 1. Emissions from Indonesian, African, and other fuels, Journal of Geophysical Research: Atmospheres 108 (2003).

[47] V. Selimovic, R.J. Yokelson, C. Warneke, J.M. Roberts, J. de Gouw, J. Reardon, D.W.T. Griffith, Aerosol optical properties and trace gas emissions by PAX and OP-FTIR for laboratory-simulated western US wildfires during FIREX, Atmos. Chem. Phys. 18 (2018) 2929-2948.

[48] G. Rein, S. Cohen, A. Simeoni, Carbon emissions from smouldering peat in shallow and strong fronts, Proceedings of the Combustion Institute 32 (2009) 2489-2496.

[49] R.R. Black, J. Aurell, A. Holder, I.J. George, B.K. Gullett, M.D. Hays, C.D. Geron, D. Tabor, Characterization of gas and particle emissions from laboratory burns of peat, Atmospheric Environment 132 (2016) 49-57.

[50] R.K. Chakrabarty, M. Gyawali, R.L.N. Yatavelli, A. Pandey, A.C. Watts, J. Knue, L.W.A. Chen, R.R. Pattison, A. Tsibart, V. Samburova, H. Moosmüller, Brown carbon aerosols from burning of boreal peatlands: microphysical properties, emission factors, and implications for direct radiative forcing, Atmos. Chem. Phys. 16 (2016) 3033-3040.

[51] C. Geron, M. Hays, Air emissions from organic soil burning on the coastal plain of North Carolina, Atmospheric Environment 64 (2013) 192-199.

[52] D. Wilson, S.D. Dixon, R.R.E. Artz, T.E.L. Smith, C.D. Evans, H.J.F. Owen, E. Archer, F. Renou-Wilson, Derivation of greenhouse gas emission factors for peatlands managed for extraction in the Republic of Ireland and the United Kingdom, Biogeosciences 12 (2015) 5291-5308.

[53] Y. Iinuma, E. Brüggemann, T. Gnauk, K. Müller, M.O. Andreae, G. Helas, R. Parmar, H. Herrmann, Source characterization of biomass burning particles: The combustion of selected European conifers, African hardwood, savanna grass, and German and Indonesian peat, Journal of Geophysical Research: Atmospheres 112 (2007).

[54] C. Bhattarai, V. Samburova, D. Sengupta, M. Iaukea-Lum, A.C. Watts, H. Moosmüller, A.Y. Khlystov, Physical and chemical characterization of aerosol in fresh and aged emissions from open combustion of biomass fuels, Aerosol Science and Technology 52 (2018) 1266-1282.

[55] A.R. Koss, K. Sekimoto, J.B. Gilman, V. Selimovic, M.M. Coggon, K.J. Zarzana, B. Yuan, B.M. Lerner, S.S. Brown, J.L. Jimenez, J. Krechmer, J.M. Roberts, C. Warneke, R.J. Yokelson, J. de Gouw, Non-methane organic gas emissions from biomass burning: identification, quantification, and emission factors from PTR-ToF during the FIREX 2016 laboratory experiment, Atmos. Chem. Phys. 18 (2018) 3299-3319.

[56] A.A. May, G.R. McMeeking, T. Lee, J.W. Taylor, J.S. Craven, I. Burling, A.P. Sullivan, S. Akagi, J.L. Collett Jr., M. Flynn, H. Coe, S.P. Urbanski, J.H. Seinfeld, R.J. Yokelson, S.M. Kreidenweis, Aerosol emissions from prescribed fires in the United States: A synthesis of laboratory and aircraft measurements, Journal of Geophysical Research: Atmospheres 119 (2014) 11,826-811,849.

[57] T.E.L. Smith, S. Evers, C.M. Yule, J.Y. Gan, In Situ Tropical Peatland Fire Emission Factors and Their Variability, as Determined by Field Measurements in Peninsula Malaysia, Global Biogeochemical Cycles 32 (2018) 18-31.

[58] Y. Hu, Experimental investigation of peat fire emissions and haze phenomena, Imperial College London, 2019.

[59] M.J. Wooster, D.L.A. Gaveau, M.A. Salim, T. Zhang, W. Xu, D.C. Green, V. Huijnen, D. Murdiyarso, D. Gunawan, N. Borchard, M. Schirrmann, B. Main, A. Sepriando, New Tropical Peatland Gas and Particulate Emissions Factors Indicate 2015 Indonesian Fires Released Far More Particulate Matter (but Less Methane) than Current Inventories Imply, Remote Sensing 10 (2018) 495.

[60] V. Huijnen, M.J. Wooster, J.W. Kaiser, D.L.A. Gaveau, J. Flemming, M. Parrington, A. Inness, D. Murdiyarso, B. Main, M. van Weele, Fire carbon emissions over maritime southeast Asia in 2015 largest since 1997, Scientific Reports 6 (2016) 26886.

[61] C. Roulston, C. Paton-Walsh, T.E.L. Smith, É.-A. Guérette, S. Evers, C.M. Yule, G. Rein, G.R. Van der Werf, Fine Particle Emissions From Tropical Peat Fires Decrease Rapidly With Time Since Ignition, Journal of Geophysical Research: Atmospheres 123 (2018) 5607-5617.

[62] R.J. Yokelson, B.H. Saharjo, C.E. Stockwell, E.I. Putra, T. Jayarathne, A. Akbar, I. Albar, D.R. Blake, L.L.B. Graham, A. Kurniawan, S. Meinardi, D. Ningrum, A.D. Nurhayati, A. Saad, N. Sakuntaladewi, E. Setianto, I.J. Simpson, E.A. Stone, S. Sutikno, A. Thomas, K.C. Ryan, M.A. Cochrane, Tropical peat fire emissions: 2019 field measurements in Sumatra and Borneo and synthesis with previous studies, Atmos. Chem. Phys. Discuss. 2022 (2022) 1-32.

[63] Y. Hamada, U. Darung, S.H. Limin, R. Hatano, Characteristics of fire-generated gas emission observed during a large peatland fire in 2009 at Kalimantan, Indonesia, Atmospheric Environment 74 (2013) 177-181.

[64] S.W. See, R. Balasubramanian, E. Rianawati, S. Karthikeyan, D.G. Streets, Characterization and Source Apportionment of Particulate Matter $\leqslant$ 2.5 μm in Sumatra, Indonesia, during a Recent Peat Fire Episode, Environmental Science & Technology 41 (2007) 3488-3494.

[65] Y. Fujii, W. Iriana, M. Oda, A. Puriwigati, S. Tohno, P. Lestari, A. Mizohata, H.S. Huboyo, Characteristics of carbonaceous aerosols emitted from peatland fire in Riau, Sumatra, Indonesia, Atmospheric Environment 87 (2014) 164-169.

[66] M.A. Santoso, E. Christensen, H.M.F. Amin, P. Palamba, Y. Hu, D.M.J. Purnomo, W. Cui, A. Pamitran, F. Richter, T.E.L. Smith, Y.S. Nugroho, G. Rein, GAMBUT field experiment of peatland wildfires in Sumatra: from ignition to spread and suppression, International Journal of Wildland Fire, (2022).

[67] R.S. Ferrarezi, S.K. Dove, M.W.v. Iersel, An Automated System for Monitoring Soil Moisture and Controlling Irrigation Using Low-cost Open-source Microcontrollers, HortTechnology hortte 25 (2015) 110.

[68] M.W.v. Iersel, M. Chappell, J.D. Lea-Cox, Sensors for Improved Efficiency of Irrigation in Greenhouse and Nursery Production, HortTechnology hortte 23 (2013) 735.

[69] R. Hartford, W. Frandsen, When It's Hot, It's Hot... Or Maybe It's Not! (Surface Flaming May Not Portend Extensive Soil Heating), International Journal of Wildland Fire 2 (1992) 139-144.

[70] A. Usup, Y. Hashimoto, H. Takahashi, H. Hayasaka, Combustion and thermal characteristics of peat fire in tropical peatland in Central Kalimantan, Indonesia, Tropics 14 (2004) 1-19.

[71] A.M. Young, P.E. Higuera, P.A. Duffy, F.S. Hu, Climatic thresholds shape northern high-latitude fire regimes and imply vulnerability to future climate change, Ecography 40 (2017) 606-617.

[72] D.J.C. M. F. Billett, J. M. Clark, C. D. Evans, M. G. Evans, N. J. Ostle, F. Worrall, A. Burden, K. J. Dinsmore, T. Jones, N. P. McNamara, L. Parry, J. G. Rowson, R. Rose, Carbon balance of UK peatlands: current state of knowledge and future research challenges, Climate Research, 13-29.

[73] S.J. Chapman, J. Bell, D. Donnelly, A. Lilly, Carbon stocks in Scottish peatlands, Soil Use and Management 25 (2009) 105-112.

[74] D.A. Stroud, T.M. Reed, M.W. Pienkowski, R. Lindsay, Birds, bogs and forestry: the peatlands of Caithness and Sutherland, 1988.

[75] M.G.R. CANNELL, R.C. DEWAR, D.G. PYATT, Conifer Plantations on Drained Peatlands in Britain: a Net Gain or Loss of Carbon?, Forestry: An International Journal of Forest Research 66 (1993) 353-369.

[76] T.J. Sloan, R.J. Payne, A.R. Anderson, C. Bain, S. Chapman, N. Cowie, P. Gilbert, R. Lindsay, D. Mauquoy, A.J. Newton, R. Andersen, Peatland afforestation in the UK and consequences for carbon storage, Mires and Peat 23 (2018) 1-17.

[77] M.H. Hancock, D. Klein, R. Andersen, N.R. Cowie, Vegetation response to restoration management of a blanket bog damaged by drainage and afforestation, Applied Vegetation Science 21 (2018) 167-178.

[78] E.G. Christensen, N. Fernandez-Anez, G. Rein, Influence of soil conditions on the multidimensional spread of smouldering combustion in shallow layers, Combustion and Flame 214 (2020) 361-370.

[79] S. Lin, Y. Liu, X. Huang, Climate-induced Arctic-boreal peatland fire and carbon loss in the 21st century, The Science of the total environment 796 (2021) 148924.

[80] B.W. Benscoter, D.K. Thompson, J.M. Waddington, M.D. Flannigan, B.M. Wotton, W.J. de Groot, M.R. Turetsky, Interactive effects of vegetation, soil moisture and bulk density on depth of burning of thick organic soils, International Journal of Wildland Fire 20 (2011) 418-429.

[81] A.C. Daniel, Effects of fuel characteristics on horizontal spread rate and ground surface temperatures of smouldering duff, International journal of wildland fire v. 29 (2020) pp. 820-831-2020 v.2029 no.2029.

[82] G.C. Krieger Filho, P. Bufacchi, F. Costa, E.V. Cortez, J.C. Andrade, K. Ribeiro, F.d.S. Costa, Smoldering characteristics of high bulk density peat, Proceedings of the Combustion Institute 38 (2021) 5053-5062.

[83] S.K. Akagi, R.J. Yokelson, C. Wiedinmyer, M.J. Alvarado, J.S. Reid, T. Karl, J.D. Crounse, P.O. Wennberg, Emission factors for open and domestic biomass burning for use in atmospheric models, Atmos. Chem. Phys. 11 (2011) 4039-4072.

[84] I. Bertschi, R.J. Yokelson, D.E. Ward, R.E. Babbitt, R.A. Susott, J.G. Goode, W.M. Hao, Trace gas and particle emissions from fires in large diameter and belowground biomass fuels, Journal of Geophysical Research: Atmospheres 108 (2003).

[85] H. Chen, W. Zhao, N. Liu, Thermal Analysis and Decomposition Kinetics of Chinese Forest Peat under Nitrogen and Air Atmospheres, Energy & Fuels 25 (2011) 797-803.

[86] M.R. Turetsky, E.S. Kane, J.W. Harden, R.D. Ottmar, K.L. Manies, E. Hoy, E.S. Kasischke, Recent acceleration of biomass burning and carbon losses in Alaskan forests and peatlands, Nature Geoscience 4 (2011) 27-31.

[87] A.L. Sinclair, L.L.B. Graham, E.I. Putra, B.H. Saharjo, G. Applegate, S.P. Grover, M.A. Cochrane, Effects of distance from canal and degradation history on peat bulk density in a degraded tropical peatland, Science of The Total Environment 699 (2020) 134199.

[88] K.J. Lees, R.R.E. Artz, D. Chandler, T. Aspinall, C.A. Boulton, J. Buxton, N.R. Cowie, T.M. Lenton, Using remote sensing to assess peatland resilience by estimating soil surface moisture and drought recovery, Science of The Total Environment 761 (2021) 143312.

[89] X. Huang, G. Rein, Downward spread of smouldering peat fire: the role of moisture, density and oxygen supply, International Journal of Wildland Fire 26 (2017) 907-918.

[90] L.E. Holst, L.A. Andersson, I. Bjerle, Investigation of peat pyrolysis under inert gas atmosphere, Fuel 70 (1991) 1017-1022.

[91] A.A. Sirin, D.A. Makarov, I. Gummert, A.A. Maslov, Y.I. Gul'be, Depth of Peat Burning and Carbon Loss during an Underground Forest Fire, Contemporary Problems of Ecology 13 (2020) 769-779.

[92] N. Kettridge, M.R. Turetsky, J.H. Sherwood, D.K. Thompson, C.A. Miller, B.W. Benscoter, M.D. Flannigan, B.M. Wotton, J.M. Waddington, Moderate drop in water table increases peatland vulnerability to post-fire regime shift, Scientific Reports 5 (2015) 8063.

[93] X. Huang, G. Rein, Computational study of critical moisture and depth of burn in peat fires, International Journal of Wildland Fire 24 (2015) 798-808.

[94] T.J. Ohlemiller, D.A. Lucca, An experimental comparison of forward and reverse smolder propagation in permeable fuel beds, Combustion and Flame 54 (1983) 131-147.

[95] F. He, W. Yi, Y. Li, J. Zha, B. Luo, Effects of fuel properties on the natural downward smoldering of piled biomass powder: Experimental investigation, Biomass and Bioenergy 67 (2014) 288-296.

[96] P. Garg, T. Roche, M. Eden, J. Matz, J.M. Oakes, C. Bellini, M.J. Gollner, Effect of moisture content and fuel type on emissions from vegetation using a steady state combustion apparatus, International Journal of Wildland Fire 31 (2022) 14-23.

[97] X. Wang, G. Chancellor, J. Evenstad, J.E. Farnsworth, A. Hase, G.M. Olson, A. Sreenath, J.K. Agarwal, A Novel Optical Instrument for Estimating Size Segregated Aerosol Mass Concentration in Real Time, Aerosol Science and Technology 43 (2009) 939-950.

[98] S.H.A. Tan, T.E.L. Smith, An optimal environment for our optimal selves? An autoethnographic account of self-tracking personal exposure to air pollution, Area 53 (2021) 353-361.

[99] S. Kingham, M. Durand, T. Aberkane, J. Harrison, J. Gaines Wilson, M. Epton, Winter comparison of TEOM, MiniVol and DustTrak PM10 monitors in a woodsmoke environment, Atmospheric Environment 40 (2006) 338-347.

[100] WHO, Air quality guidelines for particulate matter, ozone, nitrogen dioxide and sulphur dioxide. Global update 2005, World Health Organization. 38 (2006) E90038.

[101] D. Blake, A.L. Hinwood, P. Horwitz, Peat fires and air quality: Volatile organic compounds and particulates, Chemosphere 76 (2009) 419-423.